Sampling from a System-Theoretic Viewpoint

Gjerrit Meinsma*   Leonid Mirkin†

This paper studies a system-theoretic approach to the problem of reconstructing an analog signal from its samples. The idea, borrowed from earlier treatments in the control literature, is to address the problem as a hybrid model-matching problem in which performance is measured by system norms.

The paper is split into three parts. In Part I we present the paradigm and revise the lifting technique, which is our main technical tool. In Part II optimal samplers and holds are designed for various analog signal reconstruction problems. In some cases one component is fixed while the remaining are designed, in other cases all three components are designed simultaneously. No causality requirements are imposed in Part II, which allows to use frequency domain arguments, in particular the lifted frequency response as introduced in Part I. In Part III the main emphasis is placed on a systematic incorporation of causality constraints into the optimal design of reconstructors. We consider reconstruction problems, in which the sampling (acquisition) device is given and the performance is measured by the L^2-norm of the reconstruction error. The problem is solved under the constraint that the optimal reconstructor is l-causal for a given $l \geq 0$, i.e., that its impulse response is zero in the time interval $(-\infty, -lh)$, where h is the sampling period. We derive a closed-form state-space solution of the problem, which is based on the spectral factorization of a rational transfer function.

Keywords: Sampling, lifting, hybrid model matching, Shannon formula, Wiener filtering, down sampling, cardinal splines

AMS Subject Classification: 49N05, 49N10, 93B36, 93B28, 93B50, 93B51, 93C57, 93D25, 93E11, 93E24, 93E14, 94A12, 94A20

*G. Meinsma is with the Dept. of Applied Math., University of Twente, 7500 AE Enschede, The Netherlands. E-mail: *g.meinsma@utwente.nl*.

†L. Mirkin is with the Faculty of Mechanical Eng., Technion—IIT, Haifa 32000, Israel. E-mail: *mirkin@technion.ac.il*. This research was supported by THE ISRAEL SCIENCE FOUNDATION (grant No. 1238/08).
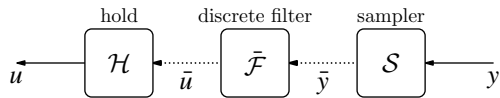
Contents

Figure 1: Hybrid signal processor (HSP), $\mathcal{F}_{\mathrm{HSP}}$

Part I: concepts and tools

1. Introduction

The problem of reconstructing a continuous-time signal from its sampled measurements may be, perhaps simplistically, described by the block-diagram in Fig. 1. Here y is a continuous-time signal, which is sampled by an A/D converter (sampler) $\mathcal{S}$, the resulting discrete-time signal $\bar{y}$ is processed by a digital filter $\bar{\mathcal{F}}$, and the output of the latter, $\bar{u}$, is converted back to continuous time by a D/A converter (hold) $\mathcal{H}$. Throughout, we refer to the (continuous-time) system from y to u as the *hybrid signal processor* (HSP) and denote it $\mathcal{F}_{\mathrm{HSP}}$.

Our goal typically is to generate u as close to y as possible. Sampling / reconstruction (SR) problems of this kind are important in numerous signal and image processing and control applications and have been extensively studied in both mathematical and engineering literature, see [18, 45, 51, 1, 15] for detailed overviews of the subject and a comprehensive bibliography. Classical studies are mainly concerned with the conditions under which perfect reconstruction of y is possible and the choice of the corresponding hold (interpolator) $\mathcal{H}$. This leads to the celebrated Sampling Theorem and its generalizations [18, 51, 15]. Such approaches, however, rely upon assumptions that are seldom realistic (e.g., require y to be bandlimited or generated by a discrete sequence), and result in interpolators that might be hard to implement or approximate.

These considerations prompted more recent studies to give up on the perfect reconstruction requirement. An example of such a setup is the reconstruction in shift-invariant spaces [45, 1], where $\bar{\mathcal{F}}$ is designed, for fixed sampling and hold circuits, to satisfy some weaker requirements. Examples of these requirements are the consistency [45], which is the perfect reconstruction of samples $\bar{y}$, or the (dual, in a sense) minimization of the error restricted to the image of $\mathcal{H}$ [11]. An advantage here is the full control over properties of $\mathcal{S}$ and $\mathcal{H}$, which may be chosen to simplify their implementation (like splines) and approximation (like truncating to impose causality constraints). This choice, however, might not be justifiable performance-wise. Moreover, the design of $\bar{\mathcal{F}}$ accounts only for a part of the reconstruction error rather than the analog error itself.

Direct optimization of analog error signals is the core of the sampled-data control theory [8, 10], which studies digital control of analog systems. Motivated by this, [23] proposed to cast SR problems as a hybrid H^∞—causal minmax—model-matching setup (the idea can be traced back to [38, 7]). This is a special case of the standard sampled-data control problem and can therefore be handled by available control methods, adopted to the relaxation of the causality of $\bar{\mathcal{F}}$. Advantages of this ap-

proach are that it explicitly addresses the analog error and does not restrict the class of input signals. The method of [23], however, is based on several intermediate transformations, which blur the structure of the solution. In fact, no closed-form formulae for this approach exist. Moreover, the design methodology adopted there is also limited to the case when both $\mathcal{S}$ and $\mathcal{H}$ are fixed.

Excluding the acquisition and reconstruction devices from the design cycle, which limits the achievable reconstruction performance, is not always justifiable. Technological constraints, which restrict the complexity of A/D and D/A circuits, become less severe taking into account the progress in hardware technology. Other constraints might merely result from limitation of existing design methods. For example, the decay rate of the interpolating kernel is considered an important factor in the choice of $\mathcal{H}$ [45]. Yet this appears to be brought about by the need to truncate it afterwards in order to impose causality constraints on the reconstructor. If these constraints were explicitly accounted for in the design stage, the kernel decay would not be so important.

This three-part paper aims at developing a systematic approach to the design of SRs, in which sampling and/or hold devices can be incorporated into the design process. Towards this end, we adopt the system-theoretic viewpoint, by which signals are modeled by systems and reconstruction performance is measured by system norms. The system-theoretic approach enables us to treat signals of different physical nature and properties (e.g., stochastic and deterministic) in a unified manner and also to incorporate causality requirements as design constraints.

The goal of this part is to present the underlying technical material required for the system-theoretic analysis of SR problems. Although many of the results presented here are not new, we believe that their compact and unified exposition is of its own tutorial value. Moreover, we do present new connections and perspectives that will play a key role in the analysis in the next parts. The part is organized as follows. In Section 2 we introduce a general optimization setup, the study of which is the leitmotif of this paper. Section 3 presents the lifting technique, which is our main technical tool, and collects some time-domain facts and definitions. In Section 4 some frequency-domain lifting definitions and results are presented. Spaces of signals and systems in the lifted domain and corresponding metrics are considered in Section 5. Finally, Section 6 presents the notions of stability and causality and their frequency-domain characterizations.

1.1. Notation

Throughout, h denotes the sampling period and $\omega_{\mathrm{N}} := \pi/h$ is the associated Nyquist frequency. The sinc function with "period" h is defined as $\mathrm{sinc}_h(t) := \sin(\omega_{\mathrm{N}}t)/(\omega_{\mathrm{N}}t)$. Signals are represented by lowercase symbols such as $y(t) : \mathbb{R} \to \mathbb{C}$ and overbars indicate discrete time signals, $\bar{y}[k] : \mathbb{Z} \to \mathbb{C}$. For any set $\mathbb{A}$ the indicator function $\mathbb{1}_{\mathbb{A}}(t)$ is 1 if $t \in \mathbb{A}$ and is zero elsewhere. The unit step (which is actually $\mathbb{1}_{\mathbb{R}+}(t)$) is denoted $\mathbb{1}(t)$ (in continuous time) and $\bar{\mathbb{1}}[k]$ in discrete time. Similarly $\delta(t)$ is the Dirac delta function (understood implicitly as the causal $\delta(t - 0^+)$) and $\bar{\delta}[k]$ is the discrete unit pulse. The number of
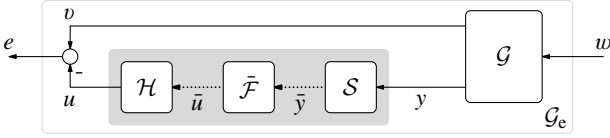
Figure 2: Sampling / reconstruction (SR) setup

elements of a vector-valued signal v is denoted by n_v.

Uppercase calligraphic symbols, like $\mathcal{G}$, denote continuous-time systems in time domains, the impulse response/kernel of which is denoted with lowercase symbols, such as g, and the corresponding transfer function/frequency response is presented by uppercase symbols, like $G(s)$ and $G(\mathrm{i}\omega)$. Discrete-time systems, kernels, etcetera are denoted by overbars, like $\bar{\mathcal{G}}$, $\bar{g}$, etc. Other more specific notation for lifted signals and systems is defined later.

By $\mathbb{Z}_l^+$ ($\mathbb{Z}_l^-$) we denote the set of all integers larger or equal to (smaller than) l. The symbols $\mathbb{T}$, $\mathbb{D}$, and $\bar{\mathbb{D}}$ stand for the unit circle ($|z| = 1$), the open unit disk ($|z| < 1$), and the closed unit disk ($|z| \leq 1$) in the complex plane, respectively. $L_{\mathbb{B}}^2(\mathbb{A})$ is the set of functions $f : \mathbb{A} \rightarrow \mathbb{B}$ that have finite norm $\|f\|_2 := (\int_{t \in \mathbb{A}} \|f(t)\|_{\mathbb{B}}^2 \, \mathrm{d}t)^{1/2}$, where $\|\cdot\|_{\mathbb{B}}$ denotes some given norm on $\mathbb{B}$ (in case $\mathbb{B} = \mathbb{C}^{n_f}$ we assume the standard Euclidean norm $|\cdot|$). Sometimes we use the notation $\mathbb{L} := L_{\mathbb{C}}^2[0, h]$. The space $\ell_{\mathbb{B}}^2(\mathbb{Z})$ is the set of $\bar{f} : \mathbb{Z} \rightarrow \mathbb{B}$ with finite norm $\|\bar{f}\|_2 := (\sum_{k \in \mathbb{Z}} \|\bar{f}[k]\|_{\mathbb{B}}^2)^{1/2}$. Some (or all) space arguments in the notation for L^2 and ℓ^2 will be dropped when they are irrelevant or clear from the context.

2. Setup

In this paper we study the SR setup shown in Fig. 2. Here v is an (unknown) analog signal, which is to be reconstructed from sampled measurements of a related analog signal y. Both v and y are modeled as outputs of a continuous-time system $\mathcal{G}$ (signal generator) driven by a common input w with known characteristics. The signal u is the reconstruction of v on the basis of y. This signal u is the output of the HSP, which is highlighted by the dark shadowed box in Fig. 2. It includes a sampler $\mathcal{S}$, a digital filter $\bar{\mathcal{F}}$, and a reconstructor, or hold, $\mathcal{H}$ (for more details see §2.2 below). Our goal then is to design an HSP (or only some of its components) to minimize a "size" (norm) of the *error system* $\mathcal{G}_{\mathrm{e}}$ (the light shadowed box in Fig. 2) which is the mapping from w to the reconstruction error $e := v - u$. Minimization of the mapping enforces that the output u of the HSP is in a sense optimally close to the signal v that we intend to reconstruct. This renders the optimal SR problem a systems optimization problem.

2.1. Paradigms

Two central aspects of the system-theoretic formulation of SR problems are the use of the signal generator $\mathcal{G}$ to *model* signals and the use of *system norms* to measure the SR performance.

These aspects, which are rather common in the control literature, are somewhat latent in the SR literature, so we start with a brief exposition of the underlying ideas.

2.1.1. Signal generator

Clearly, the reconstruction of a signal v on the basis of y makes sense only if the two signals share certain qualities. To model cross-correlations, dynamic relations, etcetera between v and y, one may choose to consider both v and y as the outcome of a (possibly fictitious) signal generator $\mathcal{G}$ driven by a common signal w having known and normalized features (such as being white or belonging to some bounded set). Below we indicate how these goals can be attained. To this end, partition the signal generator $\mathcal{G}$ compatible with the signal partition in Fig. 2 as

$$\mathcal{G} = \begin{bmatrix} \mathcal{G}_v \\ \mathcal{G}_y \end{bmatrix}.$$

The simplest choice of its components would be $\mathcal{G}_v = \mathcal{G}_y = I$, which reflects the assumptions that $v = y$ and that v is the only exogenous input. If the measured signal passes through an antialiasing filter $\mathcal{F}_{\mathrm{a}}$, we should pick $\mathcal{G}_y = \mathcal{F}_{\mathrm{a}}$ instead. If the measurement of v is corrupted by a measurement noise, n, the latter has to be included into the exogenous signal, so that $w = \begin{bmatrix} v \\ n \end{bmatrix}$ and we end up with $\mathcal{G}_v = \begin{bmatrix} I & 0 \end{bmatrix}$ and $\mathcal{G}_y = \begin{bmatrix} I & I \end{bmatrix}$ (or $\mathcal{G}_y = \mathcal{F}_{\mathrm{a}} \begin{bmatrix} I & I \end{bmatrix}$, if an antialiasing filter is present). If the velocity of y should be reconstructed, we choose $\mathcal{G}_v = \mathcal{F}_{\mathrm{d}}$, where $\mathcal{F}_{\mathrm{d}}$ is the differentiator, having the frequency response $F_{\mathrm{d}}(\mathrm{i}\omega) = \mathrm{i}\omega$. Thus, the problem of reconstructing the velocity from filtered noisy position measurements is formalized via assigning $\mathcal{G}_v = \begin{bmatrix} \mathcal{F}_{\mathrm{d}} & 0 \end{bmatrix}$, $\mathcal{G}_y = \mathcal{F}_{\mathrm{a}} \begin{bmatrix} I & I \end{bmatrix}$, and $w = \begin{bmatrix} x \\ n \end{bmatrix}$, where x is the position.

In the above examples the exogenous input w still consists of a combination of "real" signals such as position and noise, each with its own dynamical properties and physical domain/unit. To simplify their joint treatment, they can be modeled in terms of some normalized signal having favorable mathematical properties, passing through known systems. For example, if the signal to be reconstructed, v, is slow, it can be modeled as $v = \mathcal{F}_v w_v$, where $\mathcal{F}_v$ is a low-pass filter and w_v is some fictitious normalized signal. Examples of such signals are white noise in the stochastic case and the δ-impulse in the deterministic case, both of which have normalized flat spectra. A fast measurement noise, n, can then be modeled via another normalized signal, w_n, as $n = \mathcal{F}_n w_n$ for some high-pass filter $\mathcal{F}_n$. In this case, the problem of reconstructing a signal from filtered noisy measurements can be formalized via $\mathcal{G}_v = \begin{bmatrix} \mathcal{F}_v & 0 \end{bmatrix}$ and $\mathcal{G}_y = \mathcal{F}_{\mathrm{a}} \begin{bmatrix} \mathcal{F}_v & \mathcal{F}_n \end{bmatrix}$. The exogenous signal, $w = \begin{bmatrix} w_v \\ w_n \end{bmatrix}$, is then a fictitious normalized signal all components of which are on an equal footing and have similar properties; all structural properties are represented by $\mathcal{G}$.

Remark 2.1. The use of modeling filters, like $\mathcal{F}_v$ and $\mathcal{F}_n$ above, does not necessarily intend to constrain signals (e.g., v and n) to belong to a (finite-dimensional) subspace of the space of continuous-time signals, like those discussed in [51]. In many cases these filters may be thought of as functions, reshaping the metric used to measure the SR performance. Through

the choice of these filters we thus just emphasize certain aspects of signal properties, like their dominant frequency bands. ▽

2.1.2. Performance measures

The normalization of the exogenous input w makes it possible to express the size of the reconstruction error *signal e* in terms of the size of the error *system* $\mathcal{G}_e$ mapping w to e. We use two measures of the size of $\mathcal{G}_e$: its L^2 and L^∞ norms. Below we briefly discuss these formalisms. To avoid the introduction of involved technicalities at this stage, we assume for the moment that $\mathcal{G}_e$ is time invariant. Although this is practically never the case for the hybrid system in Fig. 2, extensions are conceptually straightforward (they are discussed in Section 5).

The Hilbert space $L^2_{p \times m}(i\mathbb{R})$, or simply $L^2(i\mathbb{R})$ when the dimensions are irrelevant or clear from the context, is the set of functions $F(s) : i\mathbb{R} \to \mathbb{C}^{p \times m}$ for which

$$\|F\|_2 := \left(\frac{1}{2\pi} \int_{-\infty}^{\infty} \|F(i\omega)\|_F^2 \, d\omega \right)^{1/2} < \infty, \qquad (1)$$

where $\|\cdot\|_F$ is the Frobenius matrix norm. The quantity $\|F\|_2$ is called the L^2-norm of $F(s)$. If $F(s)$ is the transfer function of an LTI system $\mathcal{F}$, we also refer to this quantity as the L^2-norm of $\mathcal{F}$ and denote it as $\|\mathcal{F}\|_2$. This norm has clear interpretations, both deterministic and stochastic, in terms of the input and output signals of $\mathcal{F}$. In the deterministic setting, it is readily seen from the Parseval's equality that $\|\mathcal{F}\|_2^2$ is the sum of the energies of the responses of $\mathcal{F}$ to δ-impulses applied at each of its m input components. In the stochastic setting, $\|\mathcal{F}\|_2^2$ is the power, that is, the sum of the variances of the p output components of $\mathcal{F}$ in the case when the input is a zero-mean unit intensity white noise process [42, Sect. 3.8].

The space $L^\infty_{p \times m}(i\mathbb{R})$, or simply $L^\infty(i\mathbb{R})$, is the set of functions $F(s) : i\mathbb{R} \to \mathbb{C}^{p \times m}$, the L^∞-norm of which,

$$\|F\|_\infty := \operatorname*{ess\,sup}_{\omega \in \mathbb{R}} \sigma_{\max}[F(i\omega)] < \infty. \qquad (2)$$

Similarly to the L^2 case, if $F(s)$ is the transfer function of an LTI system $\mathcal{F}$, the quantity defined by (2) is referred to as the L^∞-norm of $\mathcal{F}$ and denoted by $\|\mathcal{F}\|_\infty$. This norm can also be interpreted in terms of signals: $\|\mathcal{F}\|_\infty^2$ is the maximal energy of the output over all inputs of unit energy [9, Thm. A.6.26], i.e., the maximal energy gain of $\mathcal{F}$.

Returning to the setup in Fig. 2, the minimization of $\|\mathcal{G}_e\|_2$ in the stochastic case corresponds to (average) power or *mean square* minimization of the continuous-time reconstruction error e (energy minimization in the deterministic case). Thus, this is merely a hybrid version of the classical Wiener (or Kalman) filtering problem [20]. The minimization of $\|\mathcal{G}_e\|_\infty$ corresponds to the *minmax* formulation, in which the mean-square error is minimized for a worst-case input of unit energy. In fact, the L^2 and L^∞ approaches represent two extremes in our assumptions about the exogenous signals. The former assumes that these signals are completely *known*, whereas the latter—that they are completely *un*known, other than having finite power or energy. The "gray areas" in between may then be (implicitly) covered by the use of weighting filters.

Remark 2.2. It is not hard to imagine a situation where some of the exogenous inputs are known and some are not. This might call for the use of *mixed L^2/L^∞* strategies, such as minimizing the L^2-norm of a subsystem of $\mathcal{G}_e$ while keeping the L^∞-norm of the other subsystem below some prescribed level [41]. Such problems, however, result in complicated solutions that lack the structure and transparency of their pure L^2 and L^∞ counterparts. We therefore do not pursue this line here. After all, it is rarely possible to squeeze all requirements into a single optimization problem, so that the optimization in engineering should be considered as merely a *tool* to achieve meaningful and transparent solutions rather than a goal per se. ▽

The expression of the performance requirements via *system norms* simplifies the treatment of deterministic and stochastic signals via a unified formalism and brings some other (conceptual) advantages. For example, the L^∞ formulation is well suited for the sake of shaping the spectrum of the reconstruction error. To see this, consider the noise-free scalar setting and let v be modeled as $v = \mathcal{F}_v w$. Then,

$$\|\mathcal{G}_e\|_\infty < 1 \quad \Rightarrow \quad |e(i\omega)| < \frac{1}{|F_v(i\omega)|} |v(i\omega)|, \quad \forall \omega \in \mathbb{R}.$$

Thus, a desired shape of the error spectrum can be pursued via an appropriate choice of $\mathcal{F}_v$. The existence of a reconstructor guaranteeing $\|\mathcal{G}_e\|_\infty < 1$, which is the question that can be conclusively answered, is then the success indicator. Another advantage of the system-based treatment is a (relative) simplicity with which causality constraints can be imposed upon the reconstructor (see Part III of this paper).

2.2. Components

We now detail some of the components of the configuration in Fig. 2. In particular, below we address the HSP, containing a sampler, a discrete filter and a hold.

2.2.1. Sampler

By a sampling device $\mathcal{S}$ we understand any linear device transforming a function $y(t) : \mathbb{R} \to \mathbb{C}^{n_y}$ into a function $\bar{y}[k] : \mathbb{Z} \to \mathbb{C}^{n_{\bar{y}}}$. Assuming that

$$\mathcal{S}(y(\cdot - h)) = (\mathcal{S}y)[\cdot - 1],$$

which can be thought of as A/D shift invariance, a general model for such a device is

$$\bar{y} = \mathcal{S}y : \quad \bar{y}[k] = \int_{-\infty}^{\infty} \psi(kh - s) y(s) ds, \quad k \in \mathbb{Z}, \quad (3)$$

for some $\psi(t)$, called the *sampling function*. The ideal sampler $\mathcal{S}_{\mathrm{Idl}}$, generating $\bar{y}[k] = y(kh)$ and well-defined for continuous inputs, has $\psi(t) = \delta(t)$. The continuity of y can be ensured by an antialiasing filter $\mathcal{F}_a$ having the impulse response $f_a(t)$. Such a filter can always be incorporated into $\mathcal{S}$, resulting in a sampler with $\psi(t) = f_a(t)$. In fact, a general sampler of the form (3) can always be presented as the cascade of an LTI system with

the impulse response $\psi(t)$ and the ideal sampler. An important example for the developments in this paper (especially, in Part II) is the sinc-sampler, $\mathcal{S}_{\text{sinc}}$, having the sampling function $\psi_{\text{sinc}}(t) := \frac{1}{h}\text{sinc}_h(t)$. It can be viewed as the ideal lowpass filter with the cutoff frequency ω_{N} followed by the ideal sampler. Another example is the causal averaging sampler $\mathcal{S}_{\text{Av}}$, which corresponds to $\psi(t) = \frac{1}{h}\mathbb{1}_{[0,h)}(t)$.

2.2.2. Hold

By a hold device $\mathcal{H}$ we understand a linear device transforming a function $\bar{u}[k] : \mathbb{Z} \to \mathbb{C}^{n_{\bar{u}}}$ into a function $u(t) : \mathbb{R} \to \mathbb{C}^{n_u}$. Assuming D/A shift invariance, understood as

$$\mathcal{H}(\bar{u}[\cdot - 1]) = (\mathcal{H}\bar{u})(\cdot - h),$$

a general model of this device is

$$u = \mathcal{H}\bar{u} : \quad u(t) = \sum_{i \in \mathbb{Z}} \phi(t - ih)\bar{u}[i], \quad t \in \mathbb{R}, \quad (4)$$

for some *hold function*[1] $\phi(t)$. The hold function is the response of $\mathcal{H}$ to the discrete unit pulse $\bar{\delta}[i]$. The hold can also be thought of as a modulator of the input sequence $\{\bar{u}[i]\}$. The standard *zero-order hold* $\mathcal{H}_{\text{ZOH}}$, which keeps $u(t)$ constant over the intersample period, corresponds in this setting to $\phi(t) = \mathbb{1}_{[0,h)}(t)$. The predictive *first-order hold* $\mathcal{H}_{\text{FOH}}$, which is a linear interpolator of two successive input values, has the "tent" hold function $\phi(t) = (1 - |t|/h)\mathbb{1}_{[-h,h)}(t)$. It is readily seen that both these hold devices can be presented as the cascade of the *impulse-train modulator* $\mathcal{H}_{\text{ITM}}$, having the hold function $\phi(t) = \delta(t)$, and continuous-time LTI systems with the transfer functions $\frac{1-e^{-sh}}{s}$ (for $\mathcal{H}_{\text{ZOH}}$) and $\left(\frac{1-e^{-sh}}{s}\right)^2 e^{sh}$ (for $\mathcal{H}_{\text{FOH}}$). Another example of a hold device is the sinc-hold, $\mathcal{H}_{\text{sinc}}$, having the hold function $\phi_{\text{sinc}}(t) := \text{sinc}_h(t)$. This is actually the interpolator from the Sampling Theorem.

Remark 2.3. We do not restrict the input and output dimension of $\mathcal{S}$ and $\mathcal{H}$. For example, the sampler may produce a vector-valued discrete signal ($n_{\bar{y}} > 1$) from a scalar analog signal ($n_y = 1$). This renders the setup general enough to describe multirate or nonuniform sampling problems (using the polyphase decomposition). $\triangledown$

2.2.3. Discrete part

A general form of the LTI discrete-time system $\bar{\mathcal{F}}$ is the convolution model

$$\bar{u} = \bar{\mathcal{F}}\bar{y} : \quad \bar{u}[k] = \sum_{i \in \mathbb{Z}} \bar{f}[k-i]\bar{y}[i], \quad k \in \mathbb{Z}, \quad (5)$$

where the sequence $\bar{f}[k]$ is known as the *impulse response* of $\bar{\mathcal{F}}$. This system can always be absorbed into $\mathcal{S}$ or $\mathcal{H}$ via redefining the functions ψ and ϕ, respectively. When analyzing HSPs we thus may assume without loss of generality that $\bar{\mathcal{F}} = I$ or, equivalently, $\bar{f}[k] = \bar{\delta}[k]$. This assumption can also be made during the design if either sampler or hold (or both) is a design parameter. For implementation of HSPs it might however be advantageous to use a separate discrete filter.

---
[1]Thus, psi stands for sampler and phi for hold.

3. Lifting in Time Domain

Let us return now to the HSP in Fig. 1 and consider it as a continuous-time system from y to u. Assuming, without loss of generality, that $\bar{\mathcal{F}} = I$ and combining (3) and (4), we get

$$u(t) = \sum_{i \in \mathbb{Z}} \phi(t - ih) \int_{-\infty}^{\infty} \psi(ih - s)y(s)\mathrm{d}s$$
$$= \int_{-\infty}^{\infty} \sum_{i \in \mathbb{Z}} \phi(t - ih)\psi(ih - s)y(s)\mathrm{d}s.$$

Thus, $\mathcal{F}_{\text{HSP}}$ is an integral operator of the form

$$u(t) = \int_{-\infty}^{\infty} g(t, s)y(s)\mathrm{d}s \quad (6)$$

with kernel

$$g(t, s) = f_{\text{HSP}}(t, s) := \sum_{i \in \mathbb{Z}} \phi(t - ih)\psi(ih - s). \quad (7)$$

System (6) is time invariant iff $g(t, s) = g(t + \sigma, s + \sigma)$ for all $\sigma \in \mathbb{R}$. This, in general, is not the case for the kernel $f_{\text{HSP}}(t, s)$ above. Thus, operations of continuous time signals that include A/D and D/A converters are not a time-invariant operation in general. Many of the techniques that are available for LTI systems can therefore not be applied to $\mathcal{F}_{\text{HSP}}$ so easily. The time invariance can, however, be regained on noticing that

$$f_{\text{HSP}}(t, s) = f_{\text{HSP}}(t + kh, s + kh), \quad \forall k \in \mathbb{Z}. \quad (8)$$

This property, known as *h-periodicity* (or *h-shift invariance*), enables one to convert $\mathcal{F}_{\text{HSP}}$ into an equivalent shift-invariant system using the linear transformation called *lifting*, see books [8, 10] for more details and bibliography.

The lifting transformation—or simply *lifting*—can be seen as a way of separating the behavior into a fully time *in*variant discrete-time behavior and a *finite-horizon* continuous-time (intersample) behavior. Fig. 3 explains the idea and the formal

(a) $f(t)$ in continuous time   (b) $\{\check{f}[k]\}$ in the lifted domain
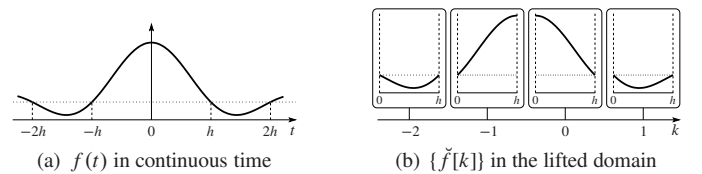
Figure 3: Lifting analog signal $f(t) = \text{sinc}_h(t)$

definition is given below:

Definition 3.1. For any signal $f : \mathbb{R} \to \mathbb{C}^{n_f}$, the *lifting* $\check{f} : \mathbb{Z} \to \{[0, h) \to \mathbb{C}^{n_f}\}$ is the sequence of functions $\{\check{f}[k]\}$ defined as

$$\check{f}[k](\tau) = f(kh + \tau), \quad k \in \mathbb{Z}, \tau \in [0, h). $$

$\triangledown$

6

In other words, with lifting we consider a function on $\mathbb{R}$ as a sequence of functions on $[0, h)$. Clearly, this incurs no loss of information, it is merely another representation of the signal. The rationale behind this representation is to "forbid" any time shift but multiples of h. This implies that if a continuous-time system $u = \mathcal{G}y$ is h-periodic, then in lifted representation, $\check{u} = \check{\mathcal{G}}\check{y}$, it is shift invariant.

More explicitly, let an h-periodic system $u = \mathcal{G}y$ be defined by the integral (6) then in the lifted domain the mapping reads

$$\check{u}[k](\tau) = u(kh + \tau) = \int_{-\infty}^{\infty} g(kh + \tau, \sigma) y(\sigma) \mathrm{d}\sigma$$

$$= \sum_{i \in \mathbb{Z}} \int_{0}^{h} g(kh + \tau, ih + \sigma) y(ih + \sigma) \mathrm{d}\sigma$$

$$= \sum_{i \in \mathbb{Z}} \int_{0}^{h} g((k - i)h + \tau, \sigma) \check{y}[i](\sigma) \mathrm{d}\sigma, \qquad (9)$$

which can be written as

$$\check{u}[k] = \sum_{i \in \mathbb{Z}} \check{G}[k - i] \check{y}[i], \qquad (10)$$

where $\check{G}[k]$, $k \in \mathbb{Z}$, is the *(lifted) impulse response* system that maps functions on $[0, h)$ to functions on $[0, h)$ as

$$(\check{G}[k]\check{w})(\tau) = \int_{0}^{h} g(kh + \tau, \sigma) \check{w}(\sigma) \mathrm{d}\sigma$$

$$= \int_{0}^{h} g(\tau, \sigma - kh) \check{w}(\sigma) \mathrm{d}\sigma, \quad \tau \in [0, h). \quad (11)$$

Mapping (10) is a standard discrete-time convolution, describing a *shift-invariant* system $\check{\mathcal{G}}$. The price to pay with lifting is the double time index: discrete (k) and continuous (τ) times.

Example 3.2. Consider the sample-and-hold circuit (Fig. 4), which is the cascade of the ideal sampler and the zero-order
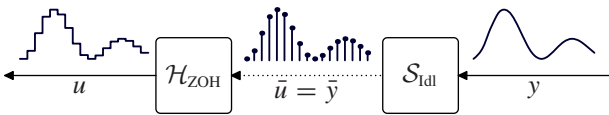

Figure 4: Sample-and-hold circuit in the time domain

hold. This system determines the relation $u(t) = y(\lfloor t/h \rfloor)$, which is clearly not time invariant. Lifting y and u transforms the sample-and-hold circuit into a discrete system, $\check{u}[k](\tau) = \check{y}[k](0)$, that is, the kth element of the lifted output is a function of the kth lifted input element only: the impulse response system at $i = 0$ acts as $(\check{G}[0]\check{y})(\tau) = \check{y}(0)$ and the others are zero, $\check{G}[i] = 0$. In the lifted domain it is therefore a static LTI system. $\qquad \triangledown$

Although it appears natural to begin with integral representations (6) (because it allows to make the lifting operators concrete), the precise integral form (11) only blurs the reasoning once the advantages of lifting sinks in. One would therefore prefer to think of lifted systems purely in discrete time (10) and suppress the finite-horizon time dependence.

Example 3.3. In the same vein, the sample-and-hold circuit from Example 3.2 in the lifted domain may be depicted as in Fig. 5. Here $\acute{\mathcal{S}}_{\mathrm{Idl}}$ is the lifted ideal sampler transforming a se-
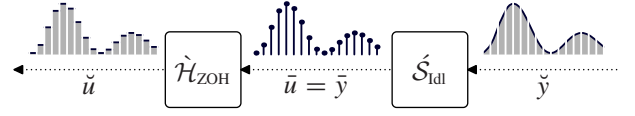

Figure 5: Sample-and-hold circuit in the lifted domain

quence of functions $\{\check{y}[k]\}$ into a sequence of numbers $\{\bar{y}[k]\}$ as $\bar{y}[k] = \check{y}[k](0)$ and $\grave{\mathcal{H}}_{\mathrm{ZOH}}$ is the lifted zero-order hold transforming a sequence of numbers $\{\bar{u}[k]\}$ into a sequence of functions $\{\check{u}[k]\}$ as $\check{u}[k](\tau) = \bar{u}[k]$ for all $\tau \in [0, h)$. Both these blocks are static discrete-time LTI systems. $\qquad \triangledown$

The reasonings of Example 3.3 apply in the general case where each time we leave the discrete signals to what they are and we lift the continuous-time signals to discrete ones. Lifting the input y of the A/D converter $\bar{y} = \mathcal{S}y$ in (3) results in the *lifted sampler*

$$\bar{y} = \acute{\mathcal{S}}\check{y} : \quad \bar{y}[k] = \sum_{i \in \mathbb{Z}} \int_{0}^{h} \psi((k - i)h - \sigma) \check{y}[i](\sigma) \mathrm{d}\sigma$$

$$=: \sum_{i \in \mathbb{Z}} \acute{S}[k - i] \check{y}[i] \qquad (12)$$

This describes a pure discrete-time shift-invariant system and we think of the operator $\acute{S}[k] : \{[0, h) \to \mathbb{C}^{n_y}\} \mapsto \mathbb{C}^{n_{\bar{y}}}$ as its impulse response. Similarly, the action of the hold device $u = \mathcal{H}\bar{u}$ in (4) after lifting its output becomes

$$\check{u} = \grave{\mathcal{H}}\bar{u} : \quad \check{u}[k] = \sum_{i \in \mathbb{Z}} \grave{H}[k - i] \bar{u}[i], \qquad (13)$$

where the operator $\check{H}[k] : \mathbb{C}^{n_{\bar{u}}} \mapsto \{[0, h) \to \mathbb{C}^{n_u}\}$ for each k is a multiplication by the lifted hold function $\check{\phi}[k]$, i.e., $(\check{H}[k]\eta)(\tau) = \check{\phi}[k](\tau)\eta$ for every $\eta \in \mathbb{C}^{n_{\bar{u}}}$. This is also a pure discrete shift-invariant system.

Example 3.4. Consider the predictive first-order hold discussed in §2.2.2. It has the hold function

$$\phi_{\mathrm{FOH}}(t) = \quad \vcenter{\hbox{}} \quad .$$

Then the lifted hold $\check{u} = \grave{\mathcal{H}}_{\mathrm{FOH}}\bar{u}$ is a discrete FIR system with support in $\{-1, 0\}$. It maps numbers $\bar{u}[k]$ to functions on $[0, h)$ as follows:

$$\check{u}[k] = \check{\phi}_{\mathrm{FOH}}[0] \bar{u}[k] + \check{\phi}_{\mathrm{FOH}}[-1] \bar{u}[k + 1]$$

$$= \quad \vcenter{\hbox{}}$$

so $\check{u}[k](\tau)$ is the straight line interpolating $\bar{u}[k]$ and $\bar{u}[k + 1]$ at $\tau = 0$ and $\tau = h$, respectively. $\qquad \triangledown$
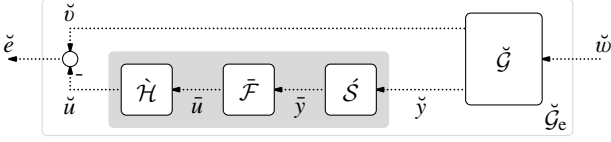
Figure 6: Sampling / reconstruction (SR) setup in the lifted domain

Remark 3.5. The various lifted systems (operators) that we have seen so far come with different accents to emphasize the dimensionality of their domain and range. The breve accent, such as in $\breve{\mathcal{G}}$, indicates that input and output space at each discrete time is infinite dimensional, $\{[0, h) \to \mathbb{C}^n\}$. Samplers $\acute{\mathcal{S}}$ map infinite-dimensional space $\{[0, h) \to \mathbb{C}^n\}$ to finite-dimensional space $\mathbb{C}^n$, which is what the acute accent indicates, and holds $\grave{\mathcal{H}}$ map finite-dimensional space to infinite-dimensional space, indicated by the grave accent. The lifted hybrid signal processor then is a mapping $\breve{\mathcal{G}}_{\mathrm{HSP}} = \grave{\mathcal{H}}\acute{\mathcal{S}}$ that goes from an infinite-dimensional space to a finite-dimensional one and back to another infinite-dimensional space again. The accents help in keeping track of the signal space dimensions. When an expression equally applies to either of these types of operators (e.g., in some definitions), we use the tilde, $\tilde{\mathcal{G}}$. $\qquad \triangledown$

Thus, by lifting all analog signals in the SR setup in Fig. 2 we end up with an equivalent discrete-time setup depicted in Fig. 6. It has two key advantages over the original representation. First, lifting puts continuous- and discrete-time signals on an equal footing. The only difference between "bar" and "breve" discrete signals is that the former are vector (or scalar) valued, whereas the latter are function valued. Conceptually, however, this difference is not more intricate than the difference between scalar and vector signals. Consequently, all systems in Fig. 2, irrespective of whether they are continuous time, discrete time, or hybrid, become pure discrete-time systems. Second, all these discrete systems are now *shift invariant*, so that many of the familiar LTI notions can be re-used almost verbatim.

The advantages come at a cost: the infinite dimensionality of certain input and output signal spaces. Yet this difficulty turns out not to be crucial and can be alleviated by exploiting the structure of the resulting operator-valued mappings.

4. Lifting in Frequency Domain

With the regained time invariance, we can apply frequency domain methods to lifted h-periodic systems and signals.

4.1. z- and Fourier transforms

Naturally, the z- and Fourier transforms of a lifted signal $\breve{f}$ are defined with respect to the discrete time index.

Definition 4.1. The *(lifted) z-transform* $\mathfrak{Z}\{\breve{f}\}$ of a lifted signal $\breve{f}$ is defined as

$$\mathfrak{Z}\{\breve{f}\} = \breve{f}(z) := \sum_{k \in \mathbb{Z}} \breve{f}[k] z^{-k}, \qquad (14)$$

for all $z \in \mathbb{C}$ for which the series converges. $\qquad \triangledown$

Definition 4.2. The *(lifted) Fourier transform* $\mathfrak{F}\{\breve{f}\}$ of a lifted $\breve{f}$ is defined as

$$\mathfrak{F}\{\breve{f}\} = \breve{f}(\mathrm{e}^{\mathrm{i}\theta}) := \sum_{k \in \mathbb{Z}} \breve{f}[k] \mathrm{e}^{-\mathrm{i}\theta k},$$

where $\theta \in [-\pi, \pi]$ is the frequency. $\qquad \triangledown$

Note that for each $z \in \mathbb{C}$ and $\theta \in [-\pi, \pi]$ the z- and Fourier transforms (if they exist) are still functions of intersample time $\tau \in [0, h)$. This is reflected by the notation $\breve{f}(z; \tau)$ and $\breve{f}(\mathrm{e}^{\mathrm{i}\theta}; \tau)$, which shall be used when these dependences are important. The lifted z-transform equals the *modified* or *advanced* z-transform as introduced by [19], but the intent is entirely different.

The following result, which to the best of our knowledge has not explicitly appeared in the literature yet, plays a key role in the subsequent analysis. It is a version of the Poisson Summation Formula, but then one that looses no information about the analog signal. Indeed the point of lifting is to maintain intersample behavior, also in frequency domain.

Theorem 4.3 (Key lifting formula). Let f be an analog signal such that $f(t)\mathrm{e}^{-s_0 t} \in L^2(\mathbb{R})$ for some $s_0 \in \mathbb{C}$. Then

$$\breve{f}(z; \tau) = \frac{1}{h} \sum_{k \in \mathbb{Z}} F(s_k) \mathrm{e}^{s_k \tau} \qquad (15)$$

for all $\tau \in [0, h)$, where $z := \mathrm{e}^{s_0 h}$ and $s_k := s_0 + \mathrm{i}2\omega_{\mathrm{N}} k$. $\qquad \triangledown$

Proof. The (regular bilateral) Laplace transform of f is

$$\begin{aligned}
F(s) &= \int_{-\infty}^{\infty} f(t)\mathrm{e}^{-st} \mathrm{d}t \\
&= \sum_{k \in \mathbb{Z}} \int_0^h f(\tau + kh)\mathrm{e}^{-s(\tau + kh)} \mathrm{d}\tau \\
&= \int_0^h \sum_{k \in \mathbb{Z}} \breve{f}[k](\tau)\mathrm{e}^{-skh} \, \mathrm{e}^{-s\tau} \mathrm{d}\tau \\
&= \int_0^h \breve{f}(\mathrm{e}^{sh}; \tau)\mathrm{e}^{-s\tau} \mathrm{d}\tau.
\end{aligned}$$

Equality (15) now follows by noting that

$$\frac{1}{h}F(s_k) = \frac{1}{h} \int_0^h \big[\breve{f}(\mathrm{e}^{s_k h}; \tau)\mathrm{e}^{-s_0 \tau}\big]\mathrm{e}^{-\mathrm{i}2\omega_{\mathrm{N}} k \tau} \mathrm{d}\tau$$

is the kth Fourier series coefficient of $\breve{f}(\mathrm{e}^{s_i h}; \tau)\mathrm{e}^{-s_0 \tau}$ (mind that $\mathrm{e}^{s_k h} = \mathrm{e}^{s_0 h} =: z$). By Plancherel's theorem, the assumption that $f(t)\mathrm{e}^{-s_0 t} \in L^2(\mathbb{R})$ assures that (15) holds in L^2-sense and therefore holds pointwise almost everywhere. $\qquad \blacksquare$

A particular case of this formula for $s_0 = \mathrm{i}\theta/h$ says that there is a bijection from the lifted Fourier transform $\breve{f}(\mathrm{e}^{\mathrm{i}\theta})$ and the classical Fourier transform $F(\mathrm{i}\omega)$:

$$F(\mathrm{i}\omega_k) = \int_0^h \breve{f}(\mathrm{e}^{\mathrm{i}\theta}; \tau)\mathrm{e}^{-\mathrm{i}\omega_k \tau} \mathrm{d}\tau, \qquad (16a)$$

$$\breve{f}(\mathrm{e}^{\mathrm{i}\theta}; \tau) = \frac{1}{h} \sum_{k \in \mathbb{Z}} F(\mathrm{i}\omega_k)\mathrm{e}^{\mathrm{i}\omega_k \tau}, \qquad (16b)$$

8

for any square integrable f, where

$$\omega_k := \frac{\theta + 2\pi k}{h} = \frac{\theta}{h} + 2\omega_\mathrm{N} k \qquad (17)$$

are aliased frequencies.

Remark 4.4. A special case of Equality (16b) corresponding to $\tau = 0$ yields the classical formula connecting Fourier transforms of an analog signal (provided it is continuous and satisfies some other mild conditions [5]) and its sampled version: $\mathfrak{F}\{\bar{f}\} = \frac{1}{h}\sum_{i\in\mathbb{Z}} F(\mathrm{i}\omega_i)$. We believe that the derivation via the use of lifting and (16b) is somewhat cleaner and more intuitive than the conventional impulse-train modulation [33] or "reverse engineering" [2] arguments. $\qquad \triangledown$

Example 4.5. To illustrate a use of formula (16b), let $f(t) = \frac{1}{h}\mathrm{sinc}_h(t)$. Since $F(\mathrm{i}\omega) = \mathbb{1}_{[-\omega_\mathrm{N},\omega_\mathrm{N}]}(\omega)$, equality (16b) yields the lifted Fourier transform $\check{f}(\mathrm{e}^{\mathrm{i}\theta}; \tau) = \frac{1}{h}\mathrm{e}^{\mathrm{i}\theta\tau/h}$ for $\theta \in [-\pi, \pi]$ and $\tau \in [0, h)$. $\qquad \triangledown$

Example 4.6. The Fourier transform of $f(t) = \frac{1}{h}\mathrm{sinc}_h^2(t)$ is the "tent" $F(\mathrm{i}\omega) = (1 - |\omega|/(2\omega_\mathrm{N}))\mathbb{1}_{[-2\omega_\mathrm{N},2\omega_\mathrm{N}]}(\omega)$. Then $\check{f}(\mathrm{e}^{\mathrm{i}\theta}; \tau) = \frac{1}{h}\mathrm{e}^{\mathrm{i}\theta\tau/h}\left(1 - \frac{|\theta|}{2\pi} + \frac{|\theta|}{2\pi}\mathrm{e}^{-\mathrm{i}2\omega_\mathrm{N}\tau\,\mathrm{sign}\,\theta}\right)$ for $\theta \in [-\pi, \pi]$ and $\tau \in [0, h)$. $\qquad \triangledown$
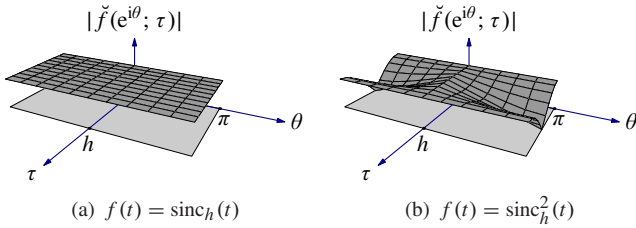
Figure 7: Amplitude $|\check{f}(\mathrm{e}^{\mathrm{i}\theta}; \tau)|$ vs. θ and τ

Fig. 7 depicts the amplitude $|\check{f}(\mathrm{e}^{\mathrm{i}\theta}; \tau)|$ as a function of $\theta \in [-\pi, \pi]$ and $\tau \in [0, h)$ for the functions considered in the above two examples. Such amplitude plots demonstrate how the amplitude spectrum of the sampled signal $f(kh + \tau)$ changes with time offset τ (for the sinc_h it does not change).

4.2. Transfer Function & Frequency Response

It is well-known that convolution (dynamic) systems become algebraic (static) if considered in the transform domain. This is also true for lifted systems as we shall see with the introduction of the lifted transfer function formalism.

The *transfer function* $\check{G}(z)$ of the lifted system (10) is formally defined as the z-transform of its impulse response

$$\check{G}(z) := \sum_{i\in\mathbb{Z}} \check{G}[i]\,z^{-i}. \qquad (18)$$

A standard index change in (10) then shows [3] that the lifted z-transforms of input and output satisfy the familiar

$$\check{u}(z) = \check{G}(z)\check{y}(z). \qquad (19)$$

It is worth recalling that the lifted impulse response $\check{G}[k]$ for each $k \in \mathbb{Z}$ is an integral operator of the form (11). Hence, so is the lifted transfer function $\check{G}(z)$. It can be shown that the "multiplication" in (19) should be understood as

$$\check{u}(z; \tau) = \int_0^h \check{g}(z; \tau, \sigma)\check{y}(z; \sigma)\mathrm{d}\sigma, \quad \tau \in [0, h), \qquad (20)$$

where $\check{g}(z; \tau, \sigma)$ is the lifted z-transform of the impulse response kernel $g(t, s)$ of $\mathcal{G}$ with respect to its first variable[2],

$$\check{g}(z; \tau, \sigma) := \sum_{k\in\mathbb{Z}} g(\tau + kh, \sigma)z^{-k}. \qquad (21)$$

Again we want to make the point here that (19) is more in the spirit of lifting than the gritty details of (20) and (21).

Example 4.7. In Example 3.3 we showed that the impulse response $\check{G}[k]$ of the cascade of the ideal sampler and the zero-order hold is such that $(\check{G}[0]\check{y})(\tau) = \check{y}(0)$ and with all other $\check{G}[k]$ zero. Therefore, the transfer function of this cascade in the lifted domain acts as $\check{G}(z)\check{y}(z) = \check{y}(z; 0)$. $\qquad \triangledown$

"Semi-lifted" elements, such as lifted sampler and hold, can be described in terms of their lifted transfer functions in the same way. The only difference from the case considered above is that either output or input space is now finite dimensional. Thus, the transfer function $\acute{S}(z)$ of the lifted sampler $\acute{\mathcal{S}}$ in (12) is a linear functional from $\{[0, h) \to \mathbb{C}^{n_y}\}$ to $\mathbb{C}^{n_{\bar{y}}}$ of the form[3]

$$\bar{y}(z) = \acute{S}(z)\check{y}(z): \quad \bar{y}(z) = \int_0^h \check{\psi}(z; -\sigma)\check{y}(z; \sigma)\mathrm{d}\sigma \qquad (22)$$

for each $z \in \mathbb{C}$ where it is defined. Here $\check{\psi}(z)$ is the lifted z-transform of the sampling function $\psi(t)$. Similarly, the transfer function $\grave{H}(z)$ of the lifted hold $\grave{\mathcal{H}}$ in (13) is an operator from $\mathbb{C}^{n_{\bar{u}}}$ to $\{[0, h) \to \mathbb{C}^{n_u}\}$ of the form

$$\check{u}(z) = \grave{H}(z)\bar{u}(z): \quad \check{u}(z; \tau) = \check{\phi}(z; \tau)\bar{u}(z) \qquad (23)$$

for each $z \in \mathbb{C}$ where it is defined. Here, $\check{\phi}(z)$ is the lifted z-transform of the hold function $\phi(t)$.

Example 4.8. Consider again the predictive first-order hold $\mathcal{H}_{\mathrm{FOH}}$ studied in Example 3.4. Inspecting the formulae in this example, it is readily seen that

$$\check{\phi}_{\mathrm{FOH}}(z; \cdot) = \check{\phi}_{\mathrm{FOH}}[-1]\,z + \check{\phi}_{\mathrm{FOH}}[0] = \underset{0 \qquad h}{\diagup\!\!\!|}\,z + \underset{0 \qquad h}{|\!\!\!\diagdown}.$$

The "static gain" of this transfer function is $\grave{H}_{\mathrm{FOH}}(1; \tau) \equiv 1$, which agrees with our understanding of this hold. $\qquad \triangledown$

Obviously, $\check{G}(\mathrm{e}^{\mathrm{i}\theta})$ will be referred to as the *(lifted) frequency response* and the transfer kernel $\check{g}(\mathrm{e}^{\mathrm{i}\theta})$ as its *frequency response kernel*. It maintains the familiar interpretation in the sense that for any fixed $\theta \in [-\pi, \pi]$ the response $\check{u} = \check{\mathcal{G}}\check{y}$ to a *(lifted)*

---

[2]Alternatively, the "$1/z$-transform" with respect to its second variable.

[3]Strictly speaking, it should be $z^{-1}\check{\psi}(z; h - \sigma)$, rather than $\check{\psi}(z; -\sigma)$ (these two are equivalent), because the intersample time variable lies in $[0, h]$. We, however, prefer to trade notational rigor for simplicity in this case.

harmonic function $\check{y}[k] = e^{i\theta k}\check{w}$ (with $\check{w} : [0, h) \to \mathbb{C}^{n_w}$) if it exists, is again harmonic [53], $\check{u}[k] = e^{i\theta k}G(e^{i\theta})\check{w}$. The absolute value $|\check{y}[k](\tau)|$ of a harmonic input does not depend on k and neither does the output. As shown in [53], if the magnitude of harmonic $\check{y}[k]$ (for whatever k) is measured in $L^2[0, h)$-sense then the maximal possible magnitude gain (power gain) at frequency θ equals the largest singular value of $G(e^{i\theta})$ as defined later on in this part, (29). This is very similar to the interpretation of the conventional frequency response of discrete-time systems.

Example 4.9. Consider the sinc-sampler $\mathcal{S}_{\text{sinc}}$ (see §2.2.1) having the sampling function $\psi_{\text{sinc}}(t) = \frac{1}{h}\text{sinc}_h(t)$. Example 4.5 then yields that the frequency response kernel of $\check{S}_{\text{sinc}}(e^{i\theta})$ is $\check{\psi}_{\text{sinc}}(e^{i\theta}; -\sigma) = \frac{1}{h}e^{-i\theta\sigma/h}$. $\quad\triangledown$

Example 4.10. The hold function of the sinc-hold $\mathcal{H}_{\text{sinc}}$ (see §2.2.2) is $\phi_{\text{sinc}}(t) = \text{sinc}_h(t)$. Therefore, the frequency response kernel of $\check{H}_{\text{sinc}}(e^{i\theta})$ is $\check{\phi}_{\text{sinc}}(e^{i\theta}; \tau) = e^{i\theta\tau/h}$. $\quad\triangledown$

5. Spaces and Norms

This section reviews the notions of signal and system norms in the lifted domain. Most results presented below are either known or quite straightforward extensions of known results that can be found in, e.g., [8], [10, Ch. 2], [9, Appendix A].

5.1. Signal Spaces and Norms

As the lifting transformation is merely a different viewpoint of analog signals, we can take it to be norm preserving. Concretely, the L^2 signal norm translates to the lifted domain as follows:

$$\|f\|_2^2 = \int_{-\infty}^{\infty} |f(t)|^2 \mathrm{d}t = \sum_{k\in\mathbb{Z}} \int_0^h |\check{f}[k](\tau)|^2 \mathrm{d}\tau$$
$$= \sum_{k\in\mathbb{Z}} \|\check{f}[k]\|_{\mathbb{L}}^2 =: \|\check{f}\|_2^2, \quad\quad (24)$$

where $\mathbb{L} := L^2[0, h)$. By analogy with the standard $\ell^2_{\mathbb{C}}(\mathbb{Z})$ space, we call the quantity defined by (24) the ℓ^2-norm of $\check{f}$ (this is a norm, just because so is the L^2-norm in continuous time) and denote the set of all lifted signals having a bounded ℓ^2-norm as $\ell^2_{\mathbb{L}}(\mathbb{Z})$, which is a Hilbert space with the obvious inner product. Thus lifting by construction is an isometric isomorphism between $L^2_{\mathbb{C}}(\mathbb{R})$ and $\ell^2_{\mathbb{L}}(\mathbb{Z})$.

Remark 5.1. All signals in the lifted SR scheme in Fig. 6 are now measured by various ℓ^2-norms. The only difference between these norms is in their "subscript spaces": $\mathbb{C}$ or $\mathbb{L}$. This difference, however, is peripheral, so we hereafter drop the subscript from the notation for ℓ^2 and related spaces. $\quad\triangledown$

With a slight abuse of notation we use $\ell^2(\mathbb{Z}_l^+)$ and $\ell^2(\mathbb{Z}_l^-)$ to denote the subspaces of $\ell^2(\mathbb{Z})$ consisting of signals that are zero in $\mathbb{Z}_l^-$ and $\mathbb{Z}_l^+$, respectively. Clearly, $\ell^2(\mathbb{Z}) = \ell^2(\mathbb{Z}_l^+) \oplus \ell^2(\mathbb{Z}_l^-)$ for every integer l. We shall need these subspaces later on to discuss causality.

We also need corresponding frequency-domain spaces. Let $\mathbb{K}$ stand for either $\mathbb{C}^n$ or $\mathbb{L}$, depending on whether our signal is a plain discrete-time signal or a lifted one. The Hilbert space $L^2(\mathbb{T})$ is the set of functions $\tilde{f}(z) : \mathbb{T} \to \mathbb{K}$, for which[4]

$$\|\tilde{f}\|_2 := \left(\frac{1}{2\pi}\int_{-\pi}^{\pi} \|\tilde{f}(e^{i\theta})\|_{\mathbb{K}}^2 \mathrm{d}\theta\right)^{1/2} < \infty.$$

The Hardy space H^2 is the set of functions $\tilde{f}(z) : \mathbb{C} \setminus \bar{\mathbb{D}} \to \mathbb{K}$ which are analytic and satisfy

$$\|\tilde{f}\|_{H^2} := \sup_{\rho>1}\left(\frac{1}{2\pi}\int_{-\pi}^{\pi} \|\tilde{f}(\rho e^{i\theta})\|_{\mathbb{K}}^2 \mathrm{d}\theta\right)^{1/2} < \infty.$$

The domain of functions in H^2 can be extended to $\mathbb{T}$ and the result is a closed subspace of $L^2(\mathbb{T})$ with $\|\tilde{f}\|_{H^2} = \|\tilde{f}\|_2$. The orthogonal complement of H^2 in $L^2(\mathbb{T})$ is denoted by $H_{\perp}^2$ and is comprised of analytic and bounded functions $\tilde{f}(z) : \mathbb{D} \to \mathbb{K}$ such that $\|\tilde{f}\|_2 < \infty$. Finally, by $z^l H^2$ we denote the space of functions $\tilde{f}(z) : \mathbb{C} \setminus \bar{\mathbb{D}} \to \mathbb{K}$ such that $z^{-l}\check{f}(z) \in H^2$.

The Parseval's identity, which is instrumental in converting energy-based optimization problems to the frequency domain, also extends to general ℓ^2 spaces. Namely, for any $\tilde{f} \in \ell^2(\mathbb{Z})$ we have that $\mathfrak{F}\{\tilde{f}\} \in L^2(\mathbb{T})$ and

$$\|\tilde{f}\|_2 = \|\mathfrak{F}\{\tilde{f}\}\|_2.$$

The Fourier transform is thus an isometric isomorphism between $\ell^2(\mathbb{Z})$ and $L^2(\mathbb{T})$. Similarly the z-transform is an isometric isomorphism between $\ell^2(\mathbb{Z}_l^+)$ and $z^l H^2$ for any l.

Example 5.2. Consider $f(t) = \frac{1}{h}\text{sinc}_h(t)$. By Example 4.5, $\|f\|_2$ can also be computed via the $L^2(\mathbb{T})$-norm of its lifted Fourier transform: $\|\check{f}\|_2^2 = \frac{1}{2\pi}\int_{-\pi}^{\pi} \|\frac{1}{h}e^{i\theta\tau/h}\|_{\mathbb{L}}^2 \mathrm{d}\theta = \frac{1}{2\pi}\int_{-\pi}^{\pi} \frac{1}{h}\mathrm{d}\theta = \frac{1}{h}$, which agrees with the direct computation of $\|f\|_2^2$. $\quad\triangledown$

5.2. Adjoint Systems and Conjugate Transfer Functions

Since both lifting and Fourier transformation preserve inner products, the adjoint of an operator is equivalent in all domains, i.e., the lifting of the adjoint operator is the adjoint of the lifted operator, and likewise for the Fourier transformed operator. It is well known that the kernel of the adjoint of $\mathcal{G}$, given in (6), is

$$g^{\sim}(t, s) := [g(s, t)]^* \quad\quad (25)$$

with * here denoting complex conjugate transpose. The *conjugate* operator $^{\sim}$ defined by (25) not only takes the complex conjugate transpose of the matrix but also interchanges the two time parameters. It is more generally defined for frequency depending functions as

$$\check{g}^{\sim}(z; \tau, \sigma) := [\check{g}(1/\bar{z}; \sigma, \tau)]^*$$

---

[4]We use the same norm symbol for several time- and frequency-domain norms. Context determines which is intended.

for then the z-transform of the conjugate is the conjugate of the z-transform (with respect to the first variable):

$$
\begin{aligned}
\mathfrak{Z}\{g^\sim(\tau,\sigma)\} &= \sum_{k\in\mathbb{Z}} g^\sim(\tau+kh,\sigma)z^{-k} \\
&= \sum_{m=-k} [g(\sigma,\tau-mh)\overline{z}^m]^* \\
&= \sum_{m\in\mathbb{Z}} [g(\sigma+mh,\tau)(1/\overline{z})^{-m}]^* = \breve{g}^\sim(z;\tau,\sigma).
\end{aligned}
$$

According to (20), (21), and the above, $\breve{g}^\sim(z;\tau,\sigma)$ hence is the kernel of the transfer function of the adjoint system $\mathcal{G}^*$. We denote this transfer function as $\breve{G}^\sim(z)$,

$$
\breve{y}(z) = \breve{G}^\sim(z)\breve{u}(z): \quad \breve{y}(z;\tau) = \int_0^h \breve{g}^\sim(z;\tau,\sigma)\breve{u}(z;\sigma)\mathrm{d}\sigma.
$$

It is readily seen that for $z = \mathrm{e}^{\mathrm{i}\theta}$ the conjugate $\breve{G}^\sim(\mathrm{e}^{\mathrm{i}\theta})$ is the adjoint of $\breve{G}(\mathrm{e}^{\mathrm{i}\theta})$ with respect to $\mathbb{L}$:

$$
\langle \breve{u}(\mathrm{e}^{\mathrm{i}\theta}), \breve{G}(\mathrm{e}^{\mathrm{i}\theta})\breve{y}(\mathrm{e}^{\mathrm{i}\theta})\rangle_{\mathbb{L}} = \langle \breve{G}^\sim(\mathrm{e}^{\mathrm{i}\theta})\breve{u}(\mathrm{e}^{\mathrm{i}\theta}), \breve{y}(\mathrm{e}^{\mathrm{i}\theta})\rangle_{\mathbb{L}}.
$$

That is, the lifted transfer function of the adjoint equals the adjoint of the lifted transfer function.

Now, the adjoint of the sampler in (3) can be derived via

$$
\begin{aligned}
\langle \mathcal{S}y, \bar{u}\rangle_{\ell^2} &= \sum_{i\in\mathbb{Z}} \bar{u}^*[i] \int_{-\infty}^{\infty} \psi(ih-s)y(s)\mathrm{d}s \\
&= \int_{-\infty}^{\infty} \left(\sum_{i\in\mathbb{Z}} [\psi(ih-s)]^*\bar{u}[i]\right)^* y(s)\mathrm{d}s \\
&= \langle y, \mathcal{S}^*\bar{u}\rangle_{L^2}.
\end{aligned}
$$

Thus, the adjoint of $\mathcal{S}$ with a sampling function $\psi(t)$ is a $\mathcal{H}$ with the hold function $\phi(t) = [\psi(-t)]^* =: \psi^\sim(t)$ (the latter is just an LTI version of (25)). This prompts a duality between the A/D and D/A conversions and also implies that the adjoint of $\mathcal{H}$ with $\phi(t)$ is $\mathcal{S}$ with $\psi(t) = \phi^\sim(t)$. The conjugate transfer function of $\acute{S}(z)$, $\acute{S}^\sim(z)$, is the following lifted hold:

$$
\breve{y}(z) = \acute{S}^\sim(z)\bar{u}(z): \quad \breve{y}(z;\tau) = \breve{\psi}^\sim(z;\tau)\bar{u}(z),
$$

with $\breve{\psi}^\sim(z;\tau) := [\breve{\psi}(1/\overline{z};-\tau)]^*$. The conjugate transfer function of $\grave{H}(z)$ is

$$
\bar{y}(z) = \grave{H}^\sim(z)\breve{u}(z): \quad \bar{y}(z) = \int_0^h \breve{\phi}^\sim(z;-\sigma)\breve{u}(z)\sigma\,\mathrm{d}\sigma,
$$

which is a lifted sampler.

The following result will be used in the next parts:

Proposition 5.3. Let $\mathcal{S}$ be a sampler, the sampling function $\psi(t)$ of which is such that $\psi(t)\mathrm{e}^{-s_0 t} \in L^2(\mathbb{R})$ for some $s_0 \in \mathbb{C}$. Then at $z = \mathrm{e}^{s_0 h}$ we have that

$$
\acute{S}(z)\acute{S}^\sim(z) = \int_0^h \breve{\psi}(z;\tau)[\breve{\psi}(1/\overline{z};\tau)]^*\mathrm{d}\tau \tag{26a}
$$

$$
= \frac{1}{h}\sum_{k\in\mathbb{Z}} \Psi(s_k)\Psi^\sim(s_k), \tag{26b}
$$

where $s_k = s_0 + \mathrm{i}2\omega_{\mathrm{N}}k$ and $\Psi(s)$ is the bilateral Laplace transform of ψ. $\qquad\triangledown$

Proof. Equality (26a) follows by routine substitution. To derive (26b), denote the integral in (26a) by M and use (16b):

$$
\begin{aligned}
M &= \frac{1}{h^2}\int_0^h \sum_{k\in\mathbb{Z}} \Psi(s_k)\mathrm{e}^{s_k\tau}\left[\sum_{i\in\mathbb{Z}} \Psi(s_i)\mathrm{e}^{s_i\tau}\right]^\sim \mathrm{d}\tau \\
&= \frac{1}{h^2}\sum_{k\in\mathbb{Z}} \Psi(s_k)\sum_{i\in\mathbb{Z}} \Psi^\sim(s_i)\int_0^h \mathrm{e}^{\mathrm{i}2\omega_{\mathrm{N}}(k-i)\tau}\mathrm{d}\tau.
\end{aligned}
$$

The result now follows by $\int_0^h \mathrm{e}^{\mathrm{i}2\omega_{\mathrm{N}}(k-i)\tau}\mathrm{d}\tau = h\,\bar{\delta}[k-i]$. $\qquad\blacksquare$

It is an immediate corollary of this result that if $\psi(t)$ is scalar, then $\acute{S}(\mathrm{e}^{\mathrm{i}\theta})\acute{S}^\sim(\mathrm{e}^{\mathrm{i}\theta}) = \|\breve{\psi}(\mathrm{e}^{\mathrm{i}\theta})\|_{\mathbb{L}}^2 = \frac{1}{h}\sum_{k\in\mathbb{Z}}|\Psi(\mathrm{i}\omega_k)|^2$, where ω_k are defined by (17). Also, by duality we have:

Proposition 5.4. Let $\mathcal{H}$ be a hold, the hold function $\phi(t)$ of which is such that $\phi(t)\mathrm{e}^{-s_0 t} \in L^2(\mathbb{R})$ for some $s_0 \in \mathbb{C}$. Then at $z = \mathrm{e}^{s_0 h}$ we have that

$$
\grave{H}^\sim(z)\grave{H}(z) = \int_0^h [\breve{\phi}(1/\overline{z};\tau)]^*\breve{\phi}(z;\tau)\mathrm{d}\tau \tag{27a}
$$

$$
= \frac{1}{h}\sum_{k\in\mathbb{Z}} \Phi^\sim(s_k)\Phi(s_k) \tag{27b}
$$

where $s_k = s_0 + \mathrm{i}2\omega_{\mathrm{N}}k$ and $\Phi(s)$ is the bilateral Laplace transform of ϕ. $\qquad\triangledown$

5.3. L^∞ System Norm

The L^∞ norm (cf. (2)) of a lifted transfer function $\tilde{G}(z): \mathbb{K}_{\mathrm{i}} \to \mathbb{K}_{\mathrm{o}}$ is defined as

$$
\|\tilde{G}\|_\infty := \operatorname*{ess\,sup}_{\theta\in[-\pi,\pi]} \sigma_{\max}[\tilde{G}(\mathrm{e}^{\mathrm{i}\theta})] < \infty, \tag{28}
$$

where the (operator) maximal singular value $\sigma_{\max}$ equals

$$
\sigma_{\max}[\tilde{G}(\mathrm{e}^{\mathrm{i}\theta})] = \sup_{\tilde{y}\in\mathbb{K}_{\mathrm{i}},\|\tilde{y}\|_{\mathbb{K}_{\mathrm{i}}}=1} \|\tilde{G}(\mathrm{e}^{\mathrm{i}\theta})\tilde{y}\|_{\mathbb{K}_{\mathrm{o}}}, \tag{29}
$$

i.e., (29) is the induced norm of $\tilde{G}(\mathrm{e}^{\mathrm{i}\theta})$. If $\tilde{G}(z)$ is the transfer function of an LTI system $\tilde{\mathcal{G}}$, we also refer to (28) as the L^∞-norm of the system and denote it as $\|\tilde{\mathcal{G}}\|_\infty$. For given $\mathbb{K}_{\mathrm{i}}$ and $\mathbb{K}_{\mathrm{o}}$ the vector space of all transfer functions with finite L^∞-norm is represented with the same symbol L^∞, so

$$
L^\infty = \{\tilde{G}:\mathbb{T}\to(\mathbb{K}_{\mathrm{i}}\to\mathbb{K}_{\mathrm{o}}) \mid \|\tilde{G}\|_\infty < \infty\}.
$$

By the arguments of [3], it can be shown that $\|\breve{\mathcal{G}}\|_\infty$ equals the $L^2(\mathbb{R})$-induced norm of its original, $\mathcal{G}$, i.e., $\|\breve{\mathcal{G}}\|_\infty = \sup_{\|y\|_2=1}\|\mathcal{G}y\|_2$. Its square, $\|\breve{\mathcal{G}}\|_\infty^2$, is therefore the maximal energy gain of the system and also equals the maximal power gain. Likewise, $\|\acute{\mathcal{S}}\|_\infty$ and $\|\grave{\mathcal{H}}\|_\infty$ equal $L^2(\mathbb{R}) \to \ell^2(\mathbb{Z})$ and $\ell^2(\mathbb{Z}) \to L^2(\mathbb{R})$ induced norms of $\mathcal{S}$ and $\mathcal{H}$, respectively.

Example 5.5. Consider the HSP $\mathcal{H}_{\mathrm{ZOH}}\mathcal{S}_\epsilon$, where $\mathcal{S}_\epsilon$ is the "almost ideal" sampler with $\psi_\epsilon(t) = \frac{1}{\epsilon}\mathbb{1}_{[0,\epsilon]}(t)$ for $0 < \epsilon < h$ (the smaller ϵ is, the more this sampler behaves like the ideal sampler). Because $\psi_\epsilon(t)$ is scalar, by Proposition 5.3 (this can also be seen via the Riesz-Fréchet theorem) we have that

$$
\|\acute{\mathcal{S}}_\epsilon\|_\infty = \sup_{\theta\in[-\pi,\pi]} \|\breve{\psi}_\epsilon(\mathrm{e}^{\mathrm{i}\theta})\|_{\mathbb{L}} = \sup_{\theta\in[-\pi,\pi]} \|\tfrac{1}{\epsilon}\mathbb{1}_{[0,\epsilon]}\|_{\mathbb{L}} = \frac{1}{\sqrt{\epsilon}}.
$$

In fact, the maximizing input having the unity norm for this system is $y_{\max}(t) = 1/\sqrt{\epsilon}\, \mathbb{1}_{[h-\epsilon,h]}(t)$ and is unique (modulo sign and h-shifts). Regarding $\mathcal{H}_{\text{ZOH}}$, it is readily seen that $\|u\|_2 = \sqrt{h}\|\bar{u}\|_2$ for every $\bar{u} \in \ell^2(\mathbb{Z})$. Thus, $\|\grave{\mathcal{H}}_{\text{ZOH}}\|_\infty = \sqrt{h}$ and any input $\bar{u}$ is maximizing. Hence, $y_{\max}$ actually maximizes the energy gain of the overall HSP $\grave{\mathcal{H}}_{\text{ZOH}}\acute{\mathcal{S}}_\epsilon$ and we have:

$$\|\grave{\mathcal{H}}_{\text{ZOH}}\acute{\mathcal{S}}_\epsilon\|_\infty = \sqrt{h}\,\|\acute{\mathcal{S}}_\epsilon\|_\infty = \sqrt{h/\epsilon}.$$

It becomes unbounded as $\epsilon \downarrow 0$, like in the L^2 case. $\triangledown$

Another space we need is the Hardy space H^∞. It is defined as the set of transfer functions $\tilde{G}(z)$, which are analytic for $z \in \mathbb{C} \setminus \bar{\mathbb{D}}$ and satisfy

$$\|\tilde{G}\|_{H^\infty} := \operatorname*{ess\,sup}_{z \in \mathbb{C}\setminus\mathbb{D}} \sigma_{\max}[\tilde{G}(z)] < \infty.$$

Like in the case with the H^2 signal space, H^∞ operators can be extended to $z \in \mathbb{T}$, resulting in a closed subspace of L^∞ with $\|\tilde{G}\|_{H^\infty} = \|\tilde{G}\|_\infty$. By $z^l H^\infty$ we then denote the subspace of L^∞ consisting of operators $\tilde{G}(z)$ such that $z^{-l}\tilde{G}(z) \in H^\infty$. Loosely speaking, H^∞ is the space of transfer functions, which are analytic and bounded in $\mathbb{C} \setminus \mathbb{D}$, whereas $z^l H^\infty$ is the space of analytic transfer functions with relaxed (if $l > 0$) or tightened (if $l < 0$) boundedness in $|z| \to \infty$.

5.4. L^2 System Norm

The L^2 norm (cf. (1)) of lifted (or semi-lifted) transfer functions $\tilde{G}(z) : \mathbb{K}_i \to \mathbb{K}_o$ is defined as

$$\|\tilde{G}\|_2 := \left(\frac{1}{2\pi h}\int_{-\pi}^{\pi}\|\tilde{G}(e^{i\theta})\|_{\text{HS}}^2\, d\theta\right)^{1/2} < \infty \qquad (30)$$

(the scaling factor will become clear soon, it is not present in the standard discrete case). Here $\|\cdot\|_{\text{HS}}$ is the Hilbert-Schmidt operator norm, which can in general be calculated as

$$\|\tilde{G}(e^{i\theta})\|_{\text{HS}}^2 = \operatorname{tr}[\tilde{G}(e^{i\theta})\tilde{G}^\sim(e^{i\theta})] = \operatorname{tr}[\tilde{G}^\sim(e^{i\theta})\tilde{G}(e^{i\theta})]$$
$$= \sum_i \sigma_i^2[\tilde{G}(e^{i\theta})],$$

with $\sigma_i[\cdot]$ the ith singular value. For integral operators $\mathbb{L} \to \mathbb{L}$ as in (20) we have that

$$\|\breve{G}(e^{i\theta})\|_{\text{HS}}^2 = \int_0^h \int_0^h \|\breve{g}(e^{i\theta};\tau,\sigma)\|_{\text{F}}^2\, d\tau\, d\sigma.$$

For semi-lifted operators, like $\acute{S}(z)$ and $\grave{H}(z)$, the calculations of the Hilbert-Schmidt norm reduce to the computation of the matrix trace (cf. Propositions 5.3 and 5.4). If $\tilde{G}(z)$ is the transfer function a (semi-) lifted system $\tilde{\mathcal{G}}$ we also refer to (30) as the L^2-norm of the system and denote it as $\|\tilde{\mathcal{G}}\|_2$. The vector space of systems with finite L^2 system norm (30) is represented simply as L^2,

$$L^2 = \{\tilde{G} : \mathbb{T} \to (\mathbb{K}_i \to \mathbb{K}_o) \mid \|\tilde{G}\|_2 < \infty\}.$$

In contrast to the ordinary L^2 norm for LTI-systems, the L^2 system norm is not equivalent to a signal norm, even though we use the same notation, $\|\cdot\|_2$ and L^2. Neither of the two system spaces L^∞ and L^2 is a subset of the other. However, if the rank of the transfer function is uniformly bounded then being in L^∞ implies being in L^2.

Proposition 5.6. Let $\tilde{G} \in L^\infty$ be such that rank $\tilde{G}(e^{i\theta}) \leq r$ for almost all $\theta \in [-\pi, \pi]$ and some $r \in \mathbb{N}$. Then $\tilde{G} \in L^2$.

Proof. Then (30) and (28) imply $\|\tilde{G}\|_2^2 \leq r\|\tilde{G}\|_\infty/h$. ∎

In particular every hold and sampler that is in L^∞ is necessarily in L^2.

The L^2 system norm defined by (30) retains familiar deterministic and stochastic interpretations. For SISO h-periodic analog systems, for instance, the norm satisfies [4]

$$\|\breve{G}\|_2^2 = \frac{1}{h}\int_0^h \|\mathcal{G}\,\delta(\cdot - \sigma)\|_{L^2(\mathbb{R})}^2\, d\sigma.$$

That is, $\|\breve{G}\|_2^2$ is the average energy of the output where the average is taken over all delta functions applied at $\sigma \in [0, h)$. For $h \downarrow 0$ this reduces to the classic LTI result. Also, stochastic interpretations are maintained: $\|\breve{G}\|_2^2$ equals the over time averaged sum of variances (power) of the output elements if the system is driven by standard white noise [4].

Example 5.7. Consider again the HSP $\mathcal{H}_{\text{ZOH}}\mathcal{S}_\epsilon$ studied in Example 5.5. As the input y to this system ranges over the delta functions applied at $\sigma \in [0, h)$ the output of the sampler ranges over $\bar{y} \equiv 0$ for $\sigma \in [0, h - \epsilon]$ and $\bar{y}[i] = \frac{1}{\epsilon}\delta[i - 1]$ for $\sigma \in [h - \epsilon, h)$. Hence for $\sigma \in [0, h - \epsilon]$ the output energy of the hold is zero while for $\sigma \in [h - \epsilon, h)$ the output energy is $\|\frac{1}{\epsilon}\mathbb{1}_{[h,2h]}\|_2^2 = \frac{h}{\epsilon^2}$. The average energy therefore equals

$$\|\grave{\mathcal{H}}_{\text{ZOH}}\acute{\mathcal{S}}_\epsilon\|_2^2 = \frac{1}{h}\int_{h-\epsilon}^h \frac{h}{\epsilon^2}\, d\tau = \frac{1}{\epsilon}.$$

The cascade of the *ideal* sampler and the zero-order hold consequently has infinite L^2 system norm.

When driven by zero mean unit intensity white noise $\breve{y}$, the samples $\bar{u} = \bar{y} = \acute{\mathcal{S}}_\epsilon \breve{y}$ for this sampler are independent and are stationary with variance $\frac{1}{\epsilon}$. The "Manhattan skyline" output $\breve{u} = \grave{\mathcal{H}}_{\text{ZOH}}\bar{u}$ shown in of Fig. 8 clearly is not stationary as an analog signal because it is piecewise constant, but it is stationary as a lifted signal. Its over time averaged power is well defined and equals $\|\grave{\mathcal{H}}_{\text{ZOH}}\acute{\mathcal{S}}_\epsilon\|_2^2 = \frac{1}{\epsilon}$. $\triangledown$
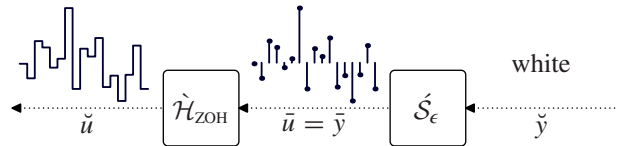

Figure 8: A periodic stationary output $\breve{u}$

Signal connotations are not that consistent in semi-lifted cases, where deterministic and stochastic interpretations might require different scaling. To be specific, to maintain the deterministic interpretation for A/D systems (averaging the output

energy over all δ-functions applied in $[0, h)$), we still need to scale the Hilbert-Schmidt norm by a factor of $1/h$. At the same time, this factor is not required to maintain the stochastic interpretation (the response to the analog white noise is a stationary discrete process then). D/A systems, on the contrary, do not need the scaling in the deterministic case, whereas do need it to maintain the stochastic meaning. We nevertheless proceed with the scaling in all cases of interest, just to keep the exposition simple.

The L^2 system norm (30) corresponds to the system inner product

$$\langle \tilde{G}, \tilde{P} \rangle_2 = \frac{1}{2\pi h} \int_{-\pi}^{\pi} \langle \tilde{G}(e^{i\theta}), \tilde{P}(e^{i\theta}) \rangle_{HS} \, d\theta \qquad (31)$$

with the Hilbert-Schmidt inner product defined as

$$\mathrm{tr}(AB^*) = \mathrm{tr}(B^*A) := \langle A, B \rangle_{HS} := \sum_i \langle A e_i, B e_i \rangle_{\mathbb{K}_o}$$

where $\{e_i\}$ is any complete orthonormal sequence of $\mathbb{K}_i$. By Parseval's theorem the inner product (31) equals

$$\langle \tilde{G}, \tilde{P} \rangle_2 = \frac{1}{h} \sum_{k \in \mathbb{Z}} \langle \tilde{G}[k], \tilde{P}[k] \rangle_{HS}$$

where $\tilde{G}[k]$ is the impulse response kernel (cf. (10), (12), (13)). It implies that two L^2 systems are orthogonal if their impulse response kernels have disjoint supports and that

$$\|\tilde{G}\|_2^2 = \frac{1}{h} \sum_{k \in \mathbb{Z}} \|\tilde{G}[k]\|_{HS}^2. \qquad (32)$$

This expression is quite useful in various applications.

Finally a note on adjoints. We take adjoints of systems (operators) always with respect to the standard L^2 and ℓ^2 *signal* inner product (24). The reason is that these are also adjoints for the other inner products such as (31). A further useful fact is that the system inner product (31) inherits from the Hilbert-Schmidt inner product the trace-like property that

$$\langle \tilde{A}, \tilde{B}\tilde{X} \rangle_2 = \langle \tilde{A}\tilde{X}^*, \tilde{B} \rangle_2 \qquad (33)$$

if $\tilde{X} \in L^\infty$ and $\tilde{A}, \tilde{B} \in L^2$.

6. Stability and Causality

This section reviews the notions of stability and causality and their expression in the lifted frequency domain.

6.1. System Stability

As HSPs, like that in Fig. 1, typically operate in open loop and their components are implemented separately, we require that each component, i.e., $\mathcal{S}$, $\bar{\mathcal{F}}$, and $\mathcal{H}$, is stable. We say that $\mathcal{S}$ is stable if it is a bounded operator $L^2(\mathbb{R}) \mapsto \ell^2(\mathbb{Z})$, $\bar{\mathcal{F}}$ is stable if it is a bounded operator $\ell^2(\mathbb{Z}) \mapsto \ell^2(\mathbb{Z})$, and $\mathcal{H}$ is stable if it is a bounded operator $\ell^2(\mathbb{Z}) \mapsto L^2(\mathbb{R})$. Obviously, in the lifted

domain, for the lifted HSP in Fig. 6, all these definitions read as the boundedness as an operator $\ell^2(\mathbb{Z}) \mapsto \ell^2(\mathbb{Z})$.

The fact that all components of the lifted HSP are LTI makes it possible to verify their stability to the (lifted) frequency domain. Indeed, because the Fourier transform is an isomorphism from $\ell^2(\mathbb{Z})$ to $L^2(\mathbb{T})$, each of the systems $\mathcal{S}$, $\bar{\mathcal{F}}$, and $\mathcal{H}$ is stable iff its lifted transfer function is a bounded operator $L^2(\mathbb{T}) \mapsto L^2(\mathbb{T})$. The following result, which is essentially the first part of [9, Thm. A.6.26], plays then a key role:

Theorem 6.1. The set of all bounded multiplication operators from $L^2(\mathbb{T})$ to $L^2(\mathbb{T})$ is L^∞. Moreover, the induced norm of an operator $\tilde{O} : L^2(\mathbb{T}) \mapsto L^2(\mathbb{T})$ is $\|\tilde{O}\|_\infty$. $\qquad \triangledown$

It follows from Theorem 6.1 that a sampler $\mathcal{S}$ is stable iff its lifted transfer function $\acute{S}(z) \in L^\infty$ and a hold $\mathcal{H}$ is stable iff its lifted transfer function $\grave{H}(z) \in L^\infty$. Propositions 5.3 and 5.4 reduce the verification of these conditions to matrix (or even scalar) operations. For example, $\mathcal{S}$ is stable iff each row of the lifted Fourier transform of its sampling function $\psi(t)$ belongs to $\mathbb{L}$ for (almost) all θ or, alternatively, iff the magnitude of the Fourier transform of each entry of $\psi(t)$ is square summable over all aliased frequencies for (almost) all baseband frequencies. The latter condition is guaranteed if the Fourier transform of the sampling function decays faster than $1/\sqrt{\omega}$ as $\omega \to \infty$, which agrees with known results about stability of the sampling operation [22].

6.2. Systems Causality

The notion of *causality* is well understood for both analog and discrete systems. Intuitively, a system is causal if its output at any time instance depends only upon its past and present inputs and does not depend on the future inputs. For a continuous-time system $\mathcal{G}$ this can be formally expressed as

$$\Pi_T \mathcal{G} (I - \Pi_T) = 0, \quad \forall T \in \mathbb{R}, \qquad (34)$$

where the *truncation operator* Π_T is defined via the relation

$$(\Pi_T u)(t) = \begin{cases} u(t) & t < T \\ 0 & t \geq T \end{cases}.$$

The discrete-time case is the same modulo the use of the discrete truncation operator $\bar{\Pi}_k$, defined similarly. If the system is time invariant, the condition need only be checked for one fixed T, e.g., for $T = 0$.

The extension of these notions to hybrid systems depends on the way in which continuous and discrete times are synchronized. Henceforth, motivated mainly by the time association in the lifting transformation, we presume that the kth discrete instance corresponds to the whole continuous-time interval $[kh, (k+1)h]$. In this case, we say that a (shift-invariant) sampler $\mathcal{S}$ is causal if

$$\bar{\Pi}_k \mathcal{S} (I - \Pi_{kh}) = 0, \quad \text{for some } k \in \mathbb{Z}, \qquad (35)$$

and a (shift-invariant) hold $\mathcal{H}$ is causal if

$$\Pi_{kh} \mathcal{H} (I - \bar{\Pi}_k) = 0, \quad \text{for some } k \in \mathbb{Z}. \qquad (36)$$

It can be verified that, according to these definitions, sampler (3) is causal iff $\psi(t) = 0$ for all $t \leq -h$ and hold (4) is causal iff $\phi(t) = 0$ for all $t < 0$. While the latter is in agreement with the criterion for continuous-time systems, the former might appear peculiar. For example, a sampler with the sampling function $\psi(t + h/2)$, which acts as $\bar{y}[k] = y(kh + h/2)$, is causal by this definition. This, however, is a matter of convention. If the implementation permits $\bar{y}[k]$ to depend only upon $y(t)$ for $t < kh$, we may require from $\mathcal{S}$ to be *strictly causal*, i.e., that $\bar{\Pi}_{k+1}\mathcal{S}\,(I - \Pi_{kh}) = 0$.

Definitions (35) and (36) can be lifted straightforwardly. To this end, note that Π_{kh} corresponds to

$$(\check{\Pi}_k \check{u})[i] = \begin{cases} \check{u}[i] & i < k \\ 0 & i \geq k \end{cases}$$

in the lifted domain. Thus, both (35) and (36) became particular cases of the general definition: an LTI (discrete / semi-lifted / lifted) system $\tilde{\mathcal{G}}$ is causal if

$$\tilde{\Pi}_k \tilde{\mathcal{G}}(I - \tilde{\Pi}_k) = 0, \quad \text{for some } k \in \mathbb{Z}. \tag{37}$$

Remark 6.2. When applied to the lifting $\check{\mathcal{G}}$ of a continuous-time system $\mathcal{G}$, definition (37) reads $\Pi_{kh}\mathcal{G}\,(I - \Pi_{kh}) = 0$. This is *not* equivalent to (34), unless $\mathcal{G}$ is time invariant. Much care must therefore be taken in analyzing causality in the lifted domain with this definition. Throughout, we use the lifted version of (37) *only* in relation to lifted HSP blocks, in which case it does reflect causality (with the convention about the sampler discussed above). $\triangledown$

We also need a more general definition. We say that an LTI system $\tilde{\mathcal{G}}$ is *l-causal* ($l \in \mathbb{Z}$) if

$$\tilde{\Pi}_{k-l}\tilde{\mathcal{G}}(I - \tilde{\Pi}_k) = 0, \quad \text{for some } k \in \mathbb{Z}. \tag{38}$$

This definition allows the output of $\tilde{\mathcal{G}}$ at the moment k to depend on its input at all moments $\leq k + l$. If $l > 0$, this effectively says that $\tilde{\mathcal{G}}$ may have l steps *preview*. If $l < 0$, (38) defines a system with the delay of $-l$. The case of $l = -1$ corresponds to strictly causal systems.

6.3. Stability with Causality Constraints

Our message in this subsection is that (l) causality can be neatly incorporated into the stability analysis, in both time and frequency domains.

Let $\tilde{\mathcal{G}}$ be a stable, i.e., bounded mapping $\ell^2(\mathbb{Z}) \to \ell^2(\mathbb{Z})$, (discrete / semi-lifted / lifted) system and consider Definition (38) for $k = 0$. It is readily seen that $\tilde{\Pi}_{-l}$ and $I - \tilde{\Pi}_0$ are the orthogonal projections from $\ell^2(\mathbb{Z})$ to $\ell^2(\mathbb{Z}_{-l}^-)$ and $\ell^2(\mathbb{Z}_0^+)$, respectively. Thus, (38) reads $\tilde{\Pi}_{-l}\tilde{\mathcal{G}}\,\ell^2(\mathbb{Z}_0^+) = 0$ or, equivalently,

$$\tilde{\mathcal{G}}\,\ell^2(\mathbb{Z}_0^+) \subset \ell^2(\mathbb{Z}) \ominus \ell^2(\mathbb{Z}_{-l}^-) = \ell^2(\mathbb{Z}_{-l}^+).$$

Thus, we just showed that an LTI system $\tilde{\mathcal{G}}$ is stable and l-causal iff it is a bounded operator $\ell^2(\mathbb{Z}_0^+) \to \ell^2(\mathbb{Z}_{-l}^+)$.

Because the z-transform is an isometric isomorphism between $\ell^2(\mathbb{Z}_l^+)$ and $z^l H^2$, the stability condition above can be

reformulated as follows: $\tilde{\mathcal{G}}$ is stable and causal iff its transfer function $\tilde{G}(z)$ is a bounded operator $H^2 \to z^l H^2$. This, in turn, translates to (relatively) easily verifiable properties of $\tilde{G}(z)$ with the help of the following result:

Theorem 6.3. The set of all bounded multiplication operators from H^2 to $z^l H^\infty$ is $z^l H^\infty$. Moreover, the induced norm of an operator $\tilde{O}: H^2 \mapsto z^l H^2$ is $\|\tilde{O}\|_\infty$. $\triangledown$

Proof. The result for $l = 0$ (i.e., for the causal case) is known, see [9, Thm. A.6.26]. To extend it to general l, note that according to the definition of $z^l H^2$,

$$\tilde{O}H^2 \subset z^l H^2 \Leftrightarrow z^{-l}(\tilde{O}H^2) \subset H^2 \Leftrightarrow (z^{-l}\tilde{O})H^2 \subset H^2.$$

According to the result for $l = 0$, the latter reads $z^{-l}\tilde{O} \in H^\infty$, leading to the first part. The second part follows by the fact that the multiplication by z^{-l} does not alter the L^∞-norm. ∎

It follows from Theorem 6.3 that $\mathcal{S}$ and $\mathcal{H}$ are stable and l-causal iff their lifted transfer functions, $\acute{S}(z)$ and $\acute{H}(z)$, respectively, belong to $z^l H^\infty$. Thus, if causality constraints are incorporated into an optimization procedure, it is no longer sufficient to look at frequency responses (transfer functions at $z \in \mathbb{T}$). The behavior of transfer functions at the whole region of $z \in \mathbb{C} \setminus \mathbb{D}$ should be accounted for. This complicates the analysis and design considerably.

7. Concluding Remarks

In this part we collected the basic concepts and technical material of lifting and lifted signals and systems, in both time and frequency domains. The key point is that lifting may losslessly recover time-invariance (in discrete time) of systems that are not time-invariant (in continuous time). From that point on most of the results are intuitively clear, but possibly technically advanced. It is this material that forms the basis for the solutions to the optimal signal reconstruction problems considered in Parts II and III of this paper.

Part II: Noncausal Solutions

8. Introduction and Problem Formulation

In Part I we introduced and expanded the lifting technique and in this part we use the machinery of Part I to solve a series of noncausal sampling / reconstruction (SR) problems. Fig. 9 shows the setup that is common to all the problems considered in this part. Here

$$\mathcal{G} = \begin{bmatrix} \mathcal{G}_v \\ \mathcal{G}_y \end{bmatrix}$$

is a given signal generator. Its upper output v is the analog signal that we want to reconstruct and the other output y is the signal that is available for sampling. The purpose of the hybrid signal processor $\mathcal{HS}$ is to produce an signal u that, in some sense, is
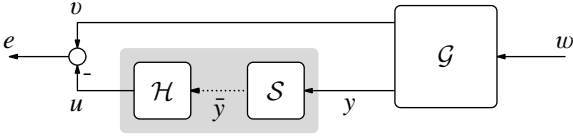
Figure 9: Sampling / reconstruction (SR) setup

optimally close the signal v. Specifically we minimize over all stable samplers $\mathcal{S}$ and/or stable holds $\mathcal{H}$ the L^2 and L^∞ norm of the error system

$$\mathcal{G}_{\mathrm{e}} = \mathcal{G}_v - \mathcal{H}\mathcal{S}\mathcal{G}_y. \tag{39}$$

Given the norm, the design problems thus split into three types

	fixed sampler	free sampler
fixed hold		Type-II
free hold	Type-III	Type-IV

These three types we consider in various settings. There is also a Type-I problem, which is when both sampler and hold are fixed and only a discrete filter (in between sampler and hold, not shown in the diagram) needs to be designed. Unlike the other three cases, Type-I problems can be reduced to equivalent discrete estimation problems, which, in turn, are solvable by standard methods. Reduction procedures, applicable to non-causal and relaxed-causal setups, are available in [8] for the L^2 norm and in [30] for the L^∞ norm. We therefore do not deal with Type-I problems in this paper.

We do not impose any causality constraints in this part. This together with the assumed stability of the components makes frequency domain solutions amenable, and the design can be done frequency-wise. The design of causal and relaxed-causal components for Type-III problems is the subject of this paper.

The so determined optimal holds recover and extend the cardinal polynomial and exponential spline hold functions of [48, 47, 49], and we identify the signal spaces for which these splines are optimal. For Type-IV problems we develop a rank characterization of hybrid signal processors and we show that the well known frequency folding [37, §6.1] also plays a role in the lifted approach, however without superimposing the foldings as is commonly done. This subsequently provides a system-theoretic interpretation of the ubiquitous Whittaker-Kotel'nikov-Shannon (WKS) Sampling Theorem, by showing that both the L^2 and the L^∞ performance criteria produce the sinc-interpolator as the optimal D/A converter and the ideal low-pass filter followed by the ideal sampler as the optimal A/D converter. This result corresponds to the case where the signal to be reconstructed has dominating low-frequency components (up to the Nyquist frequency) and is measured without noise, see also [43, 44]. Remarkably, if these conditions hold true, the optimal reconstructor is independent of properties of the analog signal [44]. Multi-channel HSPs can be designed in the same way. This recovers a series of generalized sampling results [18, 54, 34]. The machinery can also handle optimal downsampling, which is illustrated on an example. The final application in this part is optimal reconstruction in the face of noisy measurements. It is worth emphasizing that whereas

the noise-free solutions recovers known signal reconstructors (e.g. the Sampling Theorem [45]), complete solutions in the noisy case are not presently available to the best of our knowledge. Preliminary versions of some of the results presented here can be found in [26, 27].

The part is organized as follows. We begin with Type II (Section 9) and Type III (Section 10) problems. The rest of this part addresses Type IV problems. Section 11 is about a rank characterization of hybrid signal processors and in the following two sections we summarize fixed frequence singular value decompositions in lifted domain and the folding procedure. From Section 14 onwards a series of applications is discussed, beginning with a single-channel SR and the ensuing limittations on error free reconstruction. Then, in Sections 15 and 16 multi-channel SR and optimal downsampling are discussed. Finally, in Section 17 we consider SR from noisy measurements.

Notation

In this part it is convenient to refer to systems that are linear and time invariant with respect to any continuous-time shift as *LCTI* systems, and to systems that are linear and time invariant under discrete times shifts, equal to a multiple of the sampling period h, as *LDTI* systems. For the rest the notion is the same as that of Part I.

9. Type II: Fixed Hold, Optimal Sampler

Type-II (fixed hold) and Type-III (fixed sampler) problems are unconstrained projection problems which makes them easy to solve.

Lemma 9.1. Let $\mathcal{G}_v, \mathcal{G}_y, \mathcal{H} \in L^\infty$ and suppose $\|\mathcal{G}_v\|_2 < \infty$ and that $\mathcal{H}$ is a hold. Then every solution $\mathcal{S}_{\mathrm{opt}} \in L^\infty$ (if any) of the normal equations

$$\mathcal{H}^*\mathcal{G}_v\mathcal{G}_y^* = (\mathcal{H}^*\mathcal{H})\mathcal{S}_{\mathrm{opt}}(\mathcal{G}_y\mathcal{G}_y^*) \tag{40}$$

is a sampler minimizing $\|\mathcal{G}_{\mathrm{e}}\|_2$ over all $\mathcal{S} \in L^\infty$. The optimal performance level is then $\|\mathcal{G}_{\mathrm{e}}\|_2^2 = \|\mathcal{G}_v\|_2^2 - \|\mathcal{H}\mathcal{S}_{\mathrm{opt}}\mathcal{G}_y\|_2^2$. If in addition

$$(\mathcal{H}^*\mathcal{H})^{-1} \text{ and } (\mathcal{G}_y\mathcal{G}_y^*)^{-1} \text{ exist and are stable}, \tag{41}$$

then

$$\mathcal{S}_{\mathrm{opt}} = (\mathcal{H}^*\mathcal{H})^{-1}\mathcal{H}^*\mathcal{G}_v\mathcal{G}_y^*(\mathcal{G}_y\mathcal{G}_y^*)^{-1} \tag{42}$$

is the unique stable optimal sampler.

Proof. Standard projection combined with the trace-like property (33). ∎

The optimal sampler (42) can be viewed as the cascade of the LCTI system $\mathcal{G}_v\mathcal{G}_y(\mathcal{G}_y\mathcal{G}_y^*)^{-1}$, the sampler $\mathcal{H}^*$ and the discrete system $(\mathcal{H}^*\mathcal{H})^{-1}$. The first system, $\mathcal{G}_v\mathcal{G}_y(\mathcal{G}_y\mathcal{G}_y^*)^{-1}$, is actually the optimal analog filter, i.e., the filter $\mathcal{F}$ minimizing $\|\mathcal{G}_v - \mathcal{F}\mathcal{G}_y\|_2$ over all stable $\mathcal{F}$.

The above lemma is formulated representation free. To make matters concrete one can employ a specific representation. The

lifted frequency response representation is interesting because it shows that the optimal sampler

$$\check{S}_{\text{opt}}(e^{i\theta}) = [(\check{H}^*\check{H})^{-1}\check{H}^*\check{G}_v\check{G}_y^*(\check{G}_y\check{G}_y^*)^{-1}](e^{i\theta})$$

for each frequency θ satisfies the normal equations associated with the norm $\|\check{G}_e(e^{i\theta})\|_{\text{HS}}$. That is, the optimal sampler also frequency-wise minimizes the norm of the frequency response, Eqn. (30). This is a well known feature in noncausal filter design. If all signals are scalar then the Fourier transform of the optimal sampling function is probably the simplest representation. Indeed in that case $\mathcal{G}_y^*$ cancels in (40) and the optimal sampling function ϕ_{opt} then can be shown to have Fourier transform

$$\Psi_{\text{opt}}(i\omega) = \frac{h}{\sum_{k\in\mathbb{Z}}|\Phi(i(\omega+2k\omega_N))|^2}\Phi(-i\omega)\frac{G_v(i\omega)}{G_y(i\omega)}, \quad (43)$$

where $\Phi(i\omega)$ is the Fourier transform of the hold function $\phi(t)$. This follows for instance from Proposition 5.4.

The L^∞ optimal sampler is more involved but it applies to a larger class of signal generators in that $\|\mathcal{G}_v\|_2$ need not be finite. The following result is proved in Appendix A.

Lemma 9.2. Let $\mathcal{G}_v, \mathcal{G}_y, \mathcal{H} \in L^\infty$ and suppose $\mathcal{H}$ is a hold and that (41) is satisfied. Then

$$\|\mathcal{G}_e\|_\infty \geq \max(\|(I - \mathcal{H}(\mathcal{H}^*\mathcal{H})^{-1}\mathcal{H}^*)\mathcal{G}_v\|_\infty,$$
$$\|\mathcal{G}_v(I - \mathcal{G}_y^*(\mathcal{G}_y\mathcal{G}_y^*)^{-1}\mathcal{G}_y)\|_\infty) \quad (44)$$

for any stable sampler, and there exist stable samplers that achieve equality. If $\mathcal{G}_y^{-1}$ exists and is stable then the L^2-optimal (42) is also L^∞-optimal. $\qquad\triangledown$

Each term in (44) has a clear interpretation. The first term $\|(I - \mathcal{H}(\mathcal{H}^*\mathcal{H})^{-1}\mathcal{H}^*)\mathcal{G}_v\|_\infty$ is the minimal L^∞-norm for the case that $y = v$ i.e., for the case that all information about the signal v that we want to reconstruct is available for sampling. The second term, $\|\mathcal{G}_v(I-\mathcal{G}_y(\mathcal{G}_y\mathcal{G}_y^*)^{-1}\mathcal{G}_y^*)\|_\infty$, is the L^2-induced norm of the mapping $e = G_e w$ for w restricted to $w = (I - \mathcal{G}_y^*(\mathcal{G}_y\mathcal{G}_y^*)^{-1}\mathcal{G}_y)\hat{w}$. These are the signals w for which there is nothing to sample, $y = 0$. Evidently that is a lower bound for $\|\mathcal{G}_e\|_\infty$.

9.1. When $\mathcal{G}_v = \mathcal{G}_y$

Now suppose that $\mathcal{G}_v = \mathcal{G}_y$, i.e., that the signal v to be reconstructed equals the signal y available for sampling. For this case the design of L^2 optimal samplers for fixed holds is well documented [44, Section IV] and the optimal sampler is then essentially independent of the signal generator. Including the L^∞ norm we obtain:

Corollary 9.3. Let $\mathcal{G}_v = \mathcal{G}_y, \mathcal{H} \in L^\infty$ and suppose that $(\mathcal{H}^*\mathcal{H})^{-1}$ exists and is stable. Then

$$\mathcal{S}_{\text{opt}} := (\mathcal{H}^*\mathcal{H})^{-1}\mathcal{H}^* \quad (45)$$

minimizes the L^∞ norm of $\mathcal{G}_e$ with

$$\|\mathcal{G}_e\|_\infty = \|(I - \mathcal{H}(\mathcal{H}^*\mathcal{H})^{-1}\mathcal{H}^*)\mathcal{G}_v\|_\infty. \quad (46)$$

If in addition $\|\mathcal{G}_v\|_2 < \infty$, then it minimizes the L^2 norm as well with $\|\mathcal{G}_e\|_2^2 = \|\mathcal{G}_v\|_2^2 - \|\mathcal{H}(\mathcal{H}^*\mathcal{H})^{-1}\mathcal{H}^*\mathcal{G}_v\|_2^2$. $\qquad\triangledown$

Indeed $\mathcal{S}_{\text{opt}} = (\mathcal{H}^*\mathcal{H})^{-1}\mathcal{H}^*$ solves the normal equation (40) and does not depend on $\mathcal{G}_v$. Another way to think about it is that now there is a single sampler that minimizes the *signal* error norm $\|(I - \mathcal{H}\mathcal{S})\mathcal{G}_v w\|_2$ for every given exogenous input $w \in L^2$. It implies that this sampler is also L^∞-optimal. The Fourier transform (43) of the optimal sampler reduces to

$$\Psi_{\text{opt}}(i\omega) = \frac{h\Phi(-i\omega)}{\sum_{k\in\mathbb{Z}}|\Phi(i(\omega + 2k\omega_N))|^2}.$$

Example 9.4. The adjoint $\mathcal{H}^*$ is a sampler and according to §5.2, its sampling function is $\psi(t) = \phi(-t)$ with $\phi(t)$ the hold function of $\mathcal{H}$. Thus if the hold is causal then the adjoint hold (a sampler) is anti-causal, and vice-versa. The discrete filter $\bar{\mathcal{K}} := (\mathcal{H}^*\mathcal{H})^{-1}$ because of its symmetry is never causal, unless it is static. For the zero order hold, with hold function $\phi(t) = \mathbb{1}_{[0,h)}(t)$, the discrete filter $\mathcal{H}^*\mathcal{H}$ is the static gain, h. This follows from (27a). The optimal sampler (45) therefore is $\frac{1}{h}\mathcal{H}^*$. It is the sampler with sampling function $\psi(t) = \frac{1}{h}\phi(-t) = \frac{1}{h}\mathbb{1}_{(-h,0]}(t)$. It is an averaging noncausal sampler, see §2.2. $\qquad\triangledown$

The optimal sampler (45) makes $\mathcal{H}\mathcal{S}_{\text{opt}}$ the classic orthogonal projection (hence self adjoint) onto the image of $\mathcal{H}$, and we have the trivial identity that $\mathcal{S}\mathcal{H} = I$. This implies *consistency*, a term coined by [46]. In the present context consistency means that $\mathcal{S}\mathcal{H}\mathcal{S} = \mathcal{S}$. In other words, in a consistent HSP any reconstructed signal $u := \mathcal{H}\mathcal{S}y$ when reinjected into the sampler recovers the discrete signal $\mathcal{S}y$ that was injected into the hold.

The bulk of this part handles cases in which both sampler and hold are designed simultaneously (Type-IV). Obviously, this generalizes Type-II and hence also in Type-IV problems the hybrid signal processor $\mathcal{H}\mathcal{S}$ may be taken (self-adjoint) projections if $\mathcal{G}_v = \mathcal{G}_y$, and they are consistent. If causality requirements are imposed on sampler and/or hold then these properties might be lost, see Part III.

10. Type III: Fixed Sampler, Optimal Hold

Type-III problems are essentially dual to the Type-II problems that we considered in the previous section. This is why in this section we only summarize the results.

Lemma 10.1. Let $\mathcal{G}_v \in L^\infty \cap L^2$ and that a sampler $\mathcal{S}$ is given such that $\mathcal{S}\mathcal{G}_y \in L^\infty$. Then every $\mathcal{H}_{\text{opt}} \in L^\infty$ (if any) that solves the normal equation

$$\mathcal{G}_v(\mathcal{S}\mathcal{G}_y)^* = \mathcal{H}_{\text{opt}}\mathcal{S}\mathcal{G}_y(\mathcal{S}\mathcal{G}_y)^* \quad (47)$$

minimizes $\|\mathcal{G}_e\|_2$ over all $\mathcal{H} \in L^\infty$ attaining $\|\mathcal{G}_e\|_2^2 = \|\mathcal{G}_v\|_2^2 - \|\mathcal{H}_{\text{opt}}\mathcal{S}\mathcal{G}_y\|_2^2$. In particular if $(\mathcal{S}\mathcal{G}_y(\mathcal{S}\mathcal{G}_y)^*)^{-1}$ exists and is stable then

$$\mathcal{H}_{\text{opt}} = \mathcal{G}_v(\mathcal{S}\mathcal{G}_y)^*(\mathcal{S}\mathcal{G}_y(\mathcal{S}\mathcal{G}_y)^*)^{-1}. \quad (48)$$

is the unique stable optimal hold. $\qquad\triangledown$

The optimal hold (48) can be viewed as the cascade of a discrete system $(\mathcal{S}\mathcal{G}_y(\mathcal{S}\mathcal{G}_y)^*)^{-1}$, a hold $(\mathcal{S}\mathcal{G}_y)^*$ and an analog system $\mathcal{G}_v$.

Without loss of generality we can take the sampler to be ideal because its sampling function may always be absorbed into $\mathcal{G}_y$. The required stability of $\mathcal{S}_{\mathrm{Idl}}\mathcal{G}_y$ in the above lemma is then ensured if $\mathcal{G}_y$ is LCTI and whose transfer function $G(s)$ is strictly proper rational and without poles on the imaginary axis, §6.1.

The abstract solution (48) for scalar signals and LCTI signal generators $\mathcal{G}_v$ and $\mathcal{G}_y$ is compactly described via the Fourier transform of its hold function

$$\Phi_{\mathrm{opt}}(\mathrm{i}\omega) = \frac{hG_v(\mathrm{i}\omega)G_y(-\mathrm{i}\omega)}{\sum_{k\in\mathbb{Z}}|G_y(\mathrm{i}(\omega + 2k\omega_{\mathrm{N}}))|^2}, \qquad (49)$$

still under the assumption that $\mathcal{S} = \mathcal{S}_{\mathrm{Idl}}$. This follows from the $\mathrm{i}\omega$-axis version of Prop. 5.3.

10.1. When $\mathcal{G}_v = \mathcal{G}_y$

Let us return to the situation that $\mathcal{G}_v = \mathcal{G}_y$. Then once again the hybrid signal processor becomes consistent because $\mathcal{S}\mathcal{H}_{\mathrm{opt}} = I$ for the hold of (48). The normal equation (47) does not simplify much in this case. A crucial difference with Type-II is that now there is no single hold that minimizes the *signal* error norm $\|(\mathcal{G}_v - \mathcal{H}\mathcal{S}\mathcal{G}_y)w\|_2$ for all w. Typically, in fact, for almost every given $w \in L^2$ there exists a hold $\mathcal{H}_w$ that makes the reconstruction error $(\mathcal{G}_v - \mathcal{H}_w\mathcal{S}\mathcal{G}_y)w$ equal to zero[5], while no single $\mathcal{H}$ exists that does this for all w.

Let us further assume that the sampler is ideal, $\mathcal{S} = \mathcal{S}_{\mathrm{Idl}}$. For this case we will establish connections with the cardinal exponential and polynomial spline hold functions of [48, 47, 49].

Example 10.2 (Second order signal generator). Let $\mathcal{G}_v$ be the LCTI system with transfer function

$$G_v(s) = \frac{1}{(s + \alpha)^2}, \qquad \alpha > 0.$$

Clearly $\mathcal{G}_v^*\mathcal{G}_v$ has impulse response $g * g^{\sim}$ with $g(t)$ the impulse response of $\mathcal{G}$ and $g^{\sim}(t) = g(-t)$. In our case

$$(g * g^{\sim})(t) = \tfrac{1}{4\alpha^3}(1 - \alpha t)e^{\alpha t}\mathbb{1}(-t) + \tfrac{1}{4\alpha^3}(1 + \alpha t)e^{-\alpha t}\mathbb{1}(t)$$

Hence the discrete system $\bar{\mathcal{F}} := \mathcal{S}_{\mathrm{Idl}}\mathcal{G}_v(\mathcal{S}_{\mathrm{Idl}}\mathcal{G}_v)^*$ has impulse response $f[n] := (g * g^{\sim})(nh) = \frac{1}{4\alpha^3}(1 + \alpha|n|h)e^{-\alpha|n|h}$. For the optimal hold (48) we need the inverse of this filter. For that we first determine its discrete transfer function (with $r := e^{-\alpha h}$)
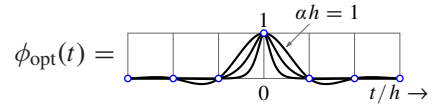
$$\bar{F}(z) = \frac{1}{4\alpha^3}\left(\frac{1 - r^2}{(1 - rz)(1 - r/z)} + \frac{\alpha h r/z}{(1 - r/z)^2} + \frac{\alpha h r z}{(1 - rz)^2}\right).$$

Its inverse, with $\beta := r(r^2(1 + \alpha h) + (\alpha h - 1))$, then reads

$$\bar{K}(z) := \bar{F}^{-1}(z) = 4\alpha^3 \frac{(1 - r/z)^2(1 - rz)^2}{\beta z^{-1} + (1 - r^2(r^2 + 4\alpha h)) + \beta z}.$$

---

[5] $\dot{H}_w(e^{\mathrm{i}\theta}) := \breve{v}(e^{\mathrm{i}\theta})/\bar{y}(e^{\mathrm{i}\theta})$ is often well defined.

The hold function of the optimal hold (48) finally can be obtained by filtering $g * g^{\sim}$ with this $\bar{\mathcal{K}}$. For the three values $\alpha h \in \{1, 5, 10\}$ this results in

For $0 < \alpha h < 1$ the plot is very similar to that for $\alpha h = 1$. Since $g * g^{\sim}$ is twice continuously differentiable, also $\phi_{\mathrm{opt}}(t)$ has this degree of smoothness. Moreover, since $g * g^{\sim}$ is piecewise exponential, the optimal hold is a spline that on each sampling interval is a sum of exponential functions. This is an example of the exponential splines of [49]. ▽

Note that the equality $\mathcal{S}_{\mathrm{Idl}}\mathcal{H}_{\mathrm{opt}} = I$ for the ideal sampler means that the hold function $\phi_{\mathrm{opt}}(t)$ at the sampling instances, kh, equals the Kronecker delta $\delta[k]$. Indeed it does in the above example.

[45, p. 575] remarks that in many cases, sequences of hold functions $\phi_n(t)$ converge towards $\mathrm{sinc}_h(t)$ as n approaches infinity. For our hold functions that would mean that often sequences of Fourier transforms

$$\Phi_{\mathrm{opt},n}(\mathrm{i}\omega) = \frac{h|G_{v,n}(\mathrm{i}\omega)|^2}{\sum_{k\in\mathbb{Z}}|G_{v,n}(\mathrm{i}(\omega + 2k\omega_{\mathrm{N}}))|^2} \qquad (50)$$

converge to $h\mathbb{1}_{[-\omega_{\mathrm{N}},\omega_{\mathrm{N}}]}$ as $n \to \infty$. This convergence occurs iff the corresponding signal generator $\mathcal{G}_{v,n}$ becomes more and more "baseband dominant" as $n \to \infty$. To be more precise, introduce the following definitions:

Definition 10.3 (Baseband dominance). A SISO LCTI system $\mathcal{W}$ is said to be *baseband dominant* if a $c \in [0, 1]$ exists such that

$$|W(\mathrm{i}\omega_k)| \leq c|W(\mathrm{i}\omega_0)| \quad \forall k \neq 0$$

and all $\omega_0 \in (-\omega_{\mathrm{N}}, \omega_{\mathrm{N}})$. If the inequality holds for a $c < 1$, then $\mathcal{W}$ is said to be *strict baseband dominant*. ▽

It is easy to see that every real system whose frequency response is monotonically decreasing over positive frequency is strict baseband dominant.

Lemma 10.4. Let $\mathcal{W}$ be an LCTI strict baseband dominant system with $W(\mathrm{i}\omega) \neq 0$ for almost every $\omega \in [-\omega_{\mathrm{N}}, \omega_{\mathrm{N}}]$ and assume that the sampler is ideal. Then for $\mathcal{G}_{v,n} := \mathcal{W}^n$ the optimal hold (48) converges to $\mathcal{H}_{\mathrm{sinc}}$ as $n \to \infty$.

Proof. For this $G_{v,n}$ the right-hand side of (50) converges to h if $\omega \in (-\omega_{\mathrm{N}}, \omega_{\mathrm{N}})$ and converges to 0 if $|\omega| > \omega_{\mathrm{N}}$. It converges to the Fourier transform of $\mathrm{sinc}_h(t)$. Stability and strict baseband dominance imply that $\|\mathcal{G}_{v,n}\|_2 < \infty$ and that the denominator in (50) is $< \infty$ for every ω. Moreover, the convergence is in L^2 signal norm, which guarantees that the limit is well defined (in both time and frequency domain). ∎

The signal interpretation of this result is intuitive: in the limit $n \to \infty$ the signals $v = \mathcal{G}_{n,v}w$ are effectively bandlimited to $[-\omega_{\mathrm{N}}, \omega_{\mathrm{N}}]$ and indeed, as Shannon dictates, holding with the sinc_h is then the best one can do (irrespective of w).

10.2. Optimal Hold for Unstable Signal Generators

A popular class of hold functions are the cardinal polynomial spline hold functions [48]. These are polynomial splines of odd degree $2n - 1$ ($n = 1, 2, \ldots$) and which are $2n - 2$ times continuously differentiable. Further they are in $L^2(\mathbb{R})$ and are required to satisfy the consistency property that $\phi(kh) = \bar{\delta}[k]$. This makes them unique. Fig. 10 shows these hold functions for $n = 1$ and $n = 2$.

Figure 10: Cardinal polynomial spline hold functions of degree 1 and 3

A natural question now is: with respect to what class of signals are these hold functions optimal? If in Example 10.2 we let α approach zero then its hold function approaches a cubic spline (this requires some work) and the signal generator approaches the double integrator $1/s^2$. It suggests that cubic cardinal polynomial splines are optimal with respect to doubly integrated white noise (integrated Brownian motion) or doubly integrated L^2 signals, so slowly varying signals. More generally, we claim the following.

Theorem 10.5. If $\mathcal{G}_v = \mathcal{G}_y$ are LCTI integrators of order n, $G_v(s) = G_y(s) = 1/s^n$ then the hold function of (50) is the unique $(2n - 2)$-smooth $(2n - 1)$-degree polynomial spline in $L^2(\mathbb{R})$ for which $\phi_{\mathrm{opt}}(kh) = \bar{\delta}[k]$. $\qquad\triangledown$

A proper proof is in Appendix A. A dubious derivation, but an insightful one nonetheless, goes as follows. Consider the normal equations $(1 - \mathcal{H}\mathcal{S}_{\mathrm{Idl}})\mathcal{G}_v\mathcal{G}_v^*\mathcal{S}_{\mathrm{Idl}}^* = 0$. Now the adjoint $\mathcal{S}_{\mathrm{Idl}}^*$ of the ideal sampler is the delta-hold operator and hence $\mathcal{G}_v\mathcal{G}_v^*\mathcal{S}_{\mathrm{Idl}}^*\bar{u}$ for any signal $\bar{u}$ is a delta-train integrated $2n$ times, i.e., some $(2n - 2)$-smooth $(2n - 1)$-degree polynomial spline. So the equality $(1-\mathcal{H}\mathcal{S}_{\mathrm{Idl}})\mathcal{G}_v\mathcal{G}_v^*\mathcal{S}_{\mathrm{Idl}}^*\bar{u} = 0$ means that the polynomial spline equals $\mathcal{H}$ applied to the sampled polynomial spline. By linearity and discrete-time invariance, it is sufficient to consider the case that $\mathcal{S}_{\mathrm{Idl}}\mathcal{G}_v\mathcal{G}_v^*\mathcal{S}_{\mathrm{Idl}}^*\bar{u}$ is the unit pulse. There is a unique polynomial spline $\phi \in L^2(\mathbb{R})$ of the given smoothness and degree that interpolates the unit pulse, see [48].

In Part III, Remark 20.7 we show, as a by product, that the hold (48) is actually the stable hold that makes the error system $(I - \mathcal{H}\mathcal{S})\mathcal{G}_v$ stable and minimizes its L^2-norm. This formulation circumvents stability of the signal generators and also applies to integrators $G_v(s) = 1/s^n$. Incidentally, since $1/s$ is strict baseband dominant, these cardinal polynomial spline functions converge towards $\mathrm{sinc}_h(t)$ as $n \to \infty$ (Lemma 10.4 and [48, § III.D]).

10.3. Singular Normal Equations

It may happen that the normal equation (47) admits a solution while the inverse needed for its explicit solution (48) is not stable or not well defined. We illustrate this by an example from [51].

Example 10.6. Even though we assumed that $\mathcal{G}_v$ is an analog system, Lemma 10.1 is actually valid for hybrid, D/A, $\mathcal{G}_v$ as well. Let $\mathcal{G}_v = \mathcal{G}_y = \mathcal{H}_v$ be the hold with hold function

and take the ideal sampler $\mathcal{S}_{\mathrm{Idl}}$. In fact, the precise shape of $\phi_v(t)$ on $[-2h, h]$ and $[h, 2h]$ is not important, but their symmetry that they add up to 1 for all intersample time,

$$\phi_v(-2h + \tau) + \phi_v(h + \tau) = 1, \quad \forall\tau \in [0, h], \qquad (51)$$

is. The cascade $\mathcal{S}_{\mathrm{Idl}}\mathcal{G}_v$ is then the discrete FIR system with the transfer function $z + 1 + z^{-1}$. In [51, p. 1095] it is claimed that then no hold $\mathcal{H}$ exists that reconstructs the input to the sampler error free, because some inverse needed in the process is not defined. That implication is not correct. The normal equation is singular but not unsolvable. To see this, note that (47) in lifted frequency domain reads

$$\dot{H}_v(z)(z + 1 + z^{-1}) = \dot{H}_{\mathrm{opt}}(z)(z + 1 + z^{-1})^2 \qquad (52)$$

and indeed $z = e^{i2\pi/3}$ is a zero of the right-most term and so that term has no stable inverse. These zeros, however, cancel against zeros of $\dot{H}_v(z)$, which can be seen via its kernel

$$\check{\phi}_v(z; \tau) = z^2\,\underline{\diagup|} + (z + 1)\,\underline{\square} + z^{-1}\,\underline{|\diagdown}$$
$$= (z + 1 + z^{-1})\,\underline{\square} + (z^2 - z^{-1})\,\underline{\diagup|} \qquad (53)$$

Therefore, the hold with the kernel

$$\phi_{\mathrm{opt}}(z; \tau) = \frac{\check{\phi}_v(z; \tau)(1 + z + z^{-1})}{(1 + z + z^{-1})^2}$$
$$= \underline{\square} + \frac{z^2 - z^{-1}}{1 + z + z^{-1}}\,\underline{\diagup|}$$
$$= \underline{\square} + (z - 1)\,\underline{\diagup|} = z\,\underline{\diagup|} + \underline{|\diagdown}$$

solves (52). This defines an FIR system, reminiscent of the predictive first-order hold (Example 3.4). In hindsight it is easy to see that this hold is optimal, and in fact it is error free (i.e., $\mathcal{G}_e = 0$).

Crucial in the derivation is the symmetry (51). If this symmetry is absent then the unit circle zeros of $z + 1 + z^{-1}$ reappear in the (unique) solution of (52) as poles, rendering it unstable. Yet even in this case one can approach the perfect reconstruction arbitrarily close by a stable $\mathcal{H}$. $\qquad\triangledown$

For LCTI signal generators $\mathcal{G}_v = \mathcal{G}_y$ and the ideal sampler, the conclusions are very similar and this, once again, is best seen from its classic Fourier transform: while the explicit formula (48) requires $\mathcal{S}_{\mathrm{Idl}}\mathcal{G}_v(\mathcal{S}_{\mathrm{Idl}}\mathcal{G}_v)^*$ to be stably invertible, for the normal equations to hold for some stable hold we merely need that its Fourier transform

$$\Phi_{\mathrm{opt}}(i\omega) = \frac{h|G_v(i\omega)|^2}{\sum_{k\in\mathbb{Z}}|G_v(i(\omega + 2k\omega_{\mathrm{N}}))|^2}$$

determines a stable system. Evidently, we have $|\Phi_{\mathrm{opt}}(\mathrm{i}\omega)| \leq h$ for every ω and so stability of the hold is, for instance, ensured if $|\omega|^{\gamma} G_v(\mathrm{i}\omega)$ is bounded for some $\gamma > 1/2$, see §6.1. Note that $\mathcal{S}_{\mathrm{Idl}}\mathcal{G}_v (\mathcal{S}_{\mathrm{Idl}}\mathcal{G}_v)^*$ is stable and stably invertible iff $\frac{1}{\epsilon} > \sum_{k \in \mathbb{Z}} |G_v(\mathrm{i}(\omega + 2k\omega_{\mathrm{N}}))|^2 > \epsilon$ for some $\epsilon \in (0, 1)$ and all $\omega \in \mathbb{R}$.

11. Rank Theorem

Samplers, by their very nature, reduce continuous-time signals to discrete-time signals. Clearly then sampling normally brings about a loss of information. Dually, the output of a hold is continuous time, but as the hold is shift-invariant and driven by a discrete signal, the richness of the set of its continuous-time outputs is limited. Typically this set is nevertheless infinite dimensional and it is difficult to get a handle on the richness of the set in time domain. In lifted frequency domain matters are transparent and in fact one can fully characterize what it means for an LDTI system to be a series interconnection of a sampler and a hold.

First, recall that the series interconnection $u = \mathcal{H}\mathcal{S}y$ in lifted frequency domain is an integral operator

$$\check{u}(\mathrm{e}^{\mathrm{i}\theta}; \tau) = \int_0^h \check{f}_{\mathrm{HSP}}(\mathrm{e}^{\mathrm{i}\theta}, \tau, \sigma) \check{y}(\mathrm{e}^{\mathrm{i}\theta}, \sigma)\mathrm{d}\sigma \quad (54)$$

whose kernel can be expressed in terms of its sampling and hold functions as

$$\check{f}_{\mathrm{HSP}}(\mathrm{e}^{\mathrm{i}\theta}; \tau, \sigma) = \check{\phi}(\mathrm{e}^{\mathrm{i}\theta}; \tau) \, \check{\psi}(\mathrm{e}^{\mathrm{i}\theta}; -\sigma), \quad (55)$$

see Appendix A for a derivation. At each θ the range of the integral operator (54) is contained in the subspace spanned by $\check{\phi}(\mathrm{e}^{\mathrm{i}\theta}; \tau)$. If the input of the hold is a channel with $n_{\bar{u}}$ elements then the dimension of this subspace is $n_{\bar{u}}$ (at most). The ramification of this observation is:

Theorem 11.1 (Rank Theorem). Let $\mathcal{F} \in L^{\infty}$ and suppose that its frequency response kernel $\check{f}(\mathrm{e}^{\mathrm{i}\theta}; \tau, \sigma)$ is piecewise continuous. Then $\mathcal{F}$ is an HSP iff there is $r \in \mathbb{N}$ such that rank $\check{F}(\mathrm{e}^{\mathrm{i}\theta}) \leq r \; \forall \theta \in [-\pi, \pi]$. In this case $r \leq \min(n_{\bar{y}}, n_{\bar{u}})$ for any HSP implementation of $\mathcal{F}$, and HSP-implementations of $\mathcal{F}$ exist for which $r = n_{\bar{y}} = n_{\bar{u}}$.

Proof. See Appendix A. ∎

The assumption on piecewise continuity of the kernel avoids issues with Lebesgue measure but other than that it is not essential to the result. It is because of this Rank Theorem that of all representations of systems, the lifted frequency response is the most useful one, at least for the design problems considered in the remainder of this part.

12. Singular Values and Optimal HSP

Having characterized HSPs as having a uniform finite rank frequency response at each θ, the design of HSPs amounts to frequency-wise approximation of given operators by finite rank operators. This begs for a Schmidt decomposition of the operator to be approximated. A Schmidt decompositions is an operator version of the singular value decomposition, SVD.

Theorem 12.1. Let $\mathcal{G} \in L^{\infty}$ and suppose that $\check{G}(\mathrm{e}^{\mathrm{i}\theta})$ at almost every $\theta \in [-\pi, \pi]$ has SVD

$$\check{G}(\mathrm{e}^{\mathrm{i}\theta}) = \sum_{k \in \mathbb{N}} \sigma_k \langle \cdot, e_k \rangle_{\mathbb{L}} v_k$$

with $\{e_1, e_2, \ldots\}$ and $\{v_1, v_2, \ldots\}$ orthonormal in $\mathbb{L}$ and $\sigma_1 \geq \sigma_2 \geq \cdots \geq 0$ (depending on θ). If the HSP

$$\check{G}_{\mathrm{HSP}}(\mathrm{e}^{\mathrm{i}\theta}) = \sum_{k=1}^{r} \sigma_k \langle \cdot, e_k \rangle_{\mathbb{L}} v_k \quad (56)$$

is well defined, it minimizes $\|\mathcal{G} - \mathcal{F}_{\mathrm{HSP}}\|_{\infty}$ over all HSPs of rank $\leq r$, attaining $\|\mathcal{G} - \mathcal{F}_{\mathrm{HSP}}\|_{\infty} = \mathrm{ess\,sup}_{\theta \in (-\pi, \pi)} \sigma_{r+1}(\theta)$. If $\mathcal{G}$ has finite L^2-norm, then the HSP (56) minimizes $\|\mathcal{G} - \mathcal{F}_{\mathrm{HSP}}\|_2$ as well, attaining $\|\mathcal{G} - \mathcal{F}_{\mathrm{HSP}}\|_2^2 = \frac{1}{2\pi h} \int_{-\pi}^{\pi} \sum_{k=r+1}^{\infty} \sigma_k^2(\theta)\mathrm{d}\theta$.

Proof. The L^2-norm and L^{∞}-norm involve nonnegative integrals over frequency θ, see (30) and (29). So if $\check{G}_{\mathrm{HSP}}(\mathrm{e}^{\mathrm{i}\theta})$ minimizes the norms for every fixed frequency then it is optimal. The rest is standard. ∎

This theorem does not settle the potentially complicated matter of existence of such SVDs and whether or not the frequency-wise defined HSP (56) can be implemented. For the applications that we have in mind, however, the SVD of $\check{G}(\mathrm{e}^{\mathrm{i}\theta})$ exists and is explicit and the pointwise HSP can be implemented as convolutions.

Typically HSPs are not LCTI and it is not hard to formalize that the subset of HSPs that are LCTI form a set of measure zero. However if $\mathcal{G}$ is LCTI then often the optimal finite-rank approximation $\mathcal{F}_{\mathrm{HSP}}$ of $\mathcal{G}$ is LCTI as well. This follows from explicit representations in the next section but it can also be understood from the fact that the L^2 and L^{∞} system norms are invariant under continuous time shift:

Lemma 12.2. Given LCTI system $\mathcal{G}$, the minimizer $\mathcal{F}_{\mathrm{HSP}}$ of $\|\mathcal{G} - \mathcal{F}_{\mathrm{HSP}}\|_2$ or $\|\mathcal{G} - \mathcal{F}_{\mathrm{HSP}}\|_{\infty}$ over noncausal LDTI HSPs of given rank is LCTI if it is unique.

Proof. The L^2- and L^{∞} norms do not depend on shifts of input and output: $\|\Delta^{\tau}(\mathcal{G} - \mathcal{F}_{\mathrm{HSP}})\Delta^{-\tau}\| = \|\mathcal{G} - \mathcal{F}_{\mathrm{HSP}}\|$ where Δ^{τ} is delay operator ($\tau \in \mathbb{R}$). By continuous time-invariance of $\mathcal{G}$ the $\mathcal{F}_{\mathrm{HSP}}$ hence is optimal iff $\Delta^{-\tau}\mathcal{F}_{\mathrm{HSP}}\Delta^{\tau}$ is optimal for all $\tau \in \mathbb{R}$. ∎

Subsequently, we shall also need the following result:

Corollary 12.3. Let $\mathcal{G}$ be as in Theorem 12.2. Then the rank-r $\mathcal{F}_{\mathrm{HSP}}$ with frequency response $\check{F}_{\mathrm{HSP}}(\mathrm{e}^{\mathrm{i}\theta}) = \sum_{k=1}^{r} \langle \cdot, v_k \rangle_{\mathbb{L}} v_k$ minimizes both $\|(I - \mathcal{F}_{\mathrm{HSP}})\mathcal{G}\|_{\infty}$ and $\|(I - \mathcal{F}_{\mathrm{HSP}})\mathcal{G}\|_2$ (provided $\|\mathcal{G}\|_2 < \infty$) with respect to stable rank-r HSPs, attaining the same norms as in Theorem 12.1.

Proof. Then $\check{G}_{\mathrm{HSP}} := \check{F}_{\mathrm{HSP}}\check{G}$ equals (56). ∎

13. SVD of LCTI Systems—Frequency Folding

LCTI systems have an explicit fixed frequency SVD. This is very similar to what [43, p. 1770] derived in discrete time and for spectral densities. We need it for signal generators:

Lemma 13.1. Let $\mathcal{G} \in L^\infty \cap L^2$. Then $\check{G}(e^{i\theta})$ exists for almost every $\theta \in [-\pi, \pi]$ and has SVD

$$\check{G}(e^{i\theta}) = \sum_{k \in \mathbb{Z}} |G(i\omega_k)| \langle \cdot, e_k \rangle_{\mathbb{L}} v_k, \tag{57}$$

in which

$$e_k(\tau) := \frac{1}{\sqrt{h}} e^{i\omega_k \tau}, \quad k \in \mathbb{Z}, \tag{58}$$

is the standard orthonormal basis of $\mathbb{L}$ and $v_k := e_k e^{i \arg G(i\omega_k)}$. The singular values in this case are well defined at almost every θ and equal $\sigma_k(\theta) = |G(i\omega_k)|$, $k \in \mathbb{Z}$, modulo ordering.

Proof. By (16b) we have that the kernel of $\check{G}(e^{i\theta})$ equals

$$\check{g}(e^{i\theta}; \tau, \sigma) = \frac{1}{h} \sum_{k \in \mathbb{Z}} G(i\omega_k) e^{i\omega_k(\tau-\sigma)} \tag{59}$$

so its frequency response, mapping $\check{w}(e^{i\theta})$ to $\check{v}(e^{i\theta})$, reads

$$\check{v}(e^{i\theta}; \tau) = \frac{1}{h} \sum_{k \in \mathbb{Z}} \int_0^h G(i\omega_k) e^{i\omega_k(\tau-\sigma)} \check{w}(e^{i\theta}; \sigma) \, d\sigma$$

$$= \sum_{k \in \mathbb{Z}} G(i\omega_k) \langle \check{w}(e^{i\theta}), e_k \rangle_{\mathbb{L}} e_k(\tau).$$

Since the functions e_k are orthonormal in $\mathbb{L}$, the absolute values $|G(i\omega_k)|$ are the singular values (modulo order). The fact that $G \in L^2 \cap L^\infty$ implies the existence of singular values and, by Plancherel, that $\check{G}(e^{i\theta})$ has finite Hilbert-Schmidt norm almost everywhere. ∎

This establishes that the singular values of $\check{G}(e^{i\theta})$ are actually the magnitudes of the continuous-time frequency response $G(i\omega)$ at all its *aliased frequencies* ω_k. This can be visualized by folding the magnitude plot of $G(i\omega)$, see Fig. 11. Folding reduces the infinite frequency bands to the finite baseband $[0, \omega_N]$ and we end up with a zig-zag plot that at each $\theta/h = \omega_0 \in [0, \omega_N]$ captures its countably many singular values $\sigma_1, \sigma_2, \ldots$. Frequency folding is well known in the literature as a way to explain aliasing or to visualize the sampled spectrum [37, §6.1]. In the lifting approach we do not add up the $G(i\omega_k)$—which would result in the sampled spectrum and thus loose intersample information—but keep them as separate entities.

Example 13.2 (WKS-block). Consider the HSP of Fig. 12. It comprises the sinc sampler

$$\bar{y} = \mathcal{S}_{\text{sinc}}(y) : \quad \bar{y}[k] = \int_{-\infty}^{\infty} \frac{1}{h} \text{sinc}_h(kh - s) y(s) \, ds \tag{60}$$

(presented in the figure as the cascade of the ideal lowpass filter $\mathcal{F}_{\text{ilp}}$ and $\mathcal{S}_{\text{Idl}}$) and the sinc-hold

$$u = \mathcal{H}_{\text{sinc}}(\bar{u}) : \quad u(t) = \sum_{i \in \mathbb{Z}} \text{sinc}_h(t - ih) \bar{u}[i]. \tag{61}$$
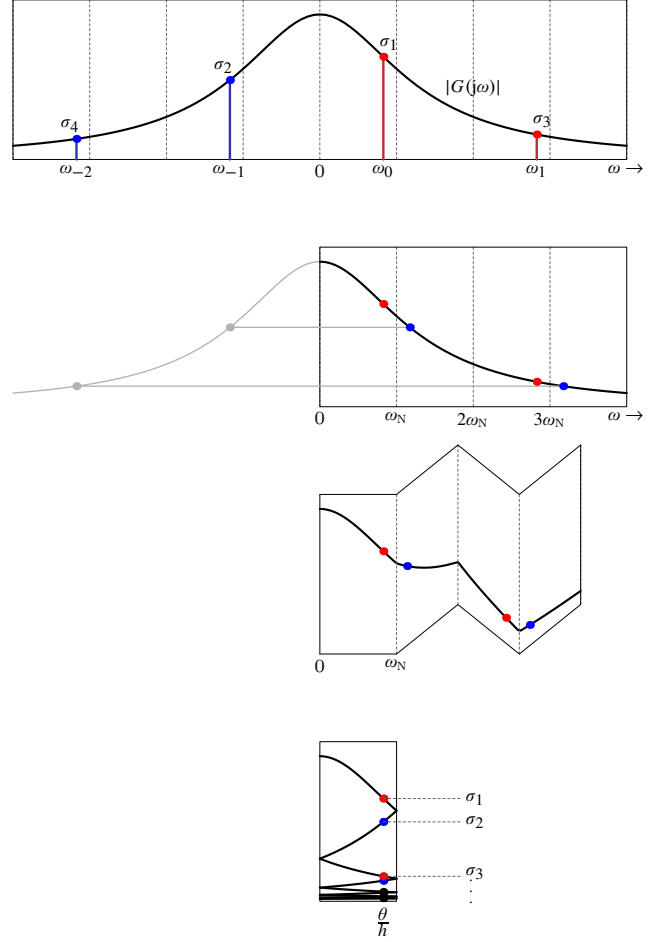

Figure 11: Frequency folding for LCTI systems: at each $\theta/h \in [0, \omega_N]$ the $\check{G}(e^{i\theta})$ has countably many singular values $\sigma_k = |\check{G}(e^{i\theta})|$, modulo ordering

Here $\xi := \mathcal{F}_{\text{ilp}} y$ is the projection of y into the space of ω_N-bandlimited signals. It follows from the Sampling Theorem that $u = \xi$ and, moreover, if y itself is ω_N-bandlimited, that we have perfect reconstruction, $u = y$. We call this system the *Whittaker-Kotel'nikov-Shannon* (WKS) block, and denote it as $\mathcal{F}_{\text{WKS}}$. According to (55) and (examples 4.9 and 4.10, the frequency response kernel of $\check{F}_{\text{WKS}}(e^{i\theta})$ is $\check{f}_{\text{WKS}}(e^{i\theta}; \tau, \sigma) = \check{\phi}_{\text{sinc}}(e^{i\theta}; \tau) \check{\psi}_{\text{sinc}}(e^{i\theta}; -\sigma) = \frac{1}{h} e^{i\theta(\tau-\sigma)/h}$. Note that this kernel has a Toeplitz structure. Together with the discrete-time invariance of $\mathcal{F}_{\text{WKS}}$, this implies that $\mathcal{F}_{\text{WKS}}$ is actually LCTI. This may appear remarkable, taking into account that generically HSPs are LDTI and typically not LCTI.

Alternatively, since the WKS-block is LCTI with the real frequency response $F(i\omega) = \mathbb{1}_{[-\omega_N, \omega_N]}(\omega)$ we have, according to Lemma 13.1, that $\check{F}(e^{i\theta}) = \langle \cdot, e_0 \rangle_{\mathbb{L}} e_0$ and that its frequency
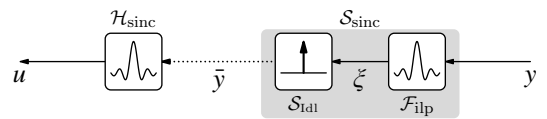

Figure 12: WKS hybrid signal processor

response kernel is $\check{f}(e^{i\theta}; \tau, \sigma) = e_0(\tau)e_0^*(\sigma) = \frac{1}{h}e^{i\theta(\tau-\sigma)/h}$. Indeed. $\triangledown$

14. Single-Channel Optimal SR

We are now in a position to formulate and solve a number of Type-IV signal reconstruction problems, i.e., problems where both sampler and hold are available for design.

In this section we return to the case that $\mathcal{G} := \mathcal{G}_v = \mathcal{G}_y$. The error system we write as $\mathcal{G}_e = (I - \mathcal{F}_{HSP})\mathcal{G} = \mathcal{G} - \mathcal{F}_{HSP}\mathcal{G}$ where $\mathcal{F}_{HSP} := \mathcal{HS}$. In this section we further restrict attention to single channel HSPs. Single-channel refers to the case that the sampled signal $\bar{y}$ is scalar, i.e., that we have only one sensor. The rank theorem thus states that rank $\check{F}_{HSP}(e^{i\theta}) \leq 1, \forall \theta \in [-\pi, \pi]$ for any such HSP. This clearly implies that the best we can do with our HSP is to match the directions and norm (Schmidt pair) corresponding to the largest singular value of $\check{G}(e^{i\theta})$ at each frequency θ and have a unit gain there. To simplify the outline, we assume that

$\mathbf{A_1}$: $\mathcal{G}$ is baseband dominant

(see Definition 10.3). $\mathbf{A_1}$ says that at each $\theta \in [-\pi, \pi]$ the largest singular value of $\check{G}(e^{i\theta})$ is attained in the baseband. By Corollary 12.3 and Lemma 13.1, the optimal rank-one $\check{F}(e^{i\theta})$ has the kernel

$$\check{f}_{HSP}(e^{i\theta}; \tau, \sigma) = v_0(\tau)v_0^*(\sigma) = \frac{1}{h}e^{i\theta(\tau-\sigma)/h},$$

meaning that the optimal HSP is actually $\mathcal{F}_{WKS}$. Thus, we just proved the following result:

Theorem 14.1. Suppose $\mathcal{G} \in L^\infty \cap L^2$ is LCTI and that it satisfies $\mathbf{A_1}$. Then the WKS block $\mathcal{F}_{WKS}$ considered in Example 13.2 is the HSP that minimizes both L^2 and L^∞ norms of $\mathcal{G}_e$, and the optimal performance indices are

$$\|(I - \mathcal{F}_{WKS})\mathcal{G}\|_2^2 = \frac{1}{\pi}\int_{\omega_N}^\infty |G(i\omega)|^2 \, d\omega \qquad (62)$$

in the L^2 case, and

$$\|(I - \mathcal{F}_{WKS})\mathcal{G}\|_\infty = \sup_{\omega > \omega_N} |G(i\omega)| \qquad (63)$$

in the L^∞ case.

This result is not new for the L^2-norm. It was derived earlier in [43] using similar methods, but then for the discrete time case. An elegant and entirely different derivation can be found in [44, p. 3593], again for the L^2 norm. Computation of the L^2 norm (62) can be done without gridding [28].

If $\mathcal{G}$ is *strict* baseband dominant then the optimal HSP is unique. Theorem 14.1 establishes that sinc-sampler (60) and sinc-hold (61) are optimal from both L^2 and L^∞ points of view. Interestingly, neither the optimal sampler nor the optimal hold depends on $\mathcal{G}$ as long as $\mathcal{G}$ is baseband dominant. Clearly under the baseband dominance assumption the norm of the reconstruction error is zero iff $G(i\omega) = 0$ almost everywhere outside the baseband $[-\omega_N, \omega_N]$. This is the classic Sampling Theorem.

If $\mathcal{G}$ is not baseband-dominant then the optimal $\mathcal{F}_{HSP}$ should account for frequency band(s) in which the frequency response

gain of $\mathcal{G}$ is dominant. In this case, the optimal sampler comprises the ideal sampler and an ideal passband filter. The frequency pattern of the latter might be rather complicated. Also, the perfect reconstruction conditions will be different in this case. The sampled signal need no longer have zero frequency content outside the baseband. Rather, we should require that $G(i\omega_k) \neq 0$ for at most one k (which is not necessarily $k = 0$). The optimal $\mathcal{F}_{HSP}$ is nonetheless selfadjoint, consistent and LCTI and its classic Fourier transform is piecewise constant having value 0 or 1, a so called brickwall filter [43].

Remark 14.2. It is straightforward to extend these ideas to multi-input-multi-output (MIMO) systems $\mathcal{G}$. In such cases, $\check{G}(i\omega_k)$ is a matrix and, for every k, has a finite number of singular values $\sigma_{k,n}(\theta)$, $n \in \mathbb{N}$, with respect to the standard Euclidean norm. Thus, at each $\theta \in [0, \pi]$ we end up with doubly indexed singular values, but the task of the HSP remains the same: to delete the largest singular value. The optimal HSP is again a (modulated) WKS-block, but then pre- and post processed by MIMO LCTI systems that select, so the say, the direction of the largest singular value of G. $\triangledown$

14.1. Fundamental Limit for Error-Free Reconstruction

The optimal mapping $\mathcal{F}_{HSP}$ selects frequency bands where $|G(i\omega)|$ is maximal and with that in mind one can obtain the upper bound

$$\|\mathcal{F}_{HSP}\mathcal{G}\|_2^2 \leq \|\mathcal{G}\|_\infty^2/h$$

and that the upper bound is tight (in a ratio sense) if $h \to \infty$ [28]. By orthogonality we also have the upper bound

$$\|\mathcal{F}_{HSP}\mathcal{G}\|_2^2 \leq \|\mathcal{G}\|_2^2.$$

The two upper bounds meet at

$$h_G := \|\mathcal{G}\|_\infty^2/\|\mathcal{G}\|_2^2,$$

which has an interesting property:

**Lemma 14.3.** Whatever $\mathcal{G}$ is, error free reconstruction is impossible for $h > h_G$. $\triangledown$

This follows from the lower bound on the error reconstruction, $\|\mathcal{G}_e\|_2^2 = \|\mathcal{G}\|_2^2 - \|\mathcal{F}_{HSP}\mathcal{G}\|_2^2 \geq \|\mathcal{G}\|_2^2 - \|\mathcal{G}\|_\infty^2/h = \|\mathcal{G}\|_2^2(1 - h_G/h)$. Stated differently, the "signal-to-error ratio" (SER) is bounded from above by

$$\text{SER} := \frac{\|\mathcal{G}\|_2^2}{\|\mathcal{G}_e\|_2^2} \leq \frac{1}{1 - h_G/h}, \quad \forall h > h_G.$$

Also the L^∞ norm gives rise to limitations on perfect reconstruction. In fact, for certain values of h the L^∞ norm may not be reducible at all if $|G(i\omega)|$ is not monotonically decaying. Indeed, suppose that the peak value of $|G(i\omega)|$ is attained at some frequency, called resonance frequency,

$$\omega_{res} := \arg\max_{\omega>0} |G(i\omega)|.$$

Suppose further that we sample at an integer fraction of the resonance frequency, i.e., at $\omega_N = \omega_{res}/k$, for some $k \in \mathbb{N}$ Then folding of $|G(i\omega)|$ shows that there are two (or more) singular values σ_k equal to $\|\mathcal{G}\|_\infty$ at either $\omega = 0$ or $\omega = \omega_N$:
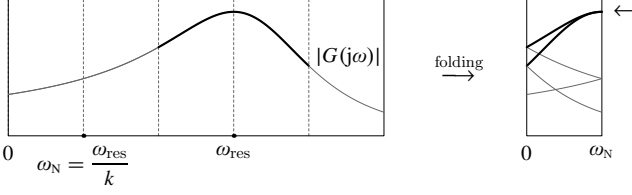
Since a single channel hybrid signal processor can cancel only one singular value, the largest singular value can not be reduced at all in this case and therefore we have:

Lemma 14.4. If $|G(i\omega)|$ is continuous and $\omega_{\text{res}} > 0$ then sampling with $\omega_N = \omega_{\text{res}}/k$ is futile: $\|\mathcal{G}_e\|_\infty = \|\mathcal{G}\|_\infty$ is the best we can do and $\mathcal{F}_{\text{HSP}} = 0$ is an L^∞-optimal solution. $\triangledown$

Example 14.5 (Resonance peaks). Consider the second order LCTI system $\mathcal{G}$ with resonance peak near $\omega = 1$,

$$G(i\omega) = \frac{1}{(i\omega + .2)^2 + 1}$$

Because of the peak, the reconstruction errors norms $\|\mathcal{G}_e\|_2$ and $\|\mathcal{G}_e\|_\infty$ need not be monotonous in the sampling period h, and indeed they are not: Fig. 13 shows the numerically computed $\|\mathcal{G}_e\|_2^2$ and $\|\mathcal{G}\|_\infty$ as a function of h. The reconstruction error norms converges to zero as $h \to 0$ and converge to $\|\mathcal{G}\|_2$ and $\|\mathcal{G}\|_\infty$ respectively as $h \to \infty$. In this example the fundamental time limit is $h_G = \|\mathcal{G}\|_\infty^2 / \|\mathcal{G}\|_2^2 = \frac{2.5^2}{125/104} = 5.2$ exactly. As predicted, the L^∞ norm can not be reduced if $\omega_N = \omega_{\text{res}}/k \approx 1/k$, that is, if $h = k\pi/\omega_{\text{res}} \approx k\pi$. As Fig. 13 suggests also the
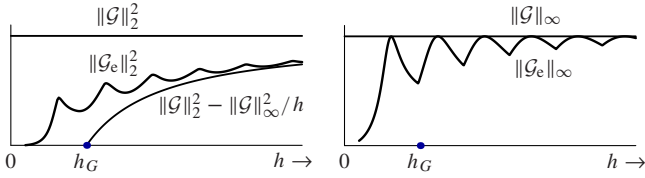

Figure 13: Optimal $\|\mathcal{G}_e\|_2^2$ (left) and $\|\mathcal{G}_e\|_\infty$ (right) as a function of h

L^2 norm is close to a local maximum at these values. This can be interpreted as being close to pathological sampling (see next subsection). $\triangledown$

14.2. Unstable Signal Generators and Pathological Sampling

To avoid technicalities it was assumed so far that the signal generator $\mathcal{G}$ is stable. But it is tempting to consider unstable signal generators as well. Bypassing the mathematical difficulties (this will be fixed later), suppose that $G(s)$ has several imaginary poles. Clearly after folding we end up with a two or more infinite singular values (poles) at some θ iff

$$\omega_a - \omega_b = 2k\omega_N \quad \text{for some poles } i\omega_a \neq i\omega_b \text{ of } G(s)$$

and certain $k \in \mathbb{Z}$. This situation is known as *pathological sampling* and it is the case when controllability and/or observability may be lost after standard discretization of a system in state

space [21]. Since an HSP can delete only one singular value, one expects that no HSP can achieve a finite norm if we have pathological sampling. If, on the other hand, no such ω_a, ω_b, and k exist then no two poles overlap after folding, and then an HSP can be found that deletes all infinite singular values (poles), rendering the error system stable. This is indeed the case. For technical reasons we formulate the result for rational $G(s)$ only:

Lemma 14.6. Suppose $G(s)$ is rational and strictly proper, but possibly with imaginary poles. Then a single channel HSP exists that renders $(I - \mathcal{F}_{\text{HSP}})\mathcal{G}$ stable iff h is not pathological with respect to $G(s)$. In that case any brick-wall filter $\check{F}_{\text{HSP}}(e^{i\theta})$ that at each θ cancels the largest singular value $\sigma_{\max}(\theta)$ of $\check{G}(e^{i\theta})$ (and leaves the other singular values unaffected) is an L^2 optimal rank-1 HSP.

Proof. See Appendix A. ∎

In particular, for the integrators $G(s) = 1/s^n$ the WKS-block once again is optimal under all $h > 0$ (no pathological sampling in this case).

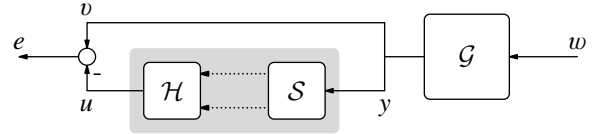## 15. Multichannel SR, Shannon Extension

Figure 14: Two-channel SR setup (Section 15)

Next we consider the setup depicted in Fig. 14. It is the case where we have two channels, i.e., *two* samplers and two holds. The HSP in this case has the form $\mathcal{F}_{\text{HSP}} = \mathcal{F}_{\text{HSP1}} + \mathcal{F}_{\text{HSP2}}$ for some *scalar* HSPs $\mathcal{F}_{\text{HSP1}}$ and $\mathcal{F}_{\text{HSP2}}$. This leads to the following rank constraint: rank $\check{F}_{\text{HSP}}(e^{i\theta}) \leq 2 \quad \forall \theta \in [-\pi, \pi]$. Assuming $2\omega_N$-baseband dominance of $\mathcal{G}$ and following the arguments of the previous section, we obtain the optimal HSP in terms of its lifted frequency response kernel as

$$\check{f}_{\text{HSP}}(e^{i\theta}; \tau, \sigma) = \frac{1}{h}\big(e^{i\omega_0(\tau - \sigma)} + e^{i\omega_{-1}(\tau - \sigma)}\big), \quad (64)$$

for $\theta \geq 0$ (the negative part follows by symmetry using the assumption that the system is real) and that the optimal L^2 and L^∞ performance indices are as in (62) and (63) with ω_N replaced by $2\omega_N$. The optimal HSP is again LCTI and its frequency response is $F_{\text{HSP}}(i\omega) = \mathbb{1}_{[-2\omega_N, 2\omega_N]}(\omega)$.

Expression (64) does not determine optimal $\mathcal{F}_{\text{HSP1}}$ and $\mathcal{F}_{\text{HSP2}}$ unambiguously. In fact, there is an infinite number of possible combinations in this case. Yet it is clear that we have perfect reconstruction iff we sample at half the Nyquist rate or faster, i.e., iff $G(i\omega)$ is zero outside $[-2\omega_N, 2\omega_N]$ (given the assumed $2\omega_N$-baseband dominance). In other words there are two scalar HSPs that, combined, can perfectly reconstruct any ω_b-bandlimited signal if *and only if* $\omega_b < 2\omega_N$.

The optimal kernel (64) naturally splits into two channels by decomposing it as

$$
\begin{aligned}
\check{f}_{\text{HSP}}(e^{i\theta}; \tau, \sigma) &= \frac{1}{h}\left(e^{i\omega_0(\tau-\sigma)} + e^{i\omega_{-1}(\tau-\sigma)}\right) \\
&= \begin{bmatrix} e^{i\omega_0\tau} & e^{i\omega_{-1}\tau} \end{bmatrix} \begin{bmatrix} \frac{1}{h}e^{-i\omega_0\sigma} \\ \frac{1}{h}e^{-i\omega_{-1}\sigma} \end{bmatrix} \\
&= \begin{bmatrix} \phi_1(e^{i\theta}) & \phi_2(e^{i\theta}) \end{bmatrix} \begin{bmatrix} \psi_1(e^{i\theta}) \\ \psi_2(e^{i\theta}) \end{bmatrix}
\end{aligned} \tag{65}
$$

with hold and sampling functions defined as

$$
\begin{bmatrix} \phi_1(e^{i\theta}) & \phi_2(e^{i\theta}) \end{bmatrix} = \begin{bmatrix} e^{i\omega_0\tau} & e^{i\omega_{-1}\tau} \end{bmatrix}
$$
$$
\begin{bmatrix} \psi_1(e^{i\theta}) \\ \psi_2(e^{i\theta}) \end{bmatrix} = \frac{1}{h}\begin{bmatrix} e^{-i\omega_0\sigma} \\ e^{-i\omega_{-1}\sigma} \end{bmatrix}.
$$

This corresponds to one channel $\mathcal{H}_1\mathcal{S}_1$ being the standard WKS-block and the other channel $\mathcal{H}_2\mathcal{S}_2$—its modulated version. Many other splittings exist. In fact (65) holds true for

$$
\begin{bmatrix} \phi_1(e^{i\theta}) & \phi_2(e^{i\theta}) \end{bmatrix} = \begin{bmatrix} e^{i\omega_0\tau} & e^{i\omega_{-1}\tau} \end{bmatrix} \bar{A}^{-1}(\theta) \tag{66}
$$
$$
\begin{bmatrix} \psi_1(e^{i\theta}) \\ \psi_2(e^{i\theta}) \end{bmatrix} = \bar{A}(\theta)\frac{1}{h}\begin{bmatrix} e^{-i\omega_0\sigma} \\ e^{-i\omega_{-1}\sigma} \end{bmatrix} \tag{67}
$$

for any 2×2 discrete system $\bar{A}(\theta)$ that is bistable (stable and having stable inverse). This way the two channels could by time varying (as continuous time systems) while we know that their sum is LCTI. An interesting and still rather general splitting is depicted in Fig. 15. Here the signal y is first given to the
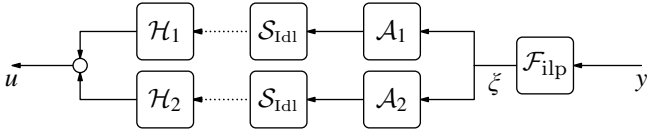

Figure 15: Alternative implementation of a two-channel HSP

ideal lowpass filter $\mathcal{F}_{\text{ilp}}$ with the cut-off frequency $2\omega_N$. With this choice, we do not need to prefilter measurements if they are already $2\omega_N$-bandlimited. The outcome is then fed to two different LCTI filters $\mathcal{A}_1$ and $\mathcal{A}_2$ followed by ideal samplers and then two holds. This corresponds to the case that

$$
\bar{A}(\theta) = \begin{bmatrix} A_1(i\omega_0) & A_1(i\omega_{-1}) \\ A_2(i\omega_0) & A_2(i\omega_{-1}) \end{bmatrix} \tag{68}
$$

if $\theta > 0$ (see Appendix A for a derivation).

Example 15.1 (Samples with derivatives). If $\mathcal{A}_1$ is the identity and $\mathcal{A}_2$ the differentiator we get a mixing matrix

$$
\bar{A}(\theta) = \begin{bmatrix} 1 & 1 \\ i\omega_0 & i\omega_{-1} \end{bmatrix}.
$$

This matrix has constant nonzero determinant $-i2\pi/h$. The hold functions (66) now become (for $\theta \in [0, \pi]$)

$$
\begin{aligned}
&\begin{bmatrix} \phi_1(e^{i\theta}) & \phi_2(e^{i\theta}) \end{bmatrix} \\
&= \begin{bmatrix} e^{i\omega_0\tau} & e^{i\omega_{-1}\tau} \end{bmatrix} A^{-1}(\theta) \\
&= \begin{bmatrix} \dfrac{e^{i\omega_0\tau}i\omega_{-1} - e^{i\omega_{-1}\tau}i\omega_0}{-i2\pi/h} & \dfrac{-e^{i\omega_0\tau} + e^{i\omega_{-1}\tau}}{-i2\pi/h} \end{bmatrix}.
\end{aligned}
$$

The inverse Fourier transformation subsequently yields (see Example 4.6] for ϕ_1) the two hold functions

$$
\phi_1(t) = \text{sinc}_h^2(t), \qquad \phi_2(t) = t\,\text{sinc}_h^2(t)
$$

and we get the well known reconstruction formula

$$
f(t) = \sum_{k\in\mathbb{Z}} \phi_1(t - kh)f(kh) + \phi_2(t - kh)f'(kh)
$$

provided $f(t)$ is $2\omega_N$-bandlimited. $\qquad\qquad \triangledown$

For two channels the mixing matrix $\bar{A}(\theta)$ is 2×2. It is straightforward to extend the ideas to more than two channels. For instance when M derivative samples, $y^{(i)}(kh)$ for $i = 0, \ldots, M - 1$, are available etcetera. The formulae are unwieldy though.

For recurring non-uniform sampling the method recovers Yen's original work [54]. In this case the formulae are manageable for any M:

Example 15.2 (Recurring non-uniform sampling). If $\mathcal{A}_1$ is the identity and $\mathcal{A}_2$ the T-delay operator $A_2(i\omega) = e^{-iT\omega}$ then the mixing matrix (68) becomes the Vandermonde matrix

$$
\bar{A}(\theta) = \begin{bmatrix} 1 & 1 \\ e^{-iT\omega_0} & e^{-iT\omega_{-1}} \end{bmatrix} \quad \text{for } \theta \in [0, \pi].
$$

It is invertible iff the delay T is not a multiple of the sampling period h, in which case

$$
\bar{A}^{-1}(\theta) = \frac{1}{e^{-iT\omega_{-1}} - e^{-iT\omega_0}} \begin{bmatrix} e^{-iT\omega_{-1}} & -1 \\ -e^{-iT\omega_0} & 1 \end{bmatrix}.
$$

Direct inverse Fourier transformation of (66) now yields the optimal hold functions

$$
\phi_1(t) = \text{sinc}_h(t)\frac{\sin(\omega_N(t + T))}{\sin(\omega_N T)}, \quad \phi_2(t) = \phi_1(-t - T)
$$

see Fig. 16. This $\phi_1(t)$ is the unique[6] $2\omega_N$-bandlimited signal that is 1 at $t = 0$ and is 0 at both all other sampling instances, kh, $k \neq 0$, and delayed sampling instances $kh - T$, $k \in \mathbb{Z}$. By symmetry $\phi_2(t) = \phi_1(-t - T)$ has comparable interpolation properties, see Fig. 16.
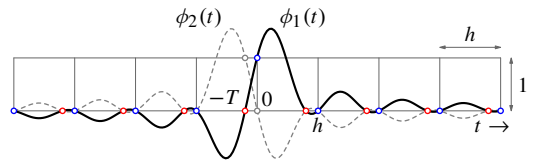
Figure 16: Optimal hold functions for $M = 2$ (Example 15.2)

If instead of 2 we have M samples every $[hk, hk + h)$ at $t = hk + T_1$, $t = hk + T_2, \ldots, t = hk + T_M$ then the M optimal sampling functions $\phi_1, \ldots, \phi_M$ are [54]

$$
\phi_n(t) = \text{sinc}_h(t + T_n)\prod_{k\neq n}\frac{\sin(\omega_N(t + T_k))}{\sin(\omega_N(-T_n + T_k))}.
$$

---

[6]Since $\mathcal{G}_{\text{e,opt}} = 0$ for any $\mathcal{G}_v$ that is $2\omega_N$-bandlimited, we have that $\mathcal{H}\mathcal{S} = I$ when restricted to $2\omega_N$-bandlimited signals. Suppose η and ζ are two $2\omega_N$-bandlimited signals with the same samples, then $\zeta = \mathcal{H}\mathcal{S}\zeta = \mathcal{H}\mathcal{S}\eta = \eta$ i.e., then they are the same.

Indeed, they satisfy the interpolation conditions and are $M\omega_{\mathrm{N}}$-bandlimited by the fact that they are M products of ω_{N}-bandlimited signals, and thus they are the solutions we seek (provided $\mathcal{G}$ is $M\omega_{\mathrm{N}}$-band dominant). $\triangledown$

Besides [54] the results in this section bears close resemblance with the generalized sampling theorems of [34], with the difference that [34] assumes from the outset that the signal is sufficiently bandlimited. Paper [50] treats the same problem but then aims at consistent rather than norm-optimal HSPs. This, however, is closely related to norm-optimality because consistency is an interpolation condition and in Footnote 6 we saw that norm-optimality under certain assumptions is equivalent to an interpolation condition.

16. Downsampling

Consider again the case $\mathcal{G} := \mathcal{G}_v = \mathcal{G}_y$, but now assume that it is itself an HSP,

$$\mathcal{G} = \mathcal{H}_{h'}\mathcal{S}_{h'} \qquad (69)$$

with a sampling period h' different from h. To maintain h-periodicity we assume that this sampling period is an integer fraction of h,

$$h' = h/m, \qquad \text{for some } m \in \mathbb{N}.$$

The problem is to find a single channel $\mathcal{F}_{\mathrm{HSP}}$ with sampling period h that minimizes the L^2 or L^∞ norm of the error system $\mathcal{G}_{\mathrm{e}}$. In the present context this is an example of downsampling by a factor m. System (69) has kernel $g(t,s) = \sum_{k\in\mathbb{Z}} \phi_{h'}(t - kh')\psi_{h'}(kh' - s)$ and it can be seen as the superposition of m advanced-delayed h-periodic systems, $g(t,s) = \sum_{n=0}^{m-1}\sum_{k\in\mathbb{Z}} \phi_{h'}(t - nh' - kh)\psi_{h'}(nh' + kh - s)$. It has frequency response kernel

$$\breve{g}(\mathrm{e}^{\mathrm{i}\theta}; \tau, \sigma) = \sum_{n=0}^{m-1} \breve{\phi}_{h'}(\mathrm{e}^{\mathrm{i}\theta}; \tau - nh')\breve{\psi}_{h'}(\mathrm{e}^{\mathrm{i}\theta}; -(\sigma - nh')).$$

Using the Key Lifting Formula for the sampling function ψ shows that

$$\breve{g}(\mathrm{e}^{\mathrm{i}\theta}; \tau, \sigma) = \sum_{k\in\mathbb{Z}}\left(\sum_{n=0}^{m-1} \phi_{h'}(\mathrm{e}^{\mathrm{i}\theta}; \tau - nh')\mathrm{e}^{-n\mathrm{i}\omega_k h'}\right)$$
$$\times \Psi(\mathrm{i}\omega_k)\frac{1}{h}\mathrm{e}^{-\mathrm{i}\omega_k\sigma}.$$
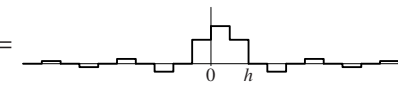
Since $\mathcal{G}$ is not LCTI it is not immediate what the fixed-frequency SVD (Lemma 13.1) is, but for certain examples of $\mathcal{G}$ it can be done:

Example 16.1 (Downsampling by factor 2**).** Let $m = 2$ and $\mathcal{G} = \mathcal{H}_{\mathrm{ZOH}}\mathcal{S}_{\mathrm{Idl}}\mathcal{G}_{\mathrm{ilp}}$, where the ideal sampler $\mathcal{S}_{\mathrm{Idl}}$ and the zero-order hold $\mathcal{H}_{\mathrm{ZOH}}$ have the sampling period $h/2$ and $\mathcal{G}_{\mathrm{ilp}}$ is the ideal lowpass filter with bandwidth $2\omega_{\mathrm{N}}$. By the bandlimitness
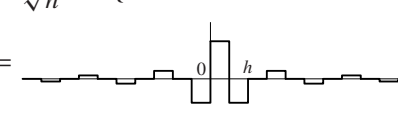
of the prefilter we have, for $\theta \in [0, \omega_{\mathrm{N}}]$,

$$\breve{g}(\mathrm{e}^{\mathrm{i}\theta}; \tau, \sigma) = \sum_{k=1,2}\left(\sum_{n=0,1} \phi_{h'}(\mathrm{e}^{\mathrm{i}\theta}; \tau - nh')\mathrm{e}^{-n\mathrm{i}\omega_k h'}\right)$$
$$\times \Psi(\mathrm{i}\omega_k)\frac{1}{h}\mathrm{e}^{-\mathrm{i}\omega_k\sigma}$$
$$= \underbrace{\begin{bmatrix} \mathbb{1}_{[0,\frac{h}{2}]}(\tau) & \mathbb{1}_{[\frac{h}{2},h]}(\tau) \end{bmatrix}\begin{bmatrix} 1 & 1 \\ \mathrm{e}^{\mathrm{i}\theta/2} & -\mathrm{e}^{\mathrm{i}\theta/2} \end{bmatrix}}_{V(\theta)}$$
$$\times \begin{bmatrix} \Psi(\mathrm{i}\omega_0) & 0 \\ 0 & \Psi(\mathrm{i}\omega_1) \end{bmatrix}\begin{bmatrix} \frac{1}{h}\mathrm{e}^{-\mathrm{i}\omega_0\sigma} \\ \frac{1}{h}\mathrm{e}^{-\mathrm{i}\omega_1\sigma} \end{bmatrix}. \quad (70)$$

The two shifted hold functions $\mathbb{1}_{[0,h/2]}(\tau)$ and $\mathbb{1}_{[h/2,h]}(\tau)$ have non-overlapping support and therefore are orthogonal (and with the same $\mathbb{L}$-norm of $\sqrt{h/2}$), making the $V(\theta)$ defined above orthogonal at each θ and $V'(\theta)V(\theta) = hI_2$. Equation (70) at each θ is therefore an SVD with singular values $\{h|\Psi(\mathrm{i}\omega_0)|, h|\Psi(\mathrm{i}\omega_1)|\}$. By Corollary 12.3, the optimal HSP should cancel the largest singular value. If Ψ is baseband dominant then according to this corollary $\breve{F}_{\mathrm{HSP}}(\mathrm{e}^{\mathrm{i}\theta}) = \langle\cdot, v_1\rangle_{\mathbb{L}} v_1$ with v_1 the θ dependent first column of $V(\theta)$ normalized to have $\mathbb{L}$-norm 1. That is, its kernel is $f_{\mathrm{HSP}}(t,s) = \phi(t)\phi(s)$ with optimal hold and sampler equal to the inverse Fourier transform of the first column of V (scaled by $\sqrt{h}$ for orthonormality),

$$\phi(t) = \psi(t) = \frac{1}{\sqrt{h}}\mathfrak{F}^{-1}\{V_1\}$$
$$= \frac{1}{\sqrt{h}}\mathfrak{F}^{-1}\left\{\mathbb{1}_{[0,h/2]}(\tau) + \mathbb{1}_{[h/2,h]}(\tau)\mathrm{e}^{\mathrm{i}\theta/2}\right\}$$
$$= \frac{1}{\sqrt{h}}\left(\mathbb{1}_{[0,h/2]}(t) + \sum_{k\in\mathbb{Z}}\mathrm{sinc}_1(k + \tfrac{1}{2})\mathbb{1}_{[h/2,h]}(t - kh)\right)$$
$$=$$

The optimal HSP is $\mathcal{S}^*\mathcal{S} = \mathcal{H}\mathcal{H}^*$. In the somewhat special case that Ψ is passband dominant in the sense that the second band is dominant, that is, $|\Psi(\mathrm{i}\omega_1)| \geq |\Psi(\mathrm{i}\omega_{k\neq 1})|, \forall\theta \in [0, \pi)$, then we should select the second column of V, rendering the optimal hold/sampler equal to

$$\phi(t) = \psi(t) = \frac{1}{\sqrt{h}}\mathfrak{F}^{-1}\{V_2\}$$
$$= \frac{1}{\sqrt{h}}\mathfrak{F}^{-1}\left\{\mathbb{1}_{[0,h/2]}(\tau) - \mathbb{1}_{[h/2,h]}(\tau)\mathrm{e}^{\mathrm{i}\theta/2}\right\}$$
$$=$$

The hold function is unique (modulo frequency dependent scaling that could be absorbed into the sampler or discrete filter) but the sampler is not unique in this case because the signal generator is singular. Neither $\mathcal{G}$ nor the optimal HSP is LCTI. $\triangledown$

17. SR with Noisy Measurements

In the final section of this part we consider the case that the signal y available for sampling is corrupted by colored noise. This very common situation can be modeled as in Fig. 17 where n is the colored noise which is seen as the output of a system $\mathcal{W}$ driven by white noise w_n, assumed to be independent of w_v which drives the system $\mathcal{G}$ that generates the signal v that we aim to reconstruct. This problem is reminiscent of Wiener filtering with the sole difference that we restrict the filters to HSPs. The error system is

$$\mathcal{G}_{\mathrm{e}} = \begin{bmatrix} \mathcal{G} & 0 \end{bmatrix} - \mathcal{F}_{\mathrm{HSP}} \begin{bmatrix} \mathcal{G} & \mathcal{W} \end{bmatrix} \qquad (71)$$

which is the mapping from (w_v, w_n) to the reconstruction error $e = v - u$. The L^∞ norm of $\mathcal{G}_{\mathrm{e}}$ corresponds to the worst-case energy of e under all v and n satisfying $\frac{|v(\mathrm{i}\omega)|^2}{|G(\mathrm{i}\omega)|^2} + \frac{|n(\mathrm{i}\omega)|^2}{|W(\mathrm{i}\omega)|^2} \leq 1$ (this, in turn, requires that the spectral densities of v and n are bounded by $|G|^2$ and $|W|^2$, respectively). The signal generators $\mathcal{G}$ and $\mathcal{W}$ are real LCTI systems, and we assume that their sum of spectra is positive everywhere:

$\mathbf{A_2}$: $|G(\mathrm{i}\omega)|^2 + |W(\mathrm{i}\omega)|^2 > 0$ for all ω.

This assumption guarantees that the optimization problems are non-singular.

The requirement that $\mathcal{F}_{\mathrm{HSP}}$ is an HSP can be viewed as a structural constraint imposed on the reconstructor (estimator). This suggests that the problem can be addressed via the solution of the unconstrained problems, where the L^2 or L^∞ norms of the error system (71) are minimized by an analog filter $\mathcal{G}$ (not necessarily an HSP). We thus start with the latter problem, following the ideas of [14].

First, recall that the L^2-norm of $\mathcal{G}_{\mathrm{e}}$, $\|\mathcal{G}_{\mathrm{e}}\|_2$, is the square root of the (operator) trace of $\mathcal{G}_{\mathrm{e}}\mathcal{G}_{\mathrm{e}}^*$ and the L^∞-norm of the error system $\|\mathcal{G}_{\mathrm{e}}\|_\infty \leq \gamma$ iff $\mathcal{G}_{\mathrm{e}}\mathcal{G}_{\mathrm{e}}^* \leq \gamma^2 I$ [14]. This is to say that the system $\mathcal{G}_{\mathrm{e}}\mathcal{G}_{\mathrm{e}}^*$ plays a central role in both optimization problems. Now,

$$\begin{aligned} \mathcal{G}_{\mathrm{e}}\mathcal{G}_{\mathrm{e}}^* &= (I - \mathcal{F})\mathcal{G}\mathcal{G}^*(I - \mathcal{F})^* + \mathcal{F}\mathcal{W}\mathcal{W}^*\mathcal{F}^* \\ &= \mathcal{G}\mathcal{G}^* - \mathcal{F}\mathcal{G}\mathcal{G}^* - \mathcal{G}\mathcal{G}^*\mathcal{F}^* + \mathcal{F}(\mathcal{G}\mathcal{G}^* + \mathcal{W}\mathcal{W}^*)\mathcal{F}^* \\ &= \mathcal{Q} + (\mathcal{G}\mathcal{G}^*\mathcal{R}^{-1} - \mathcal{F})\mathcal{R}(\mathcal{G}\mathcal{G}^*\mathcal{R}^{-1} - \mathcal{F})^*, \end{aligned} \qquad (72)$$

where $\mathcal{R} := \mathcal{G}\mathcal{G}^* + \mathcal{W}\mathcal{W}^*$ is invertible by $\mathbf{A_2}$ and, in fact, $\mathcal{G}\mathcal{G}^*\mathcal{R}^{-1}$ is then well defined and stable. Also,

$$\mathcal{Q} := \mathcal{G}(I - \mathcal{G}^*\mathcal{R}^{-1}\mathcal{G})\mathcal{G}^* = \mathcal{G}\mathcal{G}^*\mathcal{R}^{-1}\mathcal{W}\mathcal{W}^*.$$

As no causality constraints are imposed, it is readily seen [14] that the optimal solution in both L^2 and L^∞ cases is $\mathcal{F} = \mathcal{F}_{\mathrm{wiener}} := \mathcal{G}\mathcal{G}^*\mathcal{R}^{-1} = \mathcal{G}\mathcal{G}^*(\mathcal{G}\mathcal{G}^* + \mathcal{W}\mathcal{W}^*)^{-1}$ (in the L^∞ case it might be non-unique). This is the classic LCTI Wiener filter.
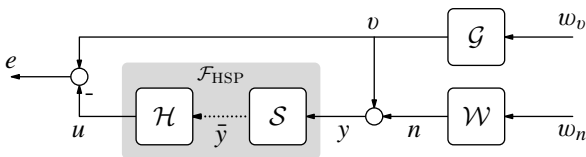

Figure 17: Setup for SR with noisy measurements (Section 17)

It is not necessarily an HSP and in fact it generally is not an HSP, and as such $\mathcal{F}_{\mathrm{wiener}}$ is not the solution we seek.

Important is that (72) can be used to reduce the original signal reconstruction problem to a simpler problem, similar to the noise-free problem studied in Section 14. This reduction, however, is different in the L^2 and L^∞ cases.

17.1. L^2 Optimization

Because of the linearity of the operator trace, (72) gives that

$$\|\mathcal{G}_{\mathrm{e}}\|_2^2 = \|\mathcal{Q}^{1/2}\|_2^2 + \|(\mathcal{F}_{\mathrm{wiener}} - \mathcal{F})\mathcal{R}^{1/2}\|_2^2. \qquad (73)$$

Hence, the L^2 signal reconstruction problem is equivalent to the problem of

$$\min_{\mathcal{F}_{\mathrm{HSP}}} \| \underbrace{\mathcal{F}_{\mathrm{wiener}}\mathcal{R}^{1/2}}_{\mathcal{G}_2} - \underbrace{\mathcal{F}_{\mathrm{HSP}}\mathcal{R}^{1/2}}_{\mathcal{F}_2} \|_2, \qquad (74)$$

which is a one-block problem. In the noise-free setting, the systems $\mathcal{R}^{1/2}$ and $\mathcal{F}_{\mathrm{wiener}}$ should be replaced with $\mathcal{G}$ and I, respectively. The presence of $\mathcal{R}^{1/2}$ and $\mathcal{F}_{\mathrm{wiener}}$ does not lead to any conceptual difference though. By the invertibility of $\mathcal{R}^{1/2}$ the series interconnection $\mathcal{F}_2$ is a rank-1 HSP iff $\mathcal{F}_{\mathrm{HSP}}$ is. Now the optimal rank-1 approximation $\mathcal{F}_2$ of an LCTI system $\mathcal{G}_2$ is itself LCTI and therefore the optimal rank-1 $\mathcal{F}_{\mathrm{HSP}} = \mathcal{F}_2\mathcal{R}^{-1/2}$ is LCTI as well. To circumvent exotic HSPs we again assume baseband dominance:

$\mathbf{A_3}$: $\mathcal{G}_2 = \mathcal{G}\mathcal{G}^*(\mathcal{G}\mathcal{G}^* + \mathcal{W}\mathcal{W}^*)^{-1/2}$ is baseband dominant.

The singular values of $\breve{G}_2(\mathrm{e}^{\mathrm{i}\theta})$ at each θ can be expressed as

$$\sigma_k = \frac{|G(\mathrm{i}\omega_k)|^2}{\sqrt{|G(\mathrm{i}\omega_k)|^2 + |W(\mathrm{i}\omega_k)|^2}} = |G(\mathrm{i}\omega_k)|\sqrt{\frac{\rho(\omega_k)}{1 + \rho(\omega_k)}},$$

where

$$\rho(\omega) := \frac{|G(\mathrm{i}\omega)|^2}{|W(\mathrm{i}\omega)|^2} \qquad (75)$$

can be interpreted as the signal-to-noise ratio spectrum.

Given $\mathbf{A_3}$, the $F_2(\mathrm{i}\omega)$ that minimizes (74) equals $G_2(\mathrm{i}\omega)$ in the baseband $\omega \in [-\omega_{\mathrm{N}}, \omega_{\mathrm{N}}]$ and is zero elsewhere. The optimal $\mathcal{F}_{\mathrm{HSP}} = \mathcal{F}_2\mathcal{R}^{-1/2}$ therefore is the LCTI system that is zero outside the baseband, and in the baseband equals $F_{\mathrm{HSP}}(\mathrm{i}\omega) = G_2(\mathrm{i}\omega)R(\mathrm{i}\omega)^{-1/2} = F_{\mathrm{wiener}}(\mathrm{i}\omega)$. In the baseband the optimal $\mathcal{F}_{\mathrm{HSP}}$ acts as the classic Wiener filter making the error $G_{\mathrm{e}}(\mathrm{i}\omega)G_{\mathrm{e}}(\mathrm{i}\omega)^*$ equal to $Q(\mathrm{e}^{\mathrm{i}\theta})$, and outside the baseband it does nothing. Therefore:

Theorem 17.1. Let $\mathcal{G}$ and $\mathcal{W}$ be real stable LCTI systems and suppose assumptions $\mathbf{A_{2\text{-}3}}$ hold. Then the HSP depicted in Fig. 18(a) minimizes the L^2 norm of $\mathcal{G}_{\mathrm{e}}$ and attains the optimal performance

$$\|\mathcal{G}_{\mathrm{e}}\|_2^2 = \frac{1}{\pi}\int_0^{\omega_{\mathrm{N}}} \frac{|G(\omega)|^2}{1 + \rho(\omega)}\mathrm{d}\omega + \frac{1}{\pi}\int_{\omega_{\mathrm{N}}}^\infty |G(\mathrm{i}\omega)|^2\mathrm{d}\omega,$$

where $F_{\mathrm{wiener}}(\mathrm{i}\omega) = \frac{\rho(\omega)}{1+\rho(\omega)}$ and $\rho(\omega)$ is defined by (75). All components are stable and the overall HSP is LCTI. $\qquad \triangledown$

(a) Configuration with analog Wiener filter $\mathcal{F}_{\text{wiener}}$

(b) Configuration with discrete filter, $\bar{K}(e^{i\theta}) = F_{\text{wiener}}(\theta/h)$
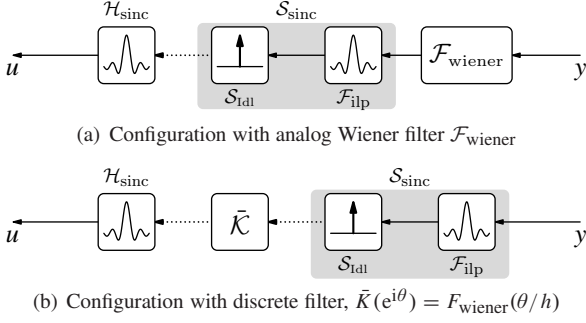
Figure 18: The optimal HSP for SR with noisy measurements

The optimal reconstructor is very similar to the WKS-block with the sole difference that the analog Wiener filter preprocesses the measurement. The frequency response of $\mathcal{F}_{\text{wiener}}$ is real valued for all frequencies, so it is noncausal (unless it is static, which happens if $\mathcal{W}$ is scalar multiple of $\mathcal{G}$). An alternative form of the optimal HSP is presented in Fig. 18(b), in which the Wiener filter is, in a sense, converted to the discrete filter $\bar{K}$ with the frequency response $\bar{K}(e^{i\theta}) = F_{\text{wiener}}(\theta/h)$. This filter is also generically noncausal. Moreover, it is normally not a rational function of $e^{i\theta}$ even if the analog Wiener filter is rational. Hence, unless $\bar{\mathcal{K}}$ is static, it is infinite dimensional.

17.2. L^{∞} Optimization

The situation here is more complicated than in the L^2 case. Clearly from (72) we have that $\mathcal{G}_e\mathcal{G}_e^* \leq \gamma^2 I$ iff

$$(\mathcal{F}_{\text{wiener}} - \mathcal{F})\mathcal{R}(\mathcal{F}_{\text{wiener}} - \mathcal{F})^* \leq \gamma^2 I - \mathcal{Q}. \qquad (76)$$

This requires that $\gamma \geq \gamma_{\text{wiener}}$, where

$$\gamma_{\text{wiener}} := \sqrt{\|\mathcal{Q}\|_{\infty}}$$

is the optimal L^{∞} performance achievable with $\mathcal{F} = \mathcal{F}_{\text{wiener}}$.

If $\gamma > \gamma_{\text{wiener}}$, the system $I - \gamma^{-2}\mathcal{Q}$ is stably invertible and then there is an HSP guaranteeing that $\|\mathcal{G}_e\|_{\infty} \leq \gamma$ iff

$$\|(I - \gamma^{-2}\mathcal{Q})^{-1/2}(\mathcal{F}_{\text{wiener}} - \mathcal{F}_{\text{HSP}})\mathcal{R}^{1/2}\|_{\infty} \leq \gamma \qquad (77)$$

for some $\mathcal{F}_{\text{HSP}}$. The system in (77) is of the one-block type

$$\underbrace{(I - \gamma^{-2}\mathcal{Q})^{-1/2}\mathcal{F}_{\text{wiener}}\mathcal{R}^{1/2}}_{\mathcal{G}_{\infty}} - \underbrace{(I - \gamma^{-2}\mathcal{Q})^{-1/2}\mathcal{F}_{\text{HSP}}\mathcal{R}^{1/2}}_{\mathcal{F}_{\infty}}$$

and, similarly to the L^2 case, $\mathcal{F}_{\infty}$ is a rank-1 HSP iff $\mathcal{F}_{\text{HSP}}$ is and by the fact that optimal rank-1 $\mathcal{F}_{\infty}$ can be taken LCTI also $\mathcal{F}_{\text{HSP}} = (I - \gamma^2\mathcal{Q})^{1/2}\mathcal{F}_{\infty}\mathcal{R}^{-1/2}$ can be taken LCTI. Now if we were to cancel the singular value $|G_{\infty}(e^{i\omega_0})|$ in the baseband then this would result in $F_{\text{HSP}}(i\omega) = F_{\text{wiener}}(i\omega)$, $\forall \omega \in [-\omega_N, \omega_N]$ and zero elsewhere. This is exactly the same HSP as in the L^2 case. This choice of $\mathcal{F}_{\text{HSP}}$ achieves $\|\mathcal{G}_e\|_{\infty} \leq \gamma$ if and only if $\sup_{\omega > \omega}|G_{\infty}(i\omega)| \leq \gamma$. This condition, at first sight, appears to hard to check. However there holds:

Lemma 17.2. Let $\gamma > \gamma_{\text{wiener}}$. Then at each ω we have $|G_{\infty}(i\omega)| \leq \gamma \iff |G(i\omega)| \leq \gamma$.

Proof. $|G_{\infty}(i\omega)| \leq \gamma$ iff (76) holds for $F(i\omega) = 0$ at the given frequency, which in turn is equivalent to $|G_e(i\omega)| \leq \gamma$, but $G_e(i\omega) = G(i\omega)$ for $F(i\omega) = 0$. ∎

This property allows to bypass baseband dominance of $\mathcal{G}_{\infty}$ (which is rather involved as $\mathcal{G}_{\infty}$ depends on γ). Sufficient is to assume baseband dominance of $\mathcal{G}$. Thus, we have:

Theorem 17.3. Suppose assumptions $\mathbf{A_1},2$ are satisfied. Then the optimal HSP is the same as that of Theorem 17.1 and

$$\|\mathcal{G}_e\|_{\infty} = \max\left\{\sup_{\omega \in [0,\omega_N]} \frac{|G(i\omega)|}{\sqrt{1 + \rho(\omega)}}, \sup_{\omega \in (\omega_N,\infty)} |G(i\omega)|\right\}$$

is the optimal L^{∞} performance level.

Proof. Let γ_{∞} be the minimal achievable norm of $\|\mathcal{G}_e\|_{\infty}$ by rank-1 $\mathcal{F}_{\text{HSP}}$. Assume first that $\gamma_{\infty} > \gamma_{\text{wiener}}$. Then $|G_{\infty}(i\omega_k)| > \gamma_{\infty}$ for at most one of the aliased frequencies ω_k, which by Lemma 17.2 is equivalent to $|G(i\omega_k)| > \gamma_{\infty}$ (for the same one k). By the baseband dominance of $\mathcal{G}$, this must be $k = 0$. I.e., the baseband has to be removed, leaving $|G_e(i\omega)| = Q^{1/2}(i\omega)$ in the baseband and $G_e(i\omega) = G(i\omega)$ elsewhere. The formula for γ_{∞} follows on noting that $Q(i\omega) = |G(i\omega)|^2/(1 + \rho(\omega))$.

If $\gamma_{\infty} = \gamma_{\text{wiener}}$ then for any $\gamma > \gamma_{\text{wiener}} = \gamma_{\infty}$ by the above argument the given $\mathcal{F}_{\text{HSP}}$ achieves $\|\mathcal{G}_e\|_{\infty} \leq \gamma$. I.e., then for any $\gamma > \gamma_{\text{wiener}}$ inequality (76) is satisfied for $\mathcal{F} = \mathcal{F}_{\text{HSP}}$. Since $\mathcal{F}_{\text{HSP}}$ is independent of γ, the inequality (76) then holds for $\gamma = \gamma_{\infty}$ as well. ∎

Both L^2 and L^{∞} equivalent one-block problems (74) and (77), respectively, can be interpreted as (weighted) approximations of the analog optimal reconstructor $\mathcal{F}_{\text{wiener}}$ by $\mathcal{F}_{\text{HSP}}$. In other words, the choice of "good" HSPs can be viewed as an attempt to imitate their analog counterparts. This interpretation merely repeats the main point of [29, Sec. 6] made in the context of the sampled-data feedback control with causal controllers.

Remark 17.4. The optimal performance indices in Theorems 17.1 and 17.3 have two components representing two extreme situations. The first of these components reflects the contribution of the baseband, $[0, \omega_N]$, and is a size of $\mathcal{Q}$ in this frequency range. The frequency response of $\mathcal{Q}$ is actually the spectrum of the estimation error under the optimal analog reconstruction. Thus, the baseband contributes, in a sense, by the optimal analog performance. The second component of the optimal indices reflects the contribution of the high-frequency range, (ω_N, ∞), and is a size of $\mathcal{G}$. Thus, high frequency components contribute by the estimator-free performance. Thus, in $[0, \omega_N]$ the sampled-data reconstructor recovers the analog performance, whereas in (ω_N, ∞) it does nothing. ▽

Remark 17.5. In the L^2 case, Theorem 17.1 requires that the function $|G(i\omega)|^2 \frac{\rho(\omega)}{1+\rho(\omega)}$ is baseband-dominant. If $|G(i\omega)|$ is baseband-dominant, this requirement is clearly guaranteed if the signal-to-noise ratio $\rho(\omega)$ is a non-increasing function of ω, which is a reasonable assumption in many applications. The

dominance requirement might fail if $\frac{\rho(\omega)}{1+\rho(\omega)}$ increases faster than $|G(i\omega)|^2$ decreases. This, in turn, is possible if the signal-to-noise ratio increases considerably faster then the spectrum of v decays. At the same time, spectral properties of $\mathcal{W}$ do not affect the baseband-dominance in the L^∞ case. $\hspace{1cm} \triangledown$

18. Concluding Remarks

The main message of this part is that the system-theoretic approach—the use of systems as signal generators to account for available information and system norms as performance measures—facilitates a unified treatment of a wide spectrum of sampling and reconstruction problems. We have considered the design of L^2 and L^∞ optimal acquisition and / or interpolation devices when no causality constraints are imposed on them. Remarkably, this single approach recovers many known HSPs derived hitherto by different methods. For example, when sampling circuits are fixed (Type III problems), certain choices of signal generators produce conventional cardinal polynomial or exponential splines as the optimal reconstructors. Another example is the recovery of the classical Sampling Theorem and its modifications (samples with derivatives, recurring non-uniform sampling) when both sampling and reconstruction devices are design parameters (Type IV problems) under different assumptions about the sampling process. We believe that the capability to reproduce known results as special cases of a general framework is an important property, offering an additional insight into both existing and the proposed approaches. The presented proofs of the continuous-time invariance of certain optimal HSPs and the necessity of a bandllimited assumption in multi-channel sampling attest to it. At the same time, we have shown that the approach can produce new solutions and interpretations, like the interplay between L^2 and L^∞ norms, leading to limitations on error free reconstruction, and optimal down-sampling and a version of the Sampling Theorem for reconstructing signals from noisy measurements. Many more extensions can be added to this list. One of them—imposing causality constraints on the design of L^2-optimal reconstructors—-will be addressed in Part III this paper.

Part III: L^2-Optimization of Reconstructors with Causality Constraints

19. Introduction and Problem Formulation

The first two parts of this paper discussed underlying technical material for the system-theoretic analysis of sampling and reconstruction (SR) problems and the design of hybrid signal processors (HSPs) when no causality constraints are imposed. The primary purpose of this part is to show, how causality constraints can be systematically incorporated into SR problems in the system-theoretic framework.

To this end, we address the (technically) simplest problem setup, depicted in Fig. 19, where v is an analog signal to be
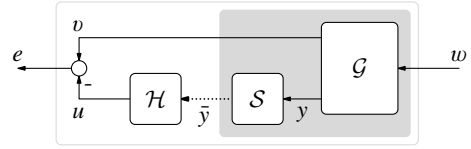

Figure 19: The problem setup

reconstructed and $\bar{y}$ is the discrete measured signal, which is the sampling of an analog signal y. Both v and y are modeled as outputs of a given continuous-time LTI system

$$\mathcal{G} = \begin{bmatrix} \mathcal{G}_v \\ \mathcal{G}_y \end{bmatrix} \tag{78}$$

driven by a common input w. To simplify the exposition, we assume that $\mathcal{G}$ is finite dimensional (i.e., its transfer function is rational) and $\mathcal{S}$ is the ideal sampler (i.e., $\bar{y}[k] = y(kh)$, where h is the sampling period), which is sufficiently general to describe the method. Nonetheless, the results can be extended to some classes of infinite-dimensional models and to more general acquisition devices. The design parameter here is the D/A reconstructor (hold) $\mathcal{H}$, which generates an estimate u of v, and the reconstruction performance is measured by the L^2-norm of the error system

$$\mathcal{G}_{\mathrm{e}} := \mathcal{G}_v - \mathcal{H}\mathcal{S}\mathcal{G}_y$$

from w to $e = v - u$. As discussed in Part I, this goal corresponds to the mean-square minimization of the (analog) error signal e assuming that w is the standard white noise. Without loss of generality we assume that $\mathcal{G}$ is causal (but not necessarily stable).

Formally, we consider the following optimization problem:

RP$_l$: Given a finite-dimensional $\mathcal{G}$, the ideal sampler $\mathcal{S}$, and $l \in \mathbb{Z}_0^+$, find a stable and l-causal (i.e., such that its hold function $\phi(t) = 0$ whenever $t < -lh$) reconstructor $\mathcal{H}$, which stabilizes the error system $\mathcal{G}_{\mathrm{e}}$ and minimizes the performance index $\mathcal{J}_l = \|\mathcal{G}_{\mathrm{e}}\|_2^2$.

The nonnegative integer l defines here the length (in sampling periods) of the preview, allowed for $\mathcal{H}$. **RP$_0$** corresponds to the causal reconstruction problem, which can be thought of as a hybrid version of the Wiener / Kalman *filtering*. This problem is currently quite well understood [6, 17]. Another limiting case, **RP$_\infty$**, is the noncausal problem addressed in Part II. It corresponds to the so-called *fixed interval smoothing*. The other cases, for positive finite l, are then hybrid versions of the *fixed lag smoothing* problem, in which context l is referred to as the smoothing lag.

To the best of our knowledge, the majority of currently available solutions to problems, similar to **RP$_l$**, in the literature address causality constraints indirectly. It appears that the most widely used approach is to design a noncausal $\mathcal{H}$ and then just truncate the anti-causal part of some particular representation of its hold function $\phi(t)$ to make it l-causal (or FIR), see [36] and the references therein. This may be justifiable only if the truncated part is insignificant, which, in turn, requires sufficiently
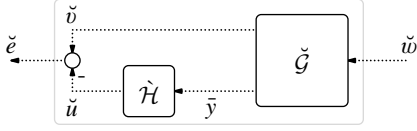
Figure 20: The problem setup in the lifted domain

fast decay[7] of $\phi(t)$. This is why the decay rate becomes an important factor in the choice of hold functions, see [45]. Yet the fast decay requirement might compromise the reconstruction performance. An alternative might be the use of parametric optimization methods, like those discussed in [16, Ch. 4] for preview-free ($l = 0$) problems. This approach, however, results in non-transparent solutions and thus cannot address important questions of the rationale, structure, and interpretations of causal reconstructors.

Having the preview length l as a part of the optimization process has a clear advantage over truncating noncausal solutions. We no longer hinge on the decay rate of $\phi(t)$ and can therefore afford to use a wider class of signal generators and, consequently, a richer set of reconstructors. Moreover, the optimization-based design makes it easy to link preview with the achievable performance, which may be used as the justification for the choice of the preview length.

This part is organized as follows. We start with the formulation and solution of $\mathbf{RP}_l$ in the lifted domain in Section 20. In Section 21 we use this solution to address the consistency of the optimal reconstruction and stabilizability conditions for some special cases. To render the lifted solution implementable and transparent in a general case, it should be converted back to the time domain—the *peeling-off* procedure. A coherent peeling-off procedure via a state-space realization of $\mathcal{G}$ (introduced in Section 22) is presented in Section 23. This section is quite technical, so a reader might probably opt for skipping it and proceed directly to Section 24, which contains the main results of this part—a complete solution of $\mathbf{RP}_l$ and a discussion of some its properties—presented in a self-contained manner. To illustrate these results, several simple examples are presented in Section 25.

Notation

We follow the notation conventions of the previous parts, so below we outline the most frequently used nonstandard definitions only. For any set $\mathbb{A}$, the indicator function $\mathbb{1}_{\mathbb{A}}(t)$ is 1 if $t \in \mathbb{A}$ and is zero elsewhere. The unit step (which is actually $\mathbb{1}_{\mathbb{R}+}(t)$) is denoted $\mathbb{1}(t)$. By $\mathbb{Z}_l^+$ we denote the set of all integers larger or equal to l. The set of natural numbers is denoted by $\mathbb{N} = \mathbb{Z}_1^+$. The symbols $\mathbb{T}$ and $\mathbb{D}$ stand for the unit circle ($|z| = 1$) and the open unit disk ($|z| < 1$) in the complex plane, respectively. We also use the convention $\mathbb{L} := L^2[0, h]$.

20. Lifted Formulation and Solution

---

[7]For example, this approach works poorly for the sinc-resonstructor from the Sampling Theorem as $\mathrm{sinc}_h(t)$ has slow decay (it is not absolutely integrable).

Our first step is to reformulate the reconstruction problem in the lifted domain. By applying the lifting transformation, the setup in Fig. 19 transforms into an equivalent LTI setup depicted in Fig. 20, where $\grave{\mathcal{H}}$ is the lifted hold (design parameter) and

$$\breve{\mathcal{G}} = \begin{bmatrix} \breve{\mathcal{G}}_v \\ \acute{\mathcal{S}}\breve{\mathcal{G}}_y \end{bmatrix} =: \begin{bmatrix} \breve{\mathcal{G}}_v \\ \acute{\mathcal{G}}_y \end{bmatrix}$$

is the lifted signal generator (given). $\mathbf{RP}_l$ can then be rewritten in terms of lifted transfer functions as follows:

$\mathbf{\breve{RP}}_l$: Given $\breve{G}$ and $l \in \mathbb{Z}_0^+$, find $\grave{H} \in z^l H^\infty$, which guarantees that $\breve{G}_e \in z^l H^\infty \cap L^2$ and minimizes $\mathcal{J}_l = \|\breve{G}_e\|_2^2$.

The time invariance of all systems in $\mathbf{\breve{RP}}_l$ makes it possible to use frequency-domain methods. In particular, we may adapt the approach of [31]. This adaptation is not straightforward as the extension of many standard methods, well known for transfer functions over finite-dimensional input and output spaces, to lifted transfer function is quite nontrivial. Moreover, some of these methods are not well exposed in the signal processing literature. For these reasons, we start with a simple particular case of $\mathbf{RP}_l$, which motivates the main steps of the theory to be developed later on.

20.1. Motivating Example

Consider the reconstruction problem with the signal generator $\mathcal{G}$ having the transfer functions

$$G_v(s) = G_y(s) = \frac{1}{s}.$$

The instability of these systems may be viewed as the reflection of incorporating non-decaying signals into the L^2 analysis. Indeed, the impulse response of $\mathcal{G}_v$ is $g_v(t) = \mathbb{1}(t)$, so we effectively minimize the energy of the reconstruction error under a step v. The requirement to stabilize the reconstruction error, which necessitates the reconstruction error e to decay, may then be considered as merely the requirement to guarantee zero steady-state error.

According to §4.2, in the lifted domain the relation $\breve{v}(z) = \breve{G}_v(z)\breve{w}(z)$ reads

$$\breve{v}(z; \tau) = \int_0^h \breve{g}_v(z; \tau, \sigma)\breve{w}(z; \sigma)\mathrm{d}\sigma,$$

where, for every $\tau, \sigma \in [0, h]$,

$$\breve{g}_v(z; \tau, \sigma) = \sum_{k \in \mathbb{Z}} \mathbb{1}(kh + \tau - \sigma)z^{-k} = \mathbb{1}(\tau - \sigma) + \sum_{k \in \mathbb{N}} z^{-k}$$
$$= \mathbb{1}(\tau - \sigma) + \frac{1}{z - 1}.$$

Thus, $\breve{G}_v(z)$ defines the relation

$$(\breve{G}_v\breve{w})(z; \tau) = \int_0^\tau \breve{w}(z; \sigma)\mathrm{d}\sigma + \int_0^h \frac{1}{z - 1}\breve{w}(z; \sigma)\mathrm{d}\sigma. \quad (79)$$

Because $\mathcal{G}_y = \mathcal{G}_v$, we have that $\bar{y}(z) = \breve{v}(z; 0)$ and, hence,

$$\bar{y}(z) = (\acute{G}_y\breve{w})(z) = \int_0^h \frac{1}{z - 1}\breve{w}(z; \sigma)\mathrm{d}\sigma.$$

These relations actually imply that $\breve{G}_v$ can be presented as

$$\breve{G}_v(z) = \breve{N}_v(z) + \dot{H}_{\text{ZOH}}(z)\acute{G}_y(z), \tag{80}$$

where $\breve{N}_v$ is defined by the first term in the right-hand side of (79) and $\dot{H}_{\text{ZOH}}$ is the (lifted) transfer function of the zero-order hold. As both $\breve{N}_v$ and $\dot{H}_{\text{ZOH}}$ are *static* lifted systems (their transfer functions are constant in z), they are stable and instabilities in the estimation channel $\breve{G}_v$ are actually of the same form as in the measurement channel $\acute{G}_y$. This, in particular, implies that the error system is stabilizable. Indeed, the trivial pick $\dot{H} = \dot{H}_{\text{ZOH}}$ produces the stable $\breve{G}_e = \breve{N}_v$. This has an intuitive explanation: if v is asymptotically constant, a piecewise-constant reconstruction of its sampled noise-free measurements yields asymptotically perfect reconstruction.

Although the zero-order hold stabilizes the error system, it is not necessarily optimal. This particular stabilizing solution, however, can be used to generate all other stabilizing solutions. To see this, consider the error transfer function $\breve{G}_e(z)$, which defines the relation

$$\breve{e}(z; \tau) = \int_0^\tau \breve{w}(z; \sigma)\mathrm{d}\sigma + \int_0^h \left(\frac{1}{z-1} - \frac{\dot{H}(z)}{z-1} \right) \breve{w}(z; \sigma)\mathrm{d}\sigma.$$

Whilst the first term of $\breve{G}_e$ is stable (it equals $\breve{N}_v$), the second term contains a singularity on $\mathbb{T}$ (at $z = 1$). Every stabilizing $\dot{H}$ must therefore cancel this singularity and this is the only requirement on stabilizing reconstructors (apart from introducing no new instabilities, of course). Thus, the requirement that $\dot{H}$ is stabilizing can be cast as the following interpolation constraint on its transfer function:

$$\dot{H}(1) \equiv 1 \quad (\forall \tau \in [0, h]). \tag{81}$$

Clearly, $\dot{H}_{\text{ZOH}}$ satisfies this constraint as $\dot{H}_{\text{ZOH}}(z) = 1$ for all z. Standard interpolation arguments [39, Thrm. 10.18] yield then that all reconstructors satisfying (81) are parametrized as

$$\dot{H}(z) = \dot{H}_{\text{ZOH}}(z) + \dot{Q}(z)\bar{M}_y(z), \tag{82}$$

where

$$\bar{M}_y(z) = \frac{z-1}{a_1 z + a_0}$$

for any fixed $|a_0| < |a_1|$ and $\dot{Q} \in z^l H^\infty$ but otherwise arbitrary. In other words, all interpolants are the parallel interconnection of a particular solution ($\dot{H}_{\text{ZOH}}$) and the cascade of a stable and proper transfer function having its zero at the interpolation point ($\bar{M}_y$) and an arbitrary stable transfer function ($\dot{Q}$). The freedom in a_1 and a_0, which does not affect $\dot{H}$ (as the term $a_1 z + a_0$ can always be canceled by $\dot{Q}$), will be exploited later on. With this parametrization, all possible stable error systems are characterized as

$$\breve{G}_e(z) = \breve{N}_v(z) - \dot{Q}(z)\acute{N}_y(z), \tag{83}$$

with $\acute{N}_y := \bar{M}_y \acute{G}_y$, which verifies

$$(\acute{N}_y \breve{w})(z) = \int_0^h \frac{1}{a_1 z + a_0} \breve{w}(z; \sigma)\mathrm{d}\sigma \tag{84}$$

and is causal and stable (i.e., $\acute{N}_y \in H^\infty$).

Once the stability issue is resolved, the solution of $\check{\mathbf{RP}}_l$ amounts to finding a $\dot{Q} \in z^l H^\infty$ minimizing the L^2-norm of $\breve{G}_e$ in (83). Note that for every such $\dot{Q}$ the resulting $\breve{G}_e \in L^2$. Indeed, the first term is in L^2 because it is a static Hilbert-Schmidt operator [55, Thrm. 8.8] and the second term is in L^2 because $\tilde{G} L^2 \subset L^2$ for all $\tilde{G} \in L^\infty$. We thus should only be concerned with the norm. By the Projection Theorem (orthogonality principle [37]) we know that the optimal $\dot{Q}$ for each l, let us call it $\dot{Q}_l$, must satisfy

$$\langle \dot{Q}\acute{N}_y, \breve{N}_v - \dot{Q}_l\acute{N}_y \rangle_2 = 0, \quad \forall \dot{Q} \in z^l H^\infty.$$

Because $\dot{Q}(z)$ is a rank-one operator for almost all $z \in \mathbb{C}$, $\dot{Q} \in z^l H^\infty \Rightarrow \dot{Q} \in L^2$ (Prop. 5.6) and we may rewrite the equation above as

$$\langle \dot{Q}, (\breve{N}_v - \dot{Q}_l\acute{N}_y)\acute{N}_y^\sim \rangle_2 = 0, \quad \forall \dot{Q} \in z^l H^\infty \cap L^2.$$

In other words, $\dot{Q}_l$ must render

$$\acute{V}^\sim - \dot{Q}_l\acute{N}_y\acute{N}_y^\sim \perp z^l H^\infty \cap L^2, \tag{85}$$

where $\acute{V} := \acute{N}_y \breve{N}_v^\sim$. The orthogonality here is equivalent to the condition that the impulse response of $\acute{V}^\sim - \dot{Q}_l\acute{N}_y\acute{N}_y^\sim$ is zero at all $k < -l$. This condition might not be easy to enforce for an arbitrary $\acute{N}_y$ of the form (84), because $\acute{N}_y\acute{N}_y^\sim$ is in general noncausal, so that the l-causality of $\dot{Q}_l$ is not preserved in $\dot{Q}_l\acute{N}_y\acute{N}_y^\sim$. Indeed, by the results of §5.2,

$$\acute{N}_y^\sim(z) = \frac{1}{a_1 z^{-1} + a_0}$$

(the zero-order hold preceeded by a discrete filter), so that

$$\acute{N}_y(z)\acute{N}_y^\sim(z) = \frac{h}{(a_1 z + a_0)(a_1 z^{-1} + a_0)}$$

is noncausal for all $a_0 > 0$. Yet if $a_0 = 0$, which is admissible, $\acute{N}_y\acute{N}_y^\sim \equiv h/a_1^2$ is static and therefore causal (and causally invertible). It is convenient to normalize this static system by choosing $a_1 = \sqrt{h}$, in which case condition (85) reads

$$\acute{V}^\sim - \dot{Q}_l \perp z^l H^\infty \cap L^2,$$

which is easy to comply by the orthogonal projection,

$$\dot{Q}_l = \text{proj}_{z^l H^\infty \cap L^2} \acute{V}^\sim.$$

This projection is merely the truncation of the impulse response of $\acute{V}^\sim$ to $\mathbb{Z}_l^+$. Because for our choice of a_1 and a_0

$$\acute{V}^\sim(z) = \breve{N}_v(z)\acute{N}_y^\sim(z) = \int_0^\tau \frac{z}{\sqrt{h}}\mathrm{d}\sigma = \frac{\tau}{\sqrt{h}} z,$$

we have:

$$\dot{Q}_l(z) = \begin{cases} 0 & \text{if } l = 0 \\ \acute{V}^\sim(z) = \frac{\tau}{\sqrt{h}} z & \text{if } l \geq 1 \end{cases}. \tag{86}$$

The optimal reconstructor is then obtained by substituting this transfer function into (82). If $l = 0$ (no preview), the optimal

reconstructor is actually the *zero-order hold*. If $l \geq 1$ (finite preview), the optimal reconstructor is the *first-order hold*:

$$\acute{H}_l(z) = \acute{H}_{\text{ZOH}}(z) + \frac{\tau z}{\sqrt{h}} \frac{z-1}{\sqrt{h}z} = \frac{\tau}{h} z + \frac{h-\tau}{h} = \acute{H}_{\text{FOH}}(z)$$

(see Example 4.8 for the last equality).

Remark 20.1. It is worth emphasizing that the optimal causal reconstructor, $\mathcal{H}_{\text{ZOH}}$, is *not* a truncated version of the optimal noncausal reconstructor, $\mathcal{H}_{\text{FOH}}$. The truncation is involved in the optimal solution, yet in an intermediate stage only. $\triangledown$

Remark 20.2. Quite interesting is that the optimal reconstructor in this case exploits only one preview step. Even if we allow a wider preview window ($l > 1$), the optimal solution is 1-causal. This property, however, is not generic in the L^2-optimization, see the discussion in [31, §IV-C]. In general, the optimal reconstructor exploits all preview available and the larger the preview length is, the better reconstruction performance is achieved, see the examples in Section 25. $\triangledown$

To complete the solution, we need to calculate the achieved optimal reconstruction performance. By orthogonality,

$$\|\breve{G}_{\text{e}}\|_2^2 = \|\breve{N}_v - \grave{Q}_l \acute{N}_y\|_2^2 = \|\breve{N}_v\|_2^2 - \|\grave{Q}_l \acute{N}_y\|_2^2$$
$$= \|\breve{N}_v\|_2^2 - \|\grave{Q}_l\|_2^2.$$

where the fact that $\acute{N}_y \acute{N}_y^\sim = I$ was used. Elementary calculus yields then that

$$\|\breve{N}_v\|_2^2 = \frac{1}{2\pi h} \int_{-\pi}^{\pi} \int_0^h \int_0^h [\mathbb{1}(\tau - \sigma)]^2 \mathrm{d}\tau \, \mathrm{d}\sigma \, \mathrm{d}\theta = \frac{h}{2}.$$

Finally, if $l = 0$, we clearly have $\|\grave{Q}_l\|_2^2 = 0$, while if $l \geq 1$, $\grave{Q}_l^\sim \grave{Q}_l \equiv h^2/3$, so that $\|\grave{Q}_l\|_2^2 = h/3$. Thus, the optimal

$$\|\breve{G}_{\text{e}}\|_2^2 = \begin{cases} h/2 & \text{if } l = 0 \\ h/6 & \text{if } l \geq 1 \end{cases},$$

which shows that the availability of preview improves the reconstruction performance by a factor of 3 in this case. Also, for all preview lengths, $\lim_{h \to 0} \|\breve{G}_{\text{e}}\|_2 = 0$, which agrees with our intuition that this signal can be perfectly reconstructed from its analog noise-free measurements. $\triangledown$

We are now in the position to describe the general solution procedure, which we split into several stages.

20.2. Stabilization of $\breve{G}_{\text{e}}$

Stability is naturally the very first issue to be addressed in solving $\mathbf{RP}_l$. As we saw in the previous subsection, the stabilization in our context amounts to canceling all instabilities of $\breve{G}$ by $\grave{\mathcal{H}}$. As $\mathcal{G}$ is assumed to be finite dimensional, $\breve{G}(z)$ has a finite number of poles in $\mathbb{C} \setminus \mathbb{D}$ (in fact, mainly in $\mathbb{T}$) and the stabilization means canceling these poles. Because $\grave{\mathcal{H}}$ must be stable and l-causal, it cannot have poles in $\mathbb{C} \setminus \mathbb{D}$, so that the stabilizability of $\breve{G}_v - \grave{H}\acute{G}_y$ should require that all unstable poles of $\breve{G}_v$ are *contained* in $\acute{G}_y$, including their multiplicities and, in the

MIMO case, directions (unstable poles of $\acute{G}_y$ that are not poles of $\breve{G}_v$ can be easily canceled out by zeros of $\grave{H}$).

For the simple system considered in the previous subsection these steps (verifying the containment condition and canceling unstable poles) are quite straightforward. This might not be true in general. The coprime factorization approach (see Appendix B) offers an elegant formalism for working this out. We start with the following result, which states that the stabilizability is equivalent to a special upper triangular form of the denominator in a left coprime factorization of $\breve{G}$:

Proposition 20.3. There exists a stabilizing $\grave{H} \in H^\infty$ iff $\breve{G}$ admits a left coprime factorization over H^∞ of the form

$$\breve{G} = \begin{bmatrix} I & \grave{M}_v \\ 0 & \bar{M}_y \end{bmatrix}^{-1} \begin{bmatrix} \breve{N}_v \\ \acute{N}_y \end{bmatrix} \tag{87}$$

for some left coprime $\bar{M}_y, \acute{N}_y \in H^\infty$ and some $\grave{M}_v, \breve{N}_v \in H^\infty$.

Proof. A lifted version of [31, Prop. 1]. ■

Remark 20.4. Note that Proposition 20.3 considers $\grave{H} \in H^\infty$, which might appear to be more restrictive than what we need ($\grave{H} \in z^l H^\infty$). It can be shown, however, that if $\breve{G}_y(z)$ is proper (i.e., bounded in $|z| > \rho$ for sufficiently large ρ), the preview has no effect on the stabilization. This is because the relaxation of the causality constraints does not relax the requirement that $\grave{H}(z)$ is analytic in $\mathbb{C} \setminus \mathbb{D}$. $\triangledown$

Factorization (87) facilitates the parametrization of the set of all stabilizing reconstructors and corresponding error systems. The following result is essentially a systematic generalization of (82) and (83):

Proposition 20.5. Let $\breve{G}$ admit a left coprime factorization as in (87). Then $\grave{H} \in z^l H^\infty$ stabilizes $\breve{G}_{\text{e}}$ iff

$$\grave{H} = -\grave{M}_v + \grave{Q}\bar{M}_y \tag{88a}$$

for some $\grave{Q} \in z^l H^\infty$. In this case,

$$\breve{G}_{\text{e}} = \breve{N}_v - \grave{Q}\acute{N}_y \tag{88b}$$

parametrizes the set of all stable error transfer functions.

Proof. A lifted version of [31, Lemma 1]. ■

20.3. Normalization and Orthogonalization

The choice of coprime factors in (87) is non-unique. Indeed, given any particular $\bar{M}_y, \grave{M}_v, \acute{N}_y$, and $\breve{N}_v$ constituting (87),

$$\begin{bmatrix} I & \grave{M}_v - \grave{R}\bar{P}\bar{M}_y \\ 0 & \bar{P}\bar{M}_y \end{bmatrix} \quad \text{and} \quad \begin{bmatrix} \breve{N}_v - \grave{R}\bar{P}\acute{N}_y \\ \bar{P}\acute{N}_y \end{bmatrix}$$

are also admissible coprime factors for every appropriately dimensioned $\grave{R} \in H^\infty$ and $\bar{P} \in H^\infty$ such that $\bar{P}^{-1} \in H^\infty$ too. We exploit this freedom to supplement the factors in (87) with desirable properties facilitating the L^2 performance analysis.

First, motivated by the analysis in §20.1, let us choose $\bar{P}$ so that the new numerator $\bar{P}\acute{N}_y$ of $\acute{G}_y$ be co-inner, i.e., such that

$$\bar{P}\acute{N}_y(\bar{P}\acute{N}_y)^\sim = \bar{P}\acute{N}_y\acute{N}_y^\sim\bar{P}^\sim = I \qquad (89)$$

(normalization). Since on the unit disk the conjugate transfer function is the adjoint, the (rational and *matrix-valued*) transfer function

$$\bar{\Phi}_y(z) := \acute{N}_y(z)\acute{N}_y^\sim(z) \qquad (90)$$

is self-adjoint on $z \in \mathbb{T}$. Equation (89) can then be rewritten as

$$\bar{\Phi}_y = \bar{P}^{-1}(\bar{P}^\sim)^{-1}. \qquad (91)$$

This shows that the required $\bar{P}$, if exists, is merely the inverse of the *spectral factor* [40] of $\bar{\Phi}_y$. The existence if this spectral factor is equivalent to the non-singularity of $\bar{\Phi}_y(z)$ on the unit disk. This condition is also the standard non-singularity condition [14] for the estimation problem associated with (88b): if it does not hold, the optimal $\dot{Q}$ might not belong to H^∞, albeit can be arbitrarily closely approximated by a stable $\dot{Q}$. To rule out such situations we assume hereafter that

A$_4$: $\bar{\Phi}_y(e^{i\theta}) > 0$ for all $\theta \in [-\pi, \pi]$.

It is worth emphasizing that this condition does not depend on the particular choice of $\acute{N}_y$ in (87). Indeed, $\acute{N}_y$ is unique (see Appendix B) modulo the left multiplication by a bi-stable $\bar{T}(z)$ (i.e., $\bar{T}, \bar{T}^{-1} \in H^\infty$), which is well-defined and nonsingular on $z \in \mathbb{T}$.

Having chosen $\bar{P}$ to guarantee (89), consider now the transfer function

$$(\check{N}_v - \grave{R}\bar{P}\acute{N}_y)(\bar{P}\acute{N}_y)^\sim = \check{N}_v\acute{N}_y^\sim\bar{P}^\sim - \grave{R}.$$

Since $\check{N}_v, \acute{N}_y, \bar{P} \in H^\infty$, the first term in the right-hand side above is an L^∞ transfer function. This transfer function can always be decomposed into causal and strictly anti-causal parts. Denote the former by $(\check{N}_v\acute{N}_y^\sim\bar{P}^\sim)_+$. It belongs to H^∞ and thus we may choose

$$\grave{R} = (\check{N}_v\acute{N}_y^\sim\bar{P}^\sim)_+, \qquad (92)$$

which guarantees that $(\check{N}_v - \grave{R}\bar{P}\acute{N}_y)(\bar{P}\acute{N}_y)^\sim$ is the transfer function of a strictly anti-causal system (that is, its conjugate belongs to $z^{-1}H^\infty$). We thus just proved the following result:

Proposition 20.6. Let **A$_4$** hold and $\check{G}$ admit a left coprime factorization as in (87). Then these factors can always be chosen so that

$$\begin{bmatrix} \check{N}_v \\ \acute{N}_y \end{bmatrix}\acute{N}_y^\sim = \begin{bmatrix} \acute{V}^\sim \\ I \end{bmatrix} \qquad (93)$$

for some $\acute{V} \in z^{-1}H^\infty$.

20.4. L^2 Optimization

Having reduced $\check{\mathbf{RP}}_l$ to a model matching over stable data, the minimization of the L^2-norm of $\check{G}_e$ follows the standard Hilbert space optimization arguments presented in §20.1. To apply these arguments, we first need to *assume* that

A$_5$: $\check{N}_v \in L^2$.

Like **A$_4$** before, this assumption does not depend on the specific choice of the factor $\check{N}_v$ in (87), as any $\check{N}_v = \check{G}_v + \check{M}_v\acute{G}_y$ at each $z \in \mathbb{T}$ is a perturbation of $\check{G}_v$ by a finite-rank operator. **A$_5$** guarantees that the error transfer function in (88b) is in L^2 for every admissible $\dot{Q}$, because $\check{G}_e(e^{i\theta})$ is merely a finite-rank perturbation of $\check{N}_v(e^{i\theta})$ at each θ, see Prop. 5.6.

By the Projection Theorem, the optimal $\dot{Q}$, denoted hereafter as $\dot{Q}_l$, should render the error system orthogonal to all possible "estimations" $\dot{Q}\acute{N}_y$, i.e.,

$$\check{N}_v - \dot{Q}_l\acute{N}_y \perp \dot{Q}\acute{N}_y, \quad \forall\dot{Q} \in z^l H^\infty.$$

As we saw through the motivating example in §20.1, this condition, combined with (93), yields that

$$\acute{V}^\sim - \dot{Q}_l \perp z^l H^\infty \cap L^2. \qquad (94)$$

This, in turn, leads to

$$\dot{Q}_l = \text{proj}_{z^l H^\infty \cap L^2}(\acute{V}^\sim). \qquad (95)$$

The required projection amounts to truncating the impulse response of $\acute{V}^\sim$ (which has support in $\mathbb{Z} \setminus \mathbb{Z}_0^+$) to $\mathbb{Z}_{-l}^+ \setminus \mathbb{Z}_0^+$, thus resulting in an FIR $\dot{Q}_l$. The optimal FIR $\dot{Q}_l$ should then be substituted instead of $\dot{Q}$ in (88a) to obtain the optimal reconstructor, we denote it $\grave{H}_l$, which is typically IIR. The optimal performance level in this case is

$$\mathcal{J}_l^2 = \|\check{N}_v\|_2^2 - \|\dot{Q}_l\|_2^2. \qquad (96)$$

Remark 20.7. It is readily seen that if there is no preview, $\dot{Q}_0 = 0$ and $\grave{H}_0 = -\check{M}_v$. The quantity $\|\check{N}_v\|_2$ is then the optimal performance level of the optimal filtering (no preview) reconstruction. In the other extreme case, $l = \infty$, the optimal $\dot{Q}_\infty = \acute{V}^\sim$ results in

$$\grave{H}_\infty = -\check{M}_v + \acute{V}^\sim\bar{M}_y = -\check{M}_v + \check{N}_v\acute{N}_y^\sim\bar{M}_y$$
$$= -\check{M}_v + (\check{G}_v + \check{M}_v\bar{M}_y^{-1}\acute{N}_y)\acute{N}_y^\sim\bar{M}_y$$
$$= \check{G}_v\acute{N}_y^\sim\bar{M}_y = \check{G}_v\acute{G}_y^\sim\bar{M}_y^\sim\bar{M}_y = \check{G}_v\acute{G}_y^\sim(\acute{G}_y\acute{G}_y^\sim)^{-1}$$

which is exactly what we had in Lemma 10.1]. The quantities $\|\dot{Q}_l\|_2^2$ and $\|\acute{V}\|_2^2 - \|\dot{Q}_l\|_2^2$ indicate the improvement with respect to the preview-free solution and the deterioration with respect to the noncausal solution, respectively, due to the finite preview of the length l. $\qquad\triangledown$

The optimal solution (95)–(96) may not yet be regarded as explicit, since it is formulated in terms of operator-valued lifted transfer functions. Every step of this solution, however, can be spelt out in the original time domain and lead to an implementable form of the optimal reconstructor and a calculable expression for the optimal performance. Following [29], we refer to this as the *peeling-off* procedure and dedicate to it Section 23 using the state-space machinery reviewed in Section 22.

Still, some insight into the problem can be gained directly from the abstract solution in the lifted domain. We demonstrate this in the next section by addressing the consistency of the optimal reconstruction and the stabilizability of the error system.

21. Intermezzi

21.1. Consistency

Following [45], we say that a reconstruction of an analog signal is *consistent* if it would yield exactly the same measurements if it was reinjected into the measurement system. Consistency is viewed as a desirable property, some design methods even effectively use it as the only requirement, see [45]. In Part II §10.1 we showed that noncausal reconstructors designed by the system-theoretic approach are always consistent, which is a pleasant byproduct of our approach (we do not impose consistency at any stage). The purpose of this subsection is to show, that this property might still be valid in the causal case, although this time some additional assumptions are required to prove the result.

Like we did in Part II, assume that $\mathcal{G}_y = \mathcal{F}\mathcal{G}_v$ for some LTI causal filter $\mathcal{F}$. This assumption means that the measurement $\bar{y}$ is produced by prefiltering v by $\mathcal{F}$ and then sampling the result by the ideal sampler $\mathcal{S}$. The consistency of the reconstructor should then read $\mathcal{S}\mathcal{F}\mathcal{H}_l\mathcal{S}\mathcal{F} = \mathcal{S}\mathcal{F}$ or, in the lifted domain,

$$\acute{F}\grave{H}_l\acute{F} = \acute{F}, \quad \text{where } \acute{F} := \acute{S}\breve{F}, \qquad (97)$$

implying that processing $\breve{u}$ with $\acute{F}$ results in $\bar{y}$ again for all $\bar{y}$ that can be produced by our measurement system. Throughout this subsection we also assume that

$\mathbf{A_6}$: $\acute{F}(z)$ is static.

This assumption holds if the analog $F(s)$ is either static or FIR with the impulse response support in $[0, h]$. An example of the latter is the case when $\bar{y}$ is v sampled with the averaging sampler $\mathcal{S}_{\text{Av}}$, §2.2.1, for which $F(s) = \frac{1}{sh}(1 - e^{-sh})$.

Consider now the optimality condition (94). Because in our case $\acute{G}_y = \acute{F}\breve{G}_v$, (87) yields that

$$\breve{N}_v = (I + \bar{M}_v\acute{F})\breve{G}_v \quad \text{and} \quad \acute{N}_y = \bar{M}_y\acute{F}\breve{G}_v.$$

Hence, $\acute{V}^\sim = (I + \bar{M}_v\acute{F})\breve{G}_v\breve{G}_v^\sim\acute{F}^\sim\bar{M}_y^\sim$ and (94) reads

$$(I + \bar{M}_v\acute{F})\breve{G}_v\breve{G}_v^\sim\acute{F}^\sim\bar{M}_y^\sim - \grave{Q}_l \perp z^l H^\infty \cap L^2. \qquad (98)$$

Because $\acute{F}$ is static, the latter equality yields that

$$\grave{T} := \acute{F}\left((I + \bar{M}_v\acute{F})\breve{G}_v\breve{G}_v^\sim\acute{F}^\sim\bar{M}_y^\sim - \grave{Q}_l\right) \perp z^l H^\infty \cap L^2 \quad (99)$$

too. In other words, the impulse response of $\grave{T}$ must have support in $\mathbb{Z} \setminus \mathbb{Z}_{-l}^+$. At the same time, it can be verified (cf. the second row of (93)) that

$$\grave{T} = (I + \acute{F}\bar{M}_v)\bar{M}_y^{-1} - \acute{F}\grave{Q}_l,$$

which is an l-causal system (the first term in its right-hand side is 0-causal and the second one is the cascade of the 0-causal $\acute{F}$ and the l-causal $\grave{Q}_l$ and thus is l-causal) and thus its impulse response must have support in $\mathbb{Z}_{-l}^+$. This contradicts (99), unless $\grave{T} = 0$. From the latter condition,

$$I + \acute{F}\bar{M}_v = \acute{F}\grave{Q}_l\bar{M}_y,$$

which reads $\acute{F}\grave{H}_l = I$ and thus verifies (97). We therefore just proved the following result:

Proposition 21.1. Let $\mathcal{G}_y = \mathcal{F}\mathcal{G}_v$ for some $\mathcal{F}$ verifying $\mathbf{A_6}$. Then the optimal reconstructor satisfies $\mathcal{S}\mathcal{F}\mathcal{H}_l = I$ and is thus consistent.

Remark 21.2. An important bit in proving Proposition 21.1 is the fact that (98) implies (99), for which we need assumption $\mathbf{A_6}$. If this assumption does not hold, (99) is no longer true. In fact, we can no longer rule out the possibility that the impulse response of $\grave{T}$ has no components in $\mathbb{Z} \setminus \mathbb{Z}_{-l}^+$. This implies that there might be situations for which a valid $\grave{T} \neq 0$ exists and, therefore, $\acute{F}\grave{H}_l \neq I$. Indeed, numerical simulations show that this happens whenever $F(s)$ is nonminimum-phase (has zeros in $\text{Re } s \geq 0$). This, however, does not necessarily imply that (97) does not hold. The question of characterizing the set of filters for which the causal optimal reconstruction is consistent is still open and is the subject of current research. ∇

21.2. Preliminary Insight into Stabilization

In this subsection we consider a relatively simple particular case of the problem, in which

$$G_v(s) = \sum_{i=1}^{n} \frac{\kappa_{v,i}}{s - \alpha_i} \quad \text{and} \quad G_y(s) = \sum_{i=1}^{n} \frac{\kappa_{y,i}}{s - \alpha_i} \qquad (100)$$

for some $\alpha_i, \kappa_{v,i}, \kappa_{y,i} \in \mathbb{C}$, $n \in \mathbb{N}$. In other words, we consider SISO (single-input / single-output) $G_v(s)$ and $G_y(s)$ with simple poles only. These assumptions simplify the exposition, so we can concentrate on the underlying ideas (although the results can be extended to MIMO systems and/or systems having multiple poles). We do not rule out the possibility that at some i either $\kappa_{v,i} = 0$ or $\kappa_{y,i} = 0$, yet not simultaneously (this would make no sense).

The impulse response kernels of these systems are

$$g_v(t) = \sum_{i=1}^{n} \kappa_{v,i} e^{\alpha_i t} \mathbb{1}(t) \quad \text{and} \quad g_y(y) = \sum_{i=1}^{n} \kappa_{y,i} e^{\alpha_i t} \mathbb{1}(t).$$

Then, the impulse response kernel of $\breve{G}_v(z)$ is $\breve{g}_v = \sum_{i=1}^{n} \breve{g}_{v,i}$, where

$$\begin{aligned}
\breve{g}_{v,i}(z; \tau, \sigma) &= \sum_{k \in \mathbb{Z}} \kappa_{v,i} e^{\alpha_i(kh+\tau-\sigma)} \mathbb{1}(kh + \tau - \sigma) z^{-k} \\
&= \kappa_{v,i} e^{\alpha_i(\tau-\sigma)} \mathbb{1}(\tau - \sigma) + \sum_{k \in \mathbb{N}} \kappa_{v,i} e^{\alpha_i(kh+\tau-\sigma)} z^{-k} \\
&= \kappa_{v,i} e^{\alpha_i(\tau-\sigma)} \mathbb{1}(\tau - \sigma) + \frac{\kappa_{v,i} e^{\alpha_i(h+\tau-\sigma)}}{z - e^{\alpha_i h}}.
\end{aligned}$$

Thus, the relation $\breve{v}(z) = \breve{G}_v(z)\breve{w}(z)$ reads

$$\begin{aligned}
\breve{v}(z; \tau) &= \int_0^\tau g_v(\tau - \sigma)\breve{w}(z; \sigma) d\sigma \\
&\quad + \sum_{i=1}^{n} \frac{\kappa_{v,i} e^{\alpha_i \tau}}{z - e^{\alpha_i h}} \int_0^h e^{\alpha_i(h-\sigma)}\breve{w}(z; \sigma) d\sigma. \quad (101)
\end{aligned}$$

Similar arguments yield that $\bar{y}(z) = \acute{G}_y(z)\breve{w}(z)$ reads

$$\bar{y}(z) = \sum_{i=1}^{n} \frac{\kappa_{y,i}}{z - e^{\alpha_i h}} \int_0^h e^{\alpha_i(h-\sigma)}\breve{w}(z; \sigma) d\sigma. \qquad (102)$$

The analysis is facilitated by the fact that we can split $\breve{G}_v$ compatibly with the partition in (101):

$$\breve{G}_v(z) = \breve{D}_v + \breve{G}_{v,\mathrm{sp}}(z).$$

The *feedthrough* term, $\breve{D}_v = \breve{G}_v(\infty)$, is bounded and static (hence, stable) and is an infinite-rank operator. The strictly proper dynamical transfer function $\breve{G}_{v,\mathrm{sp}}(z)$ is a finite-rank operator at almost every $z \in \mathbb{C}$ (cf.§11).

The error system can then be presented as

$$\breve{G}_e(z) = \breve{D}_v + \breve{G}_{v,\mathrm{sp}}(z) - \dot{H}(z)\acute{G}_y(z).$$

As $\breve{D}_v \in H^\infty$, we only need to stabilize $\breve{G}_{v,\mathrm{sp}}$ by $\dot{H}$. In other words, we may ignore the feedthrough term in the stability analysis and be only concerned with the stability of

$$\breve{G}_{e,\mathrm{sp}}(z) := \breve{G}_{v,\mathrm{sp}}(z) - \dot{H}(z)\acute{G}_y(z),$$

which is a finite-rank part of the error system that includes only strictly proper components of $\breve{G}(z)$. Using the definitions of $\breve{G}_{v,\mathrm{sp}}$ and $\acute{G}_y$, the relation $\breve{e}_{\mathrm{sp}}(z) = \breve{G}_{e,\mathrm{sp}}(z)\breve{w}(z)$ reads

$$\breve{e}_{\mathrm{sp}}(z;\tau) = \sum_{i=1}^n \frac{\kappa_{v,i}e^{\alpha_i\tau} - \dot{H}(z)\kappa_{y,i}}{z - e^{\alpha_i h}} \int_0^h e^{\alpha_i(h-\sigma)}\breve{w}(z;\sigma)\mathrm{d}\sigma.$$

The stability of this transfer function requires canceling all poles $z = e^{\alpha_i h}$ in $\mathbb{C} \setminus \mathbb{D}$, i.e., all poles with $\mathrm{Re}\,\alpha_i \geq 0$. Standard interpolation arguments yield then that this is equivalent to the existence of a rational $\dot{H} \in H^\infty$ such that

$$\kappa_{v,i}e^{\alpha_i\tau} = \dot{H}(e^{\alpha_i h})\kappa_{y,i}, \quad \forall i \text{ such that } \mathrm{Re}\,\alpha_i \geq 0. \quad (103)$$

The solvability of these equations *at each i* is clearly equivalent to the conditions that $\kappa_{y,i} \neq 0$ whenever $\kappa_{v,i} \neq 0$. These conditions actually say that every unstable pole of $G_v(s)$ is also an unstable pole of $G_y(s)$.

The solvability at each i, however, is not sufficient for the existence of an $\dot{H}(z)$ satisfying (103). That is because these interpolation constraints are not necessarily independent, even though all α_i are different. Indeed, $e^{\alpha_i h} = e^{(\alpha_i + \mathrm{i}2\omega_N k)h}$ for all $k \in \mathbb{Z}$. Hence, two different continuous-time poles α_i and α_j satisfying the condition $\alpha_i - \alpha_j = \mathrm{i}2\omega_N k$ for some integer k turn *the same* lifted pole, say z_{ij}. Therefore, if there are such poles, we have at least two interpolation constraints,

$$\kappa_{v,i}e^{\alpha_i\tau} = \dot{H}(z_{ij})\kappa_{y,i} \quad \text{and} \quad \kappa_{v,j}e^{\alpha_j\tau} = \dot{H}(z_{ij})\kappa_{y,j},$$

to be resolved simultaneously at the same point $z = z_{ij}$ and $\forall\tau \in [0, h)$. This is possible only if $\kappa_{v,i} = \kappa_{v,j} = 0$.

We thus just proved the following result:

Theorem 21.3. Let the signal generators be as in (100). Then the error system $\mathcal{G}_e$ is stabilizable iff the following two conditions hold for all i such that $\mathrm{Re}\,\alpha_i \geq 0$ and $\kappa_{v,i} \neq 0$:

1. $\kappa_{y,i} \neq 0$,

2. $\nexists j$ such that $\alpha_i - \alpha_j = \mathrm{i}2\omega_N k$ for some $k \in \mathbb{Z} \setminus \{0\}$.

Remark 21.4. Theorem 21.3 effectively says that the reconstruction error is stabilizable under sampled measurements if and only if it is stabilizable under analog measurements (the first condition) and the sampling is *non-pathological* [8] with respect to all unstable modes of $\mathcal{G}_v$ (the second condition). Curiously, there is no problem in having pathological sampling with respect to unstable modes of $\mathcal{G}_y$ that are not unstable modes of $\mathcal{G}_v$. ▽

A stabilizing $\dot{H}$, which is any stable reconstructor satisfying the interpolation constraints (103), can now be constructed by standard polynomial interpolation methods, e.g., via solving the Vandermonde system [13]. We, however, shall not flesh out this line hereafter. Rather, we pursue state-space techniques, which are rigorous, suit equally well for both SISO and MIMO systems, and results in efficient computational algorithms.

22. State-Space Setup and Preliminaries

Bring in a *minimal* state-space realizations

$$G(s) = \begin{bmatrix} G_v(s) \\ G_y(s) \end{bmatrix} = \begin{bmatrix} C_v \\ C_y \end{bmatrix}(sI - A)^{-1}B. \quad (104)$$

Minimality implies that the pair (A, B) is controllable and the pair $(\begin{bmatrix} C_v \\ C_y \end{bmatrix}, A)$ is observable. The induced realizations of G_v and G_y are not necessarily minimal as (C_v, A) and (C_y, A) need not be observable.

We implicitly assumed in (104) that $G(s)$ is *strictly proper*, i.e., that $G(\infty) = 0$. The reason is twofold: we must have $G_y(\infty) = 0$ to guarantee the stability of the ideal sampler (see §6.1) and the condition $G_v(\infty) = 0$ is effectively equivalent to $\mathbf{A_5}$ (see Remark 23.2 below). We also assume that

$\mathbf{A_7}$: the pair (C_y, e^{Ah}) is detectable in discrete time,

$\mathbf{A_8}$: the matrix C_y has full row rank.

Assumption $\mathbf{A_7}$ implies that all modes of e^{Ah} in $\mathbb{C} \setminus \mathbb{D}$ are observable through C_y. It will be shown in §23.1 that this assumption guarantees the stabilizability of the error system $\mathcal{G}_e$. $\mathbf{A_8}$, which merely rules out redundant measurements, is essentially a counterpart of $\mathbf{A_4}$.

Before we proceed to peeling-off steps, we need to review some aspects of the state-space theory for lifted systems. This is the subject matter of the rest of this section (for more details the reader is referred to [8]).

22.1. Preliminaries: State Space in the Lifted Domain

We start with the state-space realization of $G_y(s)$ in (104). As $\mathcal{G}$ is assumed to be causal, the impulse response of $\mathcal{G}_v$ in terms of its state-space realization is

$$g_v(t) = C_v e^{At} B \mathbb{1}(t).$$

Consider now the lifting $\breve{\mathcal{G}}_v$ of $\mathcal{G}_v$. It is an LTI discrete system with a transfer function $\breve{G}_v(z)$, which is an operator $\mathbb{L} \mapsto \mathbb{L}$ for

almost every $z \in \mathbb{C}$. By §4.2, the impulse response kernel of $\breve{G}_\upsilon(z)$ is

$$
\begin{aligned}
\breve{g}_\upsilon(z; \tau, \sigma) &= \sum_{k \in \mathbb{Z}} g_\upsilon(kh + \tau - \sigma) z^{-k} \\
&= C_\upsilon e^{A(\tau - \sigma)} B \, \mathbb{1}(\tau - \sigma) + \sum_{k \in \mathbb{N}} C_\upsilon e^{A(kh + \tau - \sigma)} B z^{-k} \\
&= C_\upsilon e^{A(\tau - \sigma)} B \, \mathbb{1}(\tau - \sigma) \\
&\qquad + C_\upsilon e^{A\tau} (zI - e^{Ah})^{-1} e^{-A\sigma} B,
\end{aligned}
$$

where $\tau, \sigma \in [0, h)$. Thus, we can write

$$
\breve{G}_\upsilon(z) = \breve{D}_\upsilon + \grave{C}_\upsilon(zI - \bar{A})^{-1} \acute{B}, \tag{105}
$$

where (with n denoting the state dimension of $\mathcal{G}$)

$$
\bar{A} : \mathbb{R}^n \to \mathbb{R}^n \qquad \bar{\xi} \mapsto e^{Ah} \bar{\xi}, \tag{106a}
$$

$$
\acute{B} : \mathbb{L} \to \mathbb{R}^n \qquad \breve{\upsilon} \mapsto \int_0^h e^{A(h - \sigma)} B \breve{\upsilon}(\sigma) \mathrm{d}\sigma, \tag{106b}
$$

$$
\grave{C}_\upsilon : \mathbb{R}^n \to \mathbb{L} \qquad \bar{\xi} \mapsto C_\upsilon e^{A\tau} \bar{\xi}, \tag{106c}
$$

$$
\breve{D}_\upsilon : \mathbb{L} \to \mathbb{L} \qquad \breve{\upsilon} \mapsto C_\upsilon \int_0^\tau e^{A(\tau - \sigma)} B \breve{\upsilon}(\sigma) \mathrm{d}\sigma. \tag{106d}
$$

As we can see, (105) has the form of a discrete state-space realization. The only difference from the "conventional" form is that the "B," "C," and "D" parameters of (105) are operators from or / and to infinite-dimensional space ($\mathbb{L}$), rather than plain matrices. This difference, however, is not crucial.

Eventually, we shall see that all lifted systems we face in the development of the solution of $\mathbf{RP}_l$ either have transfer functions of the form

$$
\tilde{G}(z) = \tilde{D} + \tilde{C}(zI - \bar{A})^{-1} \tilde{B} \tag{107}
$$

or are conjugate of such transfer functions. Here, we use the tilde accent to indicate that the corresponding operator, say $\tilde{O}$, might be either $\bar{O}$ or $\acute{O}$ or $\grave{O}$ or $\breve{O}$, see Remark 3.5 for our notational convention. In all cases we consider, the parameters of $\tilde{G}(z)$ are *bounded* operators. For example, the lifted transfer function of $\mathcal{G}_y$ is

$$
\acute{G}_y(z) = \bar{C}_y(zI - \bar{A})^{-1} \acute{B}, \tag{108}
$$

where $\bar{A}$ and $\acute{B}$ are as in (106a) and (106b), respectively, and $\bar{C}_y = C_y$ (just take $\tau = 0$ in (106) and replace C_υ with C_y).

Using the definition of the conjugate transfer function from §5.2, it can be shown that

$$
\tilde{G}^\sim(z) = \tilde{D}^* + \tilde{B}^*(z^{-1}I - \bar{A}')^{-1} \tilde{C}^*. \tag{109}
$$

This implies that we shall need to calculate the adjoints of the parameters of lifted state-space realizations. This usually can be done by the use of the very definition of the adjoint operator. For example, to calculate the adjoint of $\acute{B}$ in (106b), write the definition $\langle \acute{B} \breve{w}, \bar{\xi} \rangle_{\mathbb{R}^n} = \langle \breve{w}, \acute{B}^* \bar{\xi} \rangle_{\mathbb{L}}$ as

$$
\bar{\xi}' \int_0^h e^{A(h - \sigma)} \breve{w}(\sigma) \mathrm{d}\sigma = \int_0^h \left(e^{A'(h - \sigma)} \bar{\xi} \right)' \breve{w}(\sigma) \mathrm{d}\sigma.
$$

This yields

$$
\acute{B}^* : \mathbb{R}^n \to \mathbb{L} \qquad \bar{\xi} \mapsto e^{A'(h - \tau)} \bar{\xi}. \tag{110b}
$$

Analogously, it is straightforward to show that

$$
\grave{C}_\upsilon^* : \mathbb{L} \to \mathbb{R}^n \qquad \breve{\upsilon} \mapsto \int_0^h e^{A\sigma} C_\upsilon' \breve{\upsilon}(\sigma) \mathrm{d}\sigma. \tag{110c}
$$

We shall use these formulae in §§23.2 and 23.3.

Remark 22.1. If $\bar{A}$ is nonsingular, (109) can be rewritten in the form (107). This can be seen through the equality

$$
(z^{-1}I - M)^{-1} = -M^{-1} - M^{-1}(zI - M^{-1})^{-1} M^{-1}.
$$

Yet if $\bar{A}$ is singular, the transfer function in (109) is not proper and therefore has no presentation in form (107). As we cannot rule out singular $\bar{A}$, we prefer to use (109) for conjugates. $\qquad \triangledown$

Note that the "A" part in (107) is always finite dimensional. This is a fundamental property of lifted state-space realizations associated with finite-dimensional analog systems. It plays an important role in our developments. The first consequence of this fact is that the stability of (operator-valued) transfer function (107) can be verified in terms of eigenvalues of a matrix, exactly like in the case of matrix-valued transfer functions. We have:

Proposition 22.2. Let $\tilde{G}(z)$ be as in (107). Then $\tilde{G} \in H^\infty$ if $\bar{A}$ is Schur (i.e., with all eigenvalues in $\mathbb{D}$).

Proof. If $\bar{A}$ is Schur, $zI - \bar{A}$ is invertible for all $z \in \mathbb{C} \setminus \mathbb{D}$. Hence, $\tilde{G}(z)$ is analytic and bounded in $\mathbb{C} \setminus \mathbb{D}$. $\qquad \blacksquare$

Remark 22.3. The result of Proposition 22.2 can be strengthened to the "iff" statement if certain minimality assumption is made about the realization of (107). We, however need only the "if" part for our developments. $\qquad \triangledown$

Like in the matrix-valued case, the impulse response of a stable causal system having the transfer function (107) is

$$
\tilde{G}[k] = \begin{cases} 0 & \text{if } k < 0 \\ \tilde{D} & \text{if } k = 0 \\ \tilde{C} \bar{A}^{k-1} \tilde{B} & \text{otherwise} \end{cases}
$$

Using this formula, the following results can be proved:

Proposition 22.4. Let $\tilde{G}(z)$ given by (107) be the transfer function of a causal system and let $\bar{A} \in \mathbb{R}^{n \times n}$ be Schur. Then $\tilde{G} \in L^2$ iff $\tilde{D}$ is a Hilbert–Schmidt operator and in this case

$$
\|\tilde{G}\|_2^2 = \tfrac{1}{h} \|\tilde{D}\|_{\mathrm{HS}}^2 + \tfrac{1}{h} \mathrm{tr}(\tilde{C}^* \tilde{C} W_\mathrm{c}) \tag{111a}
$$

$$
= \tfrac{1}{h} \|\tilde{D}\|_{\mathrm{HS}}^2 + \tfrac{1}{h} \mathrm{tr}(W_\mathrm{o} \tilde{B} \tilde{B}^*), \tag{111b}
$$

where $W_\mathrm{c}, W_\mathrm{o} \in \mathbb{R}^{n \times n}$, verifying the Lyapunov equations

$$
W_\mathrm{c} = \bar{A} W_\mathrm{c} \bar{A}' + \tilde{B} \tilde{B}^* \quad \text{and} \quad W_\mathrm{o} = \bar{A}' W_\mathrm{o} \bar{A} + \tilde{C}^* \tilde{C},
$$

are the controllability and observability Gramians of (107), respectively.

Proof. Because $(e^{i\theta}I - \bar{A})^{-1} \in \mathbb{C}^{n \times n}$ is bounded at each $\theta \in [-\pi, \pi]$, $\tilde{G}(e^{i\theta})$ is a bounded finite-rank perturbation of $\tilde{D}$ for all possible i/o spaces. This proves the first statement. To calculate the norm, we use (32):

$$h\|\tilde{G}\|_2^2 = \|\tilde{D}\|_{\mathrm{HS}}^2 + \sum_{i \in \mathbb{N}} \|\tilde{C}\bar{A}^{i-1}\tilde{B}\|_{\mathrm{HS}}^2$$

$$= \|\tilde{D}\|_{\mathrm{HS}}^2 + \sum_{i \in \mathbb{N}} \mathrm{tr}(\tilde{C}\bar{A}^{i-1}\tilde{B}\tilde{B}^*(\bar{A}')^{i-1}\tilde{C}^*)$$

$$= \|\check{D}\|_{\mathrm{HS}}^2 + \mathrm{tr}\left(\tilde{C}^*\tilde{C}\sum_{i \in \mathbb{N}}\tilde{A}^{i-1}\tilde{B}\tilde{B}^*(\tilde{A}')^{i-1}\right)$$

$$= \|\check{D}\|_{\mathrm{HS}}^2 + \mathrm{tr}\left(\sum_{i \in \mathbb{N}}(\tilde{A}')^{i-1}\tilde{C}^*\tilde{C}\tilde{A}^{i-1} \cdot \tilde{B}\tilde{B}^*\right).$$

The result follows by the fact that the last two sums equal W_c and W_o, respectively. ∎

It is readily seen that both $\tilde{B}\tilde{B}^*$ and $\tilde{C}^*\tilde{C}$ are $n \times n$ matrices, so that the second terms in the right-hand sides of (111) are the plain matrix traces. As we shall see in §23.3 (Lemma 23.1), the evaluation of the Hilbert-Smith norm of $\tilde{D}$ also reduces to a matrix trace calculation.

23. Peeling-Off

We are now in the position to start the peeling-off procedure for the lifted solution of Section 20. Although this procedure is an important step of our development, it is quite technical and tedious. As the final results are rather transparent, we separate the development steps from the final results and a reader, only interested in the final formulae, may skip this section and proceed directly to Section 24, which is self contained.

23.1. Constructing Coprime Factors

Define $\bar{A}_1 := e^{Ah} + LC_y$ for some L such that $\bar{A}_1$ is Schur (exists by $\mathbf{A_7}$) and consider the transfer function

$$\bar{M}_y(z) = \Xi(I + C_y(zI - \bar{A}_1)^{-1}L) \in H^\infty, \qquad (112a)$$

where Ξ is any square nonsingular matrix. It can be verified that in this case $\bar{M}_y(z)C_y(zI - e^{Ah})^{-1} = \Xi C_y(zI - \bar{A}_1)^{-1}$, so

$$\acute{N}_y(z) := \bar{M}_y(z)\acute{G}_y(z) = \Xi C_y(zI - \bar{A}_1)^{-1}\acute{B} \in H^\infty, \quad (112b)$$

where $\acute{B}$ is defined by (106b). By construction, $\acute{G}_y = \bar{M}_y^{-1}\acute{N}_y$. Moreover, as shown in Lemma C.1, these factors are coprime in H^∞. Thus, for any stabilizing L and nonsingular Ξ, (112) define coprime factors of $\acute{G}_y$.

As a candidate for $\grave{M}_v$ consider then the transfer function

$$\grave{M}_v(z) = z\grave{C}_v e^{-Ah}(zI - \bar{A}_1)^{-1}L \in H^\infty, \qquad (113)$$

where $\grave{C}_v$ is as in (106c). In this case

$$\grave{C}_v(zI - e^{Ah})^{-1} + \grave{M}_v(z)C_y(zI - e^{Ah})^{-1}$$
$$= \grave{C}_v e^{-Ah}\bar{A}_1(zI - \bar{A}_1)^{-1},$$

so that $\check{N}_v := \check{G}_v + \grave{M}_v\acute{G}_y$ verifies

$$\check{N}_v(z) = \check{D}_v + \grave{C}_v e^{-Ah}\bar{A}_1(zI - \bar{A}_1)^{-1}\acute{B} \qquad (114)$$

and is indeed stable (belongs to H^∞).

Thus, the construction of a coprime factorization of $\check{G}$ as in (87) amounts to the choice of L such that $e^{Ah} + LC_y$ is Schur. The factors are then explicitly given by (112)–(114). This proves, by construction, that $\mathbf{A_7}$ guarantees the stabilizability of $\mathcal{G}_e$. The freedom we have in the choice of L and Ξ will be used to supplement the factors by property (93).

23.2. Normalization

For $\acute{N}_y$ defined by (112b),

$$\acute{N}_y^\sim(z) = \acute{B}^*(z^{-1}I - \bar{A}_1')^{-1}C_y'\Xi', \qquad (115)$$

where $\acute{B}^*$ is given in (110b). It is readily seen that

$$\acute{B}\acute{B}^* = \int_0^h e^{A\tau}BB'e^{A'\tau}d\tau =: \Gamma_w(h) > 0$$

(the positive definiteness of Γ_w for all $h > 0$ follows from the controllability of (A, B)). Hence, $\bar{\Phi}_y$ from (90) reads

$$\bar{\Phi}_y(z) = \Xi C_y(zI - \bar{A}_1)^{-1}\Gamma_w(h)(z^{-1}I - \bar{A}_1')^{-1}C_y'\Xi'.$$

The non-singularity of Γ_w, $e^{i\theta}I - \bar{A}_1$ ($\bar{A}_1$ is Schur), and Ξ yields then that $\mathbf{A_8}$ imposes $\mathbf{A_4}$.

Now, as $\bar{A}_1$ is Schur and $\Gamma_w > 0$, the Lyapunov equation

$$Y = \bar{A}_1 Y\bar{A}_1' + \Gamma_w(h) \qquad (116)$$

is solvable by $Y > 0$ for every stabilizing L. Substituting

$$\Gamma_w(h) = Y - \bar{A}_1 Y\bar{A}_1' = z^{-1}(zI - \bar{A}_1)Y + \bar{A}_1 Y(z^{-1}I - \bar{A}_1')$$

into the expression for $\bar{\Phi}_y$ above, we have:

$$\bar{\Phi}_y(z) = \Xi C_y\left(Y(I - z\bar{A}_1')^{-1} + (zI - \bar{A}_1)^{-1}\bar{A}_1 Y\right)C_y'\Xi'$$
$$= \Xi C_y YC_y'\Xi' + \bar{\Phi}_c(z) + \bar{\Phi}_c^\sim(z),$$

where $\bar{\Phi}_c(z) := \Xi C_y(zI - \bar{A}_1)^{-1}\bar{A}_1 YC_y'\Xi' \in z^{-1}H^\infty$.

We first aim at rendering $\bar{\Phi}_y$ static. This can be guaranteed if the equation

$$0 = \bar{A}_1 YC_y' = (e^{Ah} + LC_y)YC_y' \qquad (117)$$

is solvable in stabilizing L. As any such L yields $Y > 0$ and by $\mathbf{A_8}$, the matrix $C_y YC_y'$ is nonsingular and (117) is always solvable by

$$L = -e^{Ah}YC_y'(C_y YC_y')^{-1} \qquad (118)$$

Substituting this gain into (116), we end up with the following equation for Y:

$$Y = e^{Ah}Ye^{A'h} - e^{Ah}YC_y(C_y YC_y')^{-1}C_y'Ye^{A'h} + \Gamma_w(h).$$
$$(119)$$

This is a standard discrete algebraic Riccati equation (DARE) [24, 14]. $\mathbf{A_7}$ and the non-singularity of Γ_w (which, together with $\mathbf{A_8}$, implies that

$$\begin{bmatrix} e^{Ah} - e^{i\theta}I & \Gamma_w^{1/2}(h) \\ C_y & 0 \end{bmatrix}$$

is right invertible for all $\theta \in [-\pi, \pi]$) guarantee that this DARE admits a stabilizing solution $Y \geq 0$ such that $\bar{A}_1$ is Schur and $C_y Y C_y'$ is nonsingular (in fact, $Y > 0$).

Thus, by solving the DARE (119) we obtain a static $\bar{\Phi}_y(z)$. To render $\acute{N}_y$ co-inner, we can choose Ξ as any square matrix satisfying

$$\Xi'\Xi = (C_y Y C_y')^{-1} \tag{120}$$

(e.g., Ξ' may be the Cholesky factor of $(C_y Y C_y')^{-1}$), in which case $\bar{\Phi}_y(z) = I$, as required.

It is time to check the other condition in (93), which involves the product $\check{N}_v \acute{N}_y^{\sim}$. To this end, use (114) and (115) to obtain:

$$\check{N}_v \acute{N}_y^{\sim} = \check{D}_v \acute{B}^* (z^{-1}I - \bar{A}_1')^{-1} C_y' \Xi'$$
$$+ \grave{C}_v e^{-Ah} \bar{A}_1 (zI - \bar{A}_1)^{-1} \Gamma_w(h)(z^{-1}I - \bar{A}_1')^{-1} C_y' \Xi'.$$

Using the relation (it follows from (116))

$$\Gamma_w(h) = (zI - \bar{A}_1)Y\bar{A}_1' + zY(z^{-1}I - \bar{A}_1'),$$

and then (117), we have:

$$\bar{A}_1(zI - \bar{A}_1)^{-1}\Gamma_w(h)(z^{-1}I - \bar{A}_1')^{-1}C_y'$$
$$= \bar{A}_1 Y \bar{A}_1'(z^{-1}I - \bar{A}_1')^{-1}C_y' + z(zI - \bar{A}_1)^{-1}\bar{A}_1 Y C_y'$$
$$= \bar{A}_1 Y \bar{A}_1'(z^{-1}I - \bar{A}_1')^{-1}C_y'.$$

Thus, denoting

$$\grave{C}_V := \check{D}_v \acute{B}^* + \grave{C}_v e^{-Ah}\bar{A}_1 Y \bar{A}_1',$$

we end up with

$$\acute{V}^{\sim}(z) = \grave{C}_V(z^{-1}I - \bar{A}_1')^{-1}C_y'\Xi', \tag{121}$$

which is indeed the conjugate of a $z^{-1}H^\infty$ system. Thus, the (unique) choices of L and Ξ according to (118) and (120), respectively, where Y is the stabilizing solution of (119), renders the factors in (112)–(114) satisfying (93) and thus suitable for the application of the procedure of §20.4.

We conclude this section with spelling out $\grave{C}_V$ and its adjoint. Using (106d), (110b), (106c), and then (116), we obtain:

$$\grave{C}_V\bar{\xi} = C_v\left(\int_0^\tau e^{A(\tau-\sigma)}BB'e^{A'(h-\sigma)}d\sigma + e^{A(\tau-h)}\bar{A}_1 Y \bar{A}_1'\right)\bar{\xi}$$
$$= C_v e^{A(\tau-h)}(Y - \Gamma_w(h-\tau))\bar{\xi}. \tag{122}$$

The adjoint of this operator, $\grave{C}_V^* : \mathbb{L} \to \mathbb{R}^{n_v}$, transforms

$$\check{v} \mapsto \int_0^h (Y - \Gamma_w(h-\tau))e^{A'(\tau-h)}C_v'\check{v}(\tau)d\tau, \tag{123}$$

which can be verified by the direct use of the definition.

23.3. Projection

First, we establish that $\mathbf{A_5}$ does hold in our case and quantify the norm of $\check{N}_v$. To this end, define

$$\Gamma_v := \int_0^h e^{-A'\tau}C_v'C_v e^{-A\tau}d\tau, \tag{124a}$$

$$\Gamma_{vw} := \int_0^h \int_0^\tau B'e^{A'\sigma}C_v'C_v e^{A\sigma}Bd\sigma\,d\tau. \tag{124b}$$

Then the following result can be formulated:

Lemma 23.1. $\check{N}_v \in L^2$ and $\|\check{N}_v\|_2^2 = \frac{1}{h}\operatorname{tr}(\Gamma_{vw}) + \frac{1}{h}\operatorname{tr}(\Gamma_v(Y - \Gamma_w(h)))$.

Proof. It is known [55, Thrm. 8.8] that $\check{D}_v$ defined by (106d) is a Hilbert-Schmidt operator. Then the first statement follows by Proposition 22.4.

To compute the norm, we use (111a). First, it is a known fact [8, Example 12.2.2] that $\|\check{D}_v\|_{\mathrm{HS}}^2 = \operatorname{tr}(\Gamma_{vw})$. Now, it follows from (116) and the fact that $\acute{B}\acute{B}^* = \Gamma_w(h)$ that Y is actually the controllability Gramian of the realization (114) of $\check{N}_v$. Thus, the second term in the right-hand side of (111a) is

$$\operatorname{tr}(\bar{A}_1'e^{-A'h}\grave{C}_v^*\grave{C}_v e^{-Ah}\bar{A}_1 Y) = \operatorname{tr}(e^{-A'h}\grave{C}_v^*\grave{C}_v e^{-Ah}\bar{A}_1 Y \bar{A}_1').$$

The result then follows by the facts that $e^{-A'h}\grave{C}_v^*\grave{C}_v e^{-Ah} = \Gamma_v$ (just combine (110c) and (106c)) and $\bar{A}_1 Y \bar{A}_1' = Y - \Gamma_w(h)$ (see (116)). ∎

Remark 23.2. The strict properness of $G_v(s)$ in (104) is necessary for establishing that $\check{N}_v \in L^2$. Indeed, if $G_v(s) = D_v + C_v(sI - A)^{-1}B$ for some $D_v \neq 0$, the only change in $\check{N}_v$ is its feedthrough $\check{D}_v$ term, which in this case would transform $\check{v} \mapsto D_v v(\tau) + C_v\int_0^\tau e^{A(\tau-\sigma)}B\check{v}(\sigma)d\sigma$. This $\check{D}_v$ is not compact and thus not a Hilbert-Schmidt operator [55, Thrm. 8.7]. ▽

Now, consider $\acute{V}^{\sim}(z)$ from (121). Because $\bar{A}_1$ is Schur, the power series expansion $\acute{V}^{\sim}(z) = \sum_{i\in\mathbb{N}}\grave{C}_V\bar{A}_{i-1}'C_y'\Xi'z^i$ is well defined, where, with some abuse of notation, $\bar{A}_i := \bar{A}_1^i$. The coefficients of z^i are the impulse response of $\acute{V}^{\sim}$ at the time instance $-i$. By (95), the optimal $\grave{Q}$, denoted by $\grave{Q}_l$, is then the (FIR) truncation of this series to its first l terms:

$$\grave{Q}_l(z) = \grave{C}_V\sum_{i=1}^l \bar{A}_{i-1}'C_y'\Xi'z^i. \tag{125}$$

Denote

$$\grave{Q}_{l,\mathrm{tail}}(z) := z^{-l}\big(\acute{V}^{\sim}(z) - \grave{Q}_l(z)\big) = \grave{C}_V\sum_{i\in\mathbb{N}}\bar{A}_{i+l-1}'C_y'\Xi'z^i$$
$$= \grave{C}_V\bar{A}_l'(z^{-1}I - \bar{A}_1')^{-1}C_y'\Xi', \tag{126}$$

which is clearly orthogonal to $\grave{Q}_l$ in L^2. We thus may also write $\grave{Q}_l = \acute{V}^{\sim} - \grave{Q}_{l,\mathrm{tail}}$, which is a useful form to carry out state-space calculations involving $\grave{Q}_l$.

Our next step is to calculate the L^2-norm of $\grave{Q}_l$. To this end, let X be the solution of the following Lyapunov equation:

$$X = \bar{A}_1'X\bar{A}_1 + C_y'(C_y Y C_y')^{-1}C_y. \tag{127}$$

Define also the matrix

$$\Gamma_V := \int_0^h (Y - \Gamma_w(\tau)) e^{-A'\tau} C_v' C_v e^{-A\tau} (Y - \Gamma_w(\tau)) d\tau. \quad (128)$$

Then we formulate the following result:

Lemma 23.3. $\|\dot{Q}_l\|_2^2 = \frac{1}{h} \operatorname{tr}((X - \bar{A}_l' X \bar{A}_l) \Gamma_V).$

Proof. Because $\dot{Q}_l$ and $\dot{Q}_{l,\text{tail}}$ are orthogonal, the conjugate operation does not change the L^2 norm, and z^{-l} is inner,

$$\|\dot{Q}_l\|_2^2 = \|\acute{V}\|_2^2 - \|z^{-l} \dot{Q}_{l,\text{tail}}^{\sim}\|_2^2 = \|\acute{V}\|_2^2 - \|\dot{Q}_{l,\text{tail}}^{\sim}\|_2^2.$$

The first term in the right-hand side above is the norm of the lifted state-space realization $\acute{V} = \Xi C_y(zI - \bar{A}_1)^{-1} \acute{C}_V^*$ and we may use (111b) to calculate it. It is readily seen that the observability Gramian of $\acute{V}$ is X (remember (120)) and that $\acute{C}_V^* \acute{C}_V = \Gamma_V$. Thus, $\|\acute{V}\|_2^2 = \frac{1}{h} \operatorname{tr}(X\Gamma_V)$. The second term is the norm of $\dot{Q}_{l,\text{tail}}^{\sim} = \Xi C_y(zI - \bar{A}_1)^{-1} \bar{A}_l \acute{C}_V^*$, so we again use (111b) to obtain that $\|\dot{Q}_{l,\text{tail}}^{\sim}\|_2^2 = \frac{1}{h} \operatorname{tr}(X \bar{A}_l \Gamma_V \bar{A}_l') = \frac{1}{h} \operatorname{tr}(\bar{A}_l' X \bar{A}_l \Gamma_V)$. This completes the proof. ∎

23.4. Optimal Reconstructors

The last step in peeling-off the lifted solution of Section 20 is the expression for the optimal reconstructor, which amounts to combining (88a) with (125).

23.4.1. Fixed-interval ($l = \infty$) reconstructor

We start with the noncausal reconstructor, i.e., with the solution of **RP**$_\infty$. In this case, $\dot{Q}_\infty = \acute{V}^\sim$ and then

$$\dot{Q}_\infty \bar{M}_y = \acute{C}_V(z^{-1}I - \bar{A}_1')^{-1} C_y'(C_y Y C_y')^{-1} \\ + \acute{C}_V(z^{-1}I - \bar{A}_1')^{-1} C_y'(C_y Y C_y')^{-1} C_y(zI - \bar{A}_1)^{-1} L.$$

Using the relation (follows from (127))

$$C_y'(C_y Y C_y')^{-1} C_y = \bar{A}_1' X(zI - \bar{A}_1) + z(z^{-1}I - \bar{A}_1')X,$$

we can split $\dot{Q}_\infty \bar{M}_y$ into the sum of causal and anti-causal components:

$$\dot{Q}_\infty \bar{M}_y = z\acute{C}_V X(zI - \bar{A}_1)^{-1} L + \acute{C}_V(z^{-1}I - \bar{A}_1')^{-1} B_H, \quad (129)$$

where $B_H := (I - \bar{A}_1' X e^{Ah} Y) C_y'(C_y Y C_y')^{-1}$. By adding the causal solution, $-\bar{M}_v$, to this expression, we end up with

$$\dot{H}_\infty(z) = \dot{H}_c(z) + \dot{H}_{\bar{c}}(z), \quad (130)$$

where the causal part is

$$\dot{H}_c(z) = z(\acute{C}_V X - \acute{C}_v e^{-Ah})(zI - \bar{A}_1)^{-1} L$$

and the anti-causal part is

$$\dot{H}_{\bar{c}}(z) = \acute{C}_V(z^{-1}I - \bar{A}_1')^{-1} B_H.$$

It is convenient to implement both parts of the optimal solution as the cascade of the discrete filters

$$\bar{F}_c(z) = -z(zI - \bar{A}_1)^{-1} L, \qquad \bar{F}_{\bar{c}}(z) = (z^{-1}I - \bar{A}_1')^{-1} B_H,$$

and generalized holds with the hold functions $\mathcal{H}_c$ and $\mathcal{H}_{\bar{c}}$

$$\phi_c(t) = C_v e^{A(t-h)}(I - YX + \Gamma_w(h-t)X) \mathbb{1}_{[0,h]}(t),$$
$$\phi_{\bar{c}}(t) = C_v e^{A(t-h)}(Y - \Gamma_w(h-t)) \mathbb{1}_{[0,h]}(t),$$

respectively, where we used (106c) and (122) to obtain two latter formulae. It is worth emphasizing that the generalized hold functions above are (non-square) $n_v \times n$ matrices at each t.

23.4.2. Fixed-lag (finite l) reconstructor

Taking into account the equality $\dot{Q}_l = \dot{Q}_\infty - z^l \dot{Q}_{l,\text{tail}}$, we can calculate the optimal reconstructor as

$$\dot{H}_l(z) = \dot{H}_\infty(z) - z^l \dot{Q}_{l,\text{tail}}(z) \bar{M}_y(z).$$

By splitting $\dot{Q}_{l,\text{tail}} \bar{M}_y$ into causal and anti-causal parts (which can be done by the very same arguments as those we used in splitting $\dot{Q}_\infty \bar{M}_y$ in §23.4.1) and a straightforward algebra we can then end up with the following optimal reconstructor:

$$\dot{H}_l(z) = \dot{H}_c(z) + \dot{H}_{\bar{c},l}(z) + \dot{H}_{\text{corr}}(z), \quad (131)$$

where $\dot{H}_c$ is exactly as in (130), FIR

$$\dot{H}_{\bar{c},l}(z) := \acute{C}_V \sum_{i=1}^{l} \bar{A}_{i-1}' B_H z^i = z^l \acute{C}_V \sum_{i=0}^{l-1} \bar{A}_{l-1-i}' B_H z^{-i}$$

is the truncation of the impulse response of $\dot{H}_{\bar{c}}$ to $[-l, -1]$ and

$$\dot{H}_{\text{corr}}(z) := -z^{l+1} \acute{C}_V \bar{A}_l' X(zI - \bar{A}_1)^{-1} L = z^l \acute{C}_V \bar{A}_l' X \bar{F}_c(z).$$

Clearly, both $\dot{H}_{\bar{c},l}$ and $\dot{H}_{\text{corr}}$ are $z^l H^\infty$ transfer functions, so the whole $\dot{H}_l \in z^l H^\infty$ too.

24. Main Results

We are now in the position to formulate the main result of this part. To make this section self contained, we refresh some of the notation introduced in the course of the peeling-off steps of Section 23.

Aiming at triming the nomenclature, introduce the following matrix function of a real argument t:

$$\Sigma(t) = \begin{bmatrix} \Sigma_{11}(t) & \Sigma_{12}(t) \\ 0 & \Sigma_{22}(t) \end{bmatrix} := \exp\left(\begin{bmatrix} A & BB' \\ 0 & -A' \end{bmatrix} t\right). \quad (132)$$

We skip the argument when $t = h$, so that we write Σ_{ij} instead of $\Sigma_{ij}(h)$. Since $\Sigma_{11}(t) = e^{At}$ and $\Sigma_{12}(t) = \Gamma_w(t) e^{-A't}$ [8, Lemma 10.5.1], the components of $\Sigma(t)$ include several matrix exponentials, which we faced in previous sections. We shall also need the matrix Δ defined via

$$\begin{bmatrix} \Sigma & \Delta \\ 0 & \Sigma \end{bmatrix} := \exp\left(\begin{bmatrix} A & BB' & 0 & 0 \\ 0 & -A' & C_v'C_v & 0 \\ 0 & 0 & A & BB' \\ 0 & 0 & 0 & -A' \end{bmatrix} h\right), \quad (133)$$

with the natural partitioning to four sub-blocks Δ_{ij}.

Now, define the discrete algebraic Riccati equation (DARE)

$$Y = \Sigma_{11}\big(Y - YC_y'(C_yYC_y')^{-1}C_yY\big)\Sigma_{11}' + \Sigma_{12}\Sigma_{11}', \quad (134)$$

which actually equals (119). A solution Y to this equation is said to be stabilizing if C_yYC_y' is nonsingular and

$$\bar{A}_1 := \Sigma_{11}(I - YC_y'(C_yYC_y')^{-1}C_y) \quad (135)$$

is Schur (i.e., having all its eigenvalues in $\mathbb{D}$), see [24] for details. The stabilizing solution, if exists, is unique and verifies $Y = Y' \geq 0$. In this case, the discrete Lyapunov equation

$$X = \bar{A}_1'X\bar{A}_1 + C_y'(C_yYC_y')^{-1}C_y \quad (136)$$

is always solvable by an $X = X' \geq 0$ (because $\bar{A}_1$ is Schur).

The main result of this part can now be formulated:

Theorem 24.1. Let the signal generator $\mathcal{G}$ be given by the minimal realization (104) and assumptions $\mathbf{A_{7,8}}$ hold. Then the error system $\mathcal{G}_e$ is stabilizable, $\mathbf{A_{4,5}}$ hold, and DARE (134) admits a stabilizing solution $Y > 0$. The unique solution of $\mathbf{RP}_l$ is then as shown in Fig. 21, where the discrete filters are

$$\bar{F}_c(z) = z(zI - \bar{A}_1)^{-1}\Sigma_{11}YC_y'(C_yYC_y')^{-1},$$

$$\bar{F}_{\bar{c},l}(z) = \sum_{i=0}^{l-1}\bar{A}_{l-1-i}'(I - \bar{A}_1'X\Sigma_{11}Y)C_y'(C_yYC_y')^{-1}z^{l-i}$$

(here $\bar{A}_k$ stands for $\bar{A}_1^k$), and $\mathcal{H}_c$ and $\mathcal{H}_{\bar{c}}$ are hold devices with the $(n_v \times n)$-valued hold functions

$$\phi_c(\tau) = \begin{bmatrix} C_v & 0 \end{bmatrix}\Sigma(\tau - h)\begin{bmatrix} I-YX \\ -X \end{bmatrix}\mathbb{1}_{[0,h]},$$
$$\phi_{\bar{c}}(\tau) = \begin{bmatrix} C_v & 0 \end{bmatrix}\Sigma(\tau - h)\begin{bmatrix} Y \\ I \end{bmatrix}\mathbb{1}_{[0,h]},$$

respectively. The optimal performance is then calculated as

$$\mathcal{J}_l := \|\mathcal{G}_e\|_2^2 = \tfrac{1}{h}\operatorname{tr}\big(\begin{bmatrix} X_l & I - X_lY \end{bmatrix}\Delta\Sigma^{-1}\begin{bmatrix} Y \\ I \end{bmatrix}\big),$$

where $X_l := X - \bar{A}_l'X\bar{A}_l = \sum_{i=0}^{l-1}\bar{A}_i'C_y'(C_yYC_y')^{-1}C_y\bar{A}_i$.

Proof. We only need to proof the equivalence of the formulae above and the corresponding expressions obtained in Section 23. This is a matter of standard manipulations over matrix exponentials, see Appendix C for details. ∎
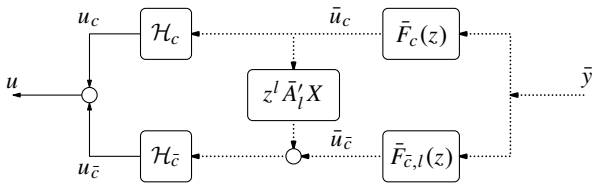
Some remarks are in order:

Figure 21: The optimal l-causal reconstructor $\mathcal{H}_l$

Remark 24.2 (Structure of $\mathcal{H}_l$). The optimal reconstructor in Fig. 21 can be viewed as the parallel interconnection:

$$\mathcal{H}_l = \mathcal{H}_{l,c} + \mathcal{H}_{l,\bar{c}} + \mathcal{H}_{l,\mathrm{corr}}.$$

The IIR causal part, $\mathcal{H}_{l,c}$, corresponds to the signal-flow channel $\bar{y} \to \bar{u}_c \to u_c$ and has the impulse response

$$\phi_{l,c}(kh + \tau) = \phi_c(\tau)\bar{A}_k\Sigma_{11}YC_y'(C_yYC_y')^{-1}$$

for all $k \in \mathbb{Z}_0^+$ and $\tau \in [0, h)$. The FIR anti-causal part, $\mathcal{H}_{l,\bar{c}}$, corresponds to the signal-flow channel $\bar{y} \to \bar{u}_{\bar{c}} \to u_{\bar{c}}$ and has the impulse response

$$\phi_{l,\bar{c}}(kh + \tau) = \phi_{\bar{c}}(\tau)\bar{A}_{-k-1}'(I - \bar{A}_1'X\Sigma_{11}Y)C_y'(C_yYC_y')^{-1}$$

for all $k \in \mathbb{Z}_{-l}^+ \setminus \mathbb{Z}_0^+$ and $\tau \in [0, h)$. The IIR correction term, $\mathcal{H}_{l,\mathrm{corr}}$, corresponds to the signal-flow channel $\bar{y} \to \bar{u}_c \to u_{\bar{c}}$ and has the impulse response

$$\phi_{l,\mathrm{corr}}(kh + \tau) = \phi_{\bar{c}}(\tau)\bar{A}_l'X\bar{A}_{l+k}\Sigma_{11}YC_y'(C_yYC_y')^{-1}$$

for all $k \in \mathbb{Z}_{-l}^+$ and $\tau \in [0, h)$.

One can see that the causal term does not depend on l at all and the anti-causal term depends on l only in the length of its support window. In fact, these two terms together are the truncation of the impulse response of the noncausal reconstructor $\mathcal{H}_\infty$ to $\mathbb{Z}_{-l}^+$. The correction term is what discriminates our solution from those available in the literature, e.g., in [45, 36]. As $l \to \infty$, this term vanishes and we recover the noncausal solution of Part II. If $l = 0$, the second term vanishes and the first and the last terms add up into the hybrid Kalman filter with the impulse response

$$\phi_0(kh + \tau) = C_v\Sigma_{11}(\tau)\Sigma_{11}^{-1}\bar{A}_k\Sigma_{11}YC_y'(C_yYC_y')^{-1},$$

defined in $k \in \mathbb{Z}_0^+$. ▽

Remark 24.3 (Implementation). The discrete IIR part of the causal and correction terms, $\bar{F}_c$, can be efficiently implemented using the state propagation. Indeed, it is readily seen that

$$\bar{u}_c[k] = \bar{A}_1\bar{u}_c[k-1] + \Sigma_{11}YC_y'(C_yYC_y')^{-1}\bar{y}[k], \quad (137)$$

which is actually the Kalman filter for the sampled state of $\mathcal{G}$. The output at each discrete instance kh is then multiplied by the fixed functions—$\phi_c(\tau)$ and $\phi_{\bar{c}}(\tau)\bar{A}_l'X$—to produce the intersample response. Equation (137) can be further simplified by noticing that $\bar{A}_1$ is always singular, which can be seen from (117). Moreover, it follows from (135) and the nonsingularity of Σ_{11} that exactly n_y eigenvalues of $\bar{A}_1$ are at the origin (here n_y stands for the dimension of y). Hence, an $(n - n_y)$-order realization of $\bar{F}_c$ can be constructed. ▽

Remark 24.4 (Optimal performance). The optimal achievable performance level, $\mathcal{J}_l$, can be rewritten in two equivalent forms:

$$\mathcal{J}_l = \mathcal{J}_0 - \mathcal{J}_{l,\mathrm{impr}} = \mathcal{J}_\infty + \mathcal{J}_{l,\mathrm{deter}},$$

where $\mathcal{J}_0$ and $\mathcal{J}_\infty$ are the optimal performance levels of $\mathbf{RP}_0$ and $\mathbf{RP}_\infty$, respectively,

$$\mathcal{J}_{l,\mathrm{impr}} := \tfrac{1}{h}\operatorname{tr}\big((X - \bar{A}_l'X\bar{A}_l)\begin{bmatrix} I & -Y \end{bmatrix}\Delta\Sigma^{-1}\begin{bmatrix} Y \\ I \end{bmatrix}\big)$$

is the improvement with respect to the preview-free case due to the preview of length l, and

$$\mathcal{J}_{l,\text{deter}} := \tfrac{1}{h} \operatorname{tr}\left(\bar{A}'_l X \bar{A}_l \begin{bmatrix} I & -Y \end{bmatrix} \Delta \Sigma^{-1} \begin{bmatrix} Y \\ I \end{bmatrix}\right)$$

is the deterioration with respect to the noncausal case due to imposing l-causality constraints. The quantities $\mathcal{J}_{l,\text{impr}}$ and $\mathcal{J}_{l,\text{deter}}$ may be useful in choosing the smoothing lag l. ▽

24.1. When $G_v = G_y$

In terms of the state-space data (104), this corresponds to the case when $C_v = C_y$. We are concerned with the behavior of the optimal hold function, $\phi_l(t)$, especially at the sampling instances. The following result can be formulated:

Proposition 24.5. Let $C_v = C_y$ and $l \in \mathbb{N}$. Then the impulse response of the optimal reconstructor $\phi_l(t)$ is continuous and such that $\phi_l(kh) = \bar{\delta}[k]$ (Kronecker delta).

Proof. Because ϕ_c and $\phi_{\bar{c}}$ are continuous, we only need to consider the continuity of $\phi_l(t)$ at $t = kh$, i.e., show that $\phi_l(kh^-) = \phi_l(kh)$. We shall show this for each one of the three components of ϕ_l described in Remark 24.2. To this end, note that

$$\Sigma^{-1} = \begin{bmatrix} \Sigma_{11}^{-1} & -\Sigma_{11}^{-1}\Sigma_{12}\Sigma'_{11} \\ 0 & \Sigma'_{11} \end{bmatrix}$$

(remember, $\Sigma_{22}^{-1} = \Sigma'_{11}$). Using this formula and also (134), (135) and (117), we have:

$$\phi_c(0) = C_y \Sigma_{11}^{-1}(I - (Y - \Sigma_{12}\Sigma'_{11})X)$$
$$= C_y \Sigma_{11}^{-1}(I - \Sigma_{11}Y\bar{A}'_1 X) = C_y \Sigma_{11}^{-1}.$$

Thus, $\phi_c(0)\bar{A}_1 = C_y(I - YC'_y(C_yYC'_y)^{-1}C_y) = 0$, so that

$$\phi_{l,c}(kh) = \begin{cases} I & \text{if } k = 0 \\ 0 & \text{otherwise} \end{cases}.$$

Now, using (136) and then (117),

$$\phi_c(h) = C_y(I - YX)$$
$$= C_y(I - Y(\bar{A}'_1 X \bar{A}_1 + C'_y(C_yYC'_y)^{-1}C_y))$$
$$= C_y Y \bar{A}'_1 X \bar{A}_1 = 0,$$

so that $\phi_{l,c}(kh^-) = 0$ for all $k \in \mathbb{N}$. Next,

$$\phi_{\bar{c}}(0) = C_y \Sigma_{11}^{-1}(Y - \Sigma_{12}\Sigma'_{11}) = C_y Y \bar{A}'_1 = 0,$$

from which $\phi_{l,\bar{c}}(kh) = \phi_{l,\text{corr}}(kh) = 0$. Finally,

$$\phi_{\bar{c}}(h)\bar{A}'_1 = C_y Y \bar{A}'_1 = 0$$

and we have

$$\phi_{l,\bar{c}}(kh^-) = \begin{cases} I & \text{if } k = -1 \\ 0 & \text{otherwise} \end{cases}$$

and $\phi_{l,\text{corr}}(kh^-) = 0$ for all $k \in \mathbb{Z}^+_{1-l}$. ∎

As a matter of fact, the proof of continuity fails if $l = 0$. In this case $\phi_{l,\text{corr}}(kh^-) \neq 0$ as there is no $\bar{A}'_l$ between $\phi_{\bar{c}}(h)$ and X. Note also that the second statement of Proposition 24.5 reproves the consistency of the optimal reconstruction, the fact we already proved in §21.1 by different arguments.

25. Examples

To illustrate the proposed solution, we consider two simple academic, albeit quite informative, examples. In both cases the simplicity of the problems enables us to solve them analytically.

25.1. $G_v(s) = G_y(s) = \frac{1}{s^2}$ (causal cubic splines)

This choice of the signal generator might be suitable for a low-pass dominant signal. The presence of unstable poles at the origin might be thought of as the reflection of the zero steady-state error for step and ramp components of v. This problem can also be viewed as reconstructing the position of a rigid body from its sampled measurement assuming that the acceleration is white process.

Bring in a possible state-space realization:

$$G(s) = \begin{bmatrix} 1 & 0 \\ \hline 1 & 0 \end{bmatrix} \left(sI - \begin{bmatrix} 0 & 1/h \\ 0 & 0 \end{bmatrix}\right)^{-1} \begin{bmatrix} 0 \\ h \end{bmatrix}.$$

Obviously, $\mathbf{A_8}$ holds. As $\mathrm{e}^{Ah} = \begin{bmatrix} 1 & 1 \\ 0 & 1 \end{bmatrix}$, the observability matrix of (C_y, e^{Ah}) is $\begin{bmatrix} 1 & 0 \\ 1 & 1 \end{bmatrix}$, which is nonsingular. Hence, $\mathbf{A_7}$ holds too and the problem is solvable.

Denoting

$$\alpha := \sqrt{3} - 2 \approx -0.2679, \qquad (138)$$

the formulae of Theorem 24.1 yield the discrete filters

$$\bar{F}_c(z) = \begin{bmatrix} 4 - \sqrt{3} \\ 3 - \sqrt{3} \end{bmatrix} + \begin{bmatrix} 1 \\ 1 \end{bmatrix} \frac{6\alpha}{z - \alpha},$$

$$\bar{F}_{\bar{c}}(z) = \frac{6z}{h^3}\left(\begin{bmatrix} 3\sqrt{3} - 3 \\ -\sqrt{3} \end{bmatrix}\sum_{i=1}^{l-1}(\alpha z)^{l-i} + \begin{bmatrix} 4 - 3\sqrt{3} \\ 1 - \sqrt{3} \end{bmatrix}\right),$$

the "correction" gain (if $l \geq 1$)

$$\bar{A}'_l X = \frac{\alpha^l}{h^3}\begin{bmatrix} 6\sqrt{3} & 3 - 3\sqrt{3} \\ -3 - 3\sqrt{3} & \sqrt{3} \end{bmatrix},$$

and the hold functions

$$\phi_c(\tilde{\tau}) = \frac{1 - \tilde{\tau}}{\sqrt{3} + 1}\begin{bmatrix} -2\tilde{\tau}^2 + \tilde{\tau} + \sqrt{3} + 1 \\ \tilde{\tau}^2 + \frac{\sqrt{3}-1}{2}\tilde{\tau} - \sqrt{3} - 1 \end{bmatrix}' \mathbb{1}_{[0,h]},$$

$$\phi_{\bar{c}}(\tilde{\tau}) = \frac{h^3\tilde{\tau}}{6}\begin{bmatrix} -\tilde{\tau}^2 + 3\tilde{\tau} + \sqrt{3} & 3\tilde{\tau} + \sqrt{3} \end{bmatrix}\mathbb{1}_{[0,h]},$$

where $\tilde{\tau} := \tau/h$ is the normalized intersample time. Note that $\bar{F}_c(z)$ is a first-order transfer function, which agrees with the discussion at the end of Remark 24.3.

Now, combining discrete filters with corresponding holds, we end up with the impulse response of the optimal reconstructor of the form $\phi_l(t) = \phi_\infty(t) + \phi_{l,\text{corr}}(t)$, where ϕ_∞ is the impulse response of the optimal noncausal reconstructor:

$$\phi_\infty((k + \tilde{\tau})h) = \begin{cases} \phi_1(1 - \tilde{\tau})\alpha^{-k-1} & \text{if } -l \leq k \leq -2 \\ \phi_0(1 - \tilde{\tau}) & \text{if } k = -1 \\ \phi_0(\tilde{\tau}) & \text{if } k = 0 \\ \phi_1(\tilde{\tau})\alpha^k & \text{if } k \geq 1 \end{cases}$$

and $\phi_{l,\text{corr}}$ is the impulse response of the correction term:

$$\phi_{l,\text{corr}}((k+\tilde{\tau})h) = \begin{cases} -\phi_1(1-\tilde{\tau})\frac{3-\sqrt{3}}{3}\alpha^{l-1} & \text{if } k = -l \\ -\phi_1(1-\tilde{\tau})\alpha^{2l+k-1} & \text{if } k \geq 1-l \end{cases}$$

where

$$\phi_0(\tilde{\tau}) := (1-\tilde{\tau})(1+\tilde{\tau}-(3\sqrt{3}-4)\tilde{\tau}^2),$$
$$\phi_1(\tilde{\tau}) := 3\tilde{\tau}(1-\tilde{\tau})(1-(\sqrt{3}-1)\tilde{\tau}).$$

The resulting impulse responses $\phi_l(t)$ of the optimal reconstructor $\mathcal{H}_l$ for $l = 1$ and $l = 2$ are shown in Fig. 22. As l in-
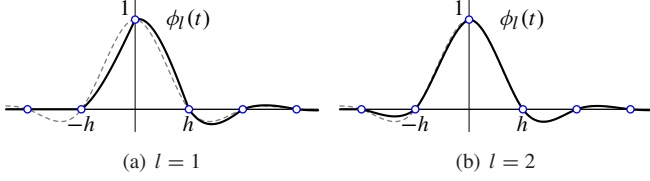

(a) $l = 1$ (b) $l = 2$

Figure 22: Causal cardinal cubic splines with preview l

creases, the correction term vanishes, so $\phi_3(t)$ is then barely distinguishable from the truncated noncausal solution $\phi_\infty(t)$, which is shown in gray dashed lines in Fig. 22. For small l, however, $\phi_{l,\text{corr}}$ is important.

Remark 25.1. We already saw in Part II Thm. 10.5 that ϕ_∞ is the standard cardinal cubic spline [45]. We may therefore regard ϕ_l, which minimizes the very same criterion, as a *causal cardinal cubic spline*. This extention is not unique though. For example, ϕ_∞ is optimal for the L^∞ criterion as well. Yet when causality constraints are imposed, the L^2 and L^∞ solutions no longer coincide. Hence, we may expect that the L^∞ criterion will produce different causal splines. ▽

Remark 25.2. Unlike earlier efforts in producing causal version of cardinal cubic splines, see [36] and the references therein, the rationale behind our solution is not the truncation of a anti-causal part of the noncausal spline, but rather the minimization of the same (analog) performance index under the causality constraint. This can be regarded as an *implicit* approach to the design of causal splines. As a result, however, our solution does not maintain the smoothness properties of the noncausal solution ϕ_∞, which is a C^2 function. Our solution ϕ_l is only a C^0 function, it is *not* differentiable at the knots $t = kh$ due to the correction term $\phi_{l,\text{corr}}$. This is clearly seen in Fig. 22(a). ▽

The optimal performance

$$\mathcal{J}_l = \frac{10\sqrt{3}-3-11(3+2\sqrt{3})\alpha^{2l}}{2520}h^3$$

is proportional to h^3. As l increases, $\mathcal{J}_l$ decreases exponentially to $\mathcal{J}_\infty$. The following table gives some indications about the decay rate:

l	0	1	2	3
$\mathcal{J}_l/\mathcal{J}_\infty$	5.9653	1.3565	1.0256	1.0018

As we can see, one step preview makes a big difference with respect to the causal reconstruction: it reduces the achievable performance level from $\approx 500\%$ of $\mathcal{J}_\infty$ to $\approx 36\%$ of it. With three steps preview we are already within 2 per mill of $\mathcal{J}_\infty$.

Comparisons

Following [36], consider the problem of reconstructing the bandlimited triangle wave (see Fig. 23(a))

$$v(t) = \sum_{i=1}^{4} \frac{8(-1)^{i-1}}{(2i-1)^2\pi^2}\sin\left(\frac{2\pi(2i-1)}{16h}t\right) \tag{139}$$

from its samples $\bar{y}[k] = v(kh)$. Our aim here is to compare the reconstruction of his signal by the causal splines ϕ_l with that by the noncausal cubic splines ϕ_∞ and by the causal splines proposed by in [36]. The last three plots in Fig. 23 present

(a) Signal to be reconstructed, (139)

(b) Reconstruction error for $l = 1$ ($P_{u_\infty-u_1} = 5.5428 \times 10^{-5}$)

(c) Reconstruction error for $l = 2$ ($P_{u_\infty-u_2} = 3.9795 \times 10^{-6}$)

(d) Reconstruction error for $l = 3$ ($P_{u_\infty-u_3} = 2.8572 \times 10^{-7}$)
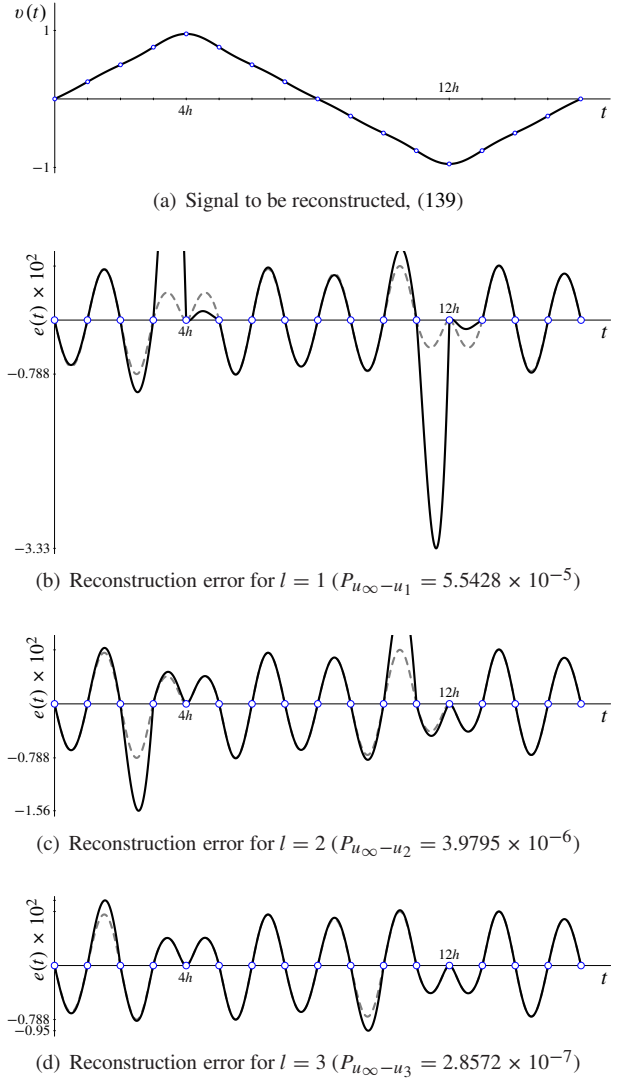
Figure 23: Reconstructing a bandlimited triangle wave

steady-state (stationary) reconstruction errors $e(t)$ over one period of $16h$ for three different smoothing lags l (1, 2, 3) together

with the noncausal case (dashed gray lines)[8]. Consistency in all cases shows up through the zero error at the sampling instances $t = kh$. One can see that the error in noncausal reconstruction is symmetric around the points $4h$ and $12h$, which are the points where $v(t)$ abruptly changes its direction (in between, v is close to the ramp, for which the reconstructions are optimal). The symmetry is not maintained in causal solutions. This is especially visible in the case of $l = 1$, where the preview available to the reconstructor is too short to anticipate this direction change.

To quantify the deviation from the reconstruction with the noncausal splines, we use the power $P_{u_\infty - u_l}$ of the difference between $u_\infty(t)$ and $u_l(t)$, which are the signals reconstructed by the noncausal and l-causal splines, respectively (by the signal power we understand $P_\xi := \lim_{T \to \infty} \frac{1}{T} \int_{-T/2}^{T/2} \xi^2(t) dt$). Remarkably, each additional preview step reduces this quantity by the very same factor: $1/\alpha^2 = 7 + 4\sqrt{3} \approx 13.93$.

The case of $l = 3$ (Fig. 23(d)) corresponds to the setup studied by Petrinović, so we may compare our reconstructor (causal spline) with those proposed in [36]. We consider the C-cascade splines proposed there, which produced the best reconstruction for this $v(t)$ over all other causal splines considered in [36]. It is readily seen from Fig. 23(d) that our reconstruction virtually coincides with that obtained by the noncausal spline in every interval but in $(h, 2h)$ and $(9h, 10h)$. Reconstruction errors with the causal splines proposed by Petrinović are visibly different from the noncausal case in every interval, see [36, Fig. 6]. This impression is confirmed quantitatively: $P_{u_\infty - u_{\text{C-cas}}} = 2.1322 \times 10^{-6}$ is larger than $P_{u_\infty - u_3}$ almost by a factor of 7.5. The peak value of the analog error in our case, 0.0095, is also some 5% smaller than that attainable by the causal C-cascade splines.

Another option for comparing causal cubic splines is via the power of the deviation from the noncausal reconstruction of a single harmonic $v(t) = \sin(\omega(t + \theta))$, averaged over $\theta \in [0, h]$. Fig. 24 presents the ratio between such powers for our recon-
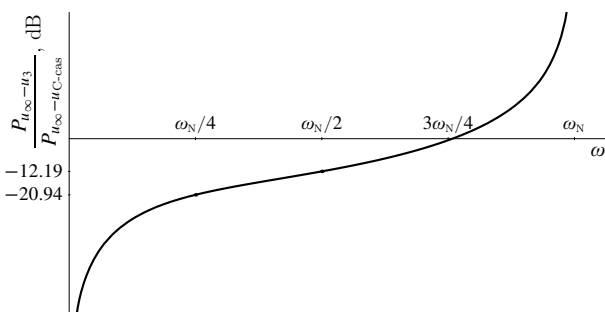

Figure 24: Comparison with C-cascade cubic splines of [36] for $l = 3$

structor and for the causal C-cascade cubic spline of [36] as a function of the frequency ω. This plot shows that ϕ_l is, in a sense, a better approximation of ϕ_∞ up to about three quarters of the Nyquist frequency ω_N, after which the causal C-cascade

splines become a more accurate imitation of ϕ_∞. In the frequency range $(3\omega_N/4, \omega_N)$, however, the reconstruction is rather inaccurate. The peak value of the reconstruction error there is at least 25% of the input magnitude. This might question the suitability of the cubic splines for reconstructing such rapid signals.

It is also possible to analyze directly the reconstruction errors, $v - u_l$ and $v - u_{\text{C-cas}}$, to compare causal splines. In our case this would produce a wider high-frequency area, where the the causal C-cascade splines yield more accurate reconstruction. Such a comparison, however, might be confusing as there is quite wide frequency band, where causal splines produce better reconstruction than ϕ_∞.

25.2. $G_v(s) = \frac{1}{s}$ and $G_y(s) = \frac{1}{s^2}$

This problem can be viewed as reconstructing the velocity of a rigid body from sampled measurement of the position assuming, like in the previous example, that the acceleration is white process. In this case we may choose

$$G(s) = \begin{bmatrix} 0 & 1/h \\ \hline 1 & 0 \end{bmatrix} \left(sI - \begin{bmatrix} 0 & 1/h \\ 0 & 0 \end{bmatrix} \right)^{-1} \begin{bmatrix} 0 \\ h \end{bmatrix}$$

so that the only difference from the first example is the C_v parameter. This, in turn, implies that only ϕ_c and $\phi_{\bar{c}}$ change comparing with the previous example (the other components do not depend on C_v). We have:

$$\phi_c(\tilde{\tau}) = \frac{1}{(\sqrt{3} + 1)h} \begin{bmatrix} 6\tilde{\tau}^2 - 6\tilde{\tau} - \sqrt{3} \\ -3\tilde{\tau}^2 + (3 - \sqrt{3})\tilde{\tau} + \frac{3\sqrt{3}+1}{2} \end{bmatrix}' \mathbb{1}_{[0,h]},$$

$$\phi_{\bar{c}}(\tilde{\tau}) = \frac{h^2}{6} \begin{bmatrix} -3\tilde{\tau}^2 + 6\tilde{\tau} + \sqrt{3} & 6\tilde{\tau} + \sqrt{3} \end{bmatrix} \mathbb{1}_{[0,h]},$$

with $\tilde{\tau} := \tau/h$, as in §25.1.

The impulse response of the optimal reconstructor is again of the form $\phi_l(t) = \phi_\infty(t) + \phi_{l,\text{corr}}(t)$, for the same ϕ_∞ and $\phi_{l,\text{corr}}$ as in the previous example, modulo the substitutions

$$\phi_0(\tilde{\tau}) \to \frac{d}{d\tilde{\tau}} \phi_0(\tilde{\tau}) = \frac{3}{h} \tilde{\tau}(2 - 2\sqrt{3} + (3\sqrt{3} - 4)\tilde{\tau}),$$

$$\phi_1(\tilde{\tau}) \to \frac{d}{d\tilde{\tau}} \phi_1(\tilde{\tau}) = \frac{3}{h} (1 - 2\sqrt{3}\tilde{\tau} + 3(\sqrt{3} - 1)\tilde{\tau}^2)$$

(and then $\phi_i(1 - \tilde{\tau}) \to -\frac{d}{d\tilde{\tau}} \phi_i(1 - \tilde{\tau})$, $i = 0, 1$), so that this ϕ_l is the derivative of the impulse response of the causal cubic splines in the previous example. This, actually, implies that the optimal reconstruction in this case is *consistent*. Indeed, integrating and then sampling this impulse response (this is exactly our measurement system) will produce the Kroneker delta. The impulse response plots for the cases of $l = 1$ and $l = 2$ are presented in Fig. 25. These impulse responses are no longer continuous functions of t, although the noncausal solution (gray dashed lines) is. This was expectable, taking into account the non-differentiability of the causal cubic splines in Fig. 22 at the sampling points.

The optimal performance

$$\mathcal{J}_l = \frac{(3 + 2\sqrt{3})(1 + 3\alpha^{2l})}{60} h$$
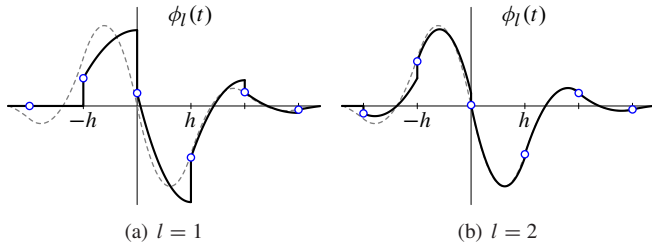
(a) $l = 1$ (b) $l = 2$

Figure 25: Impulse responses of velocity reconstructors with preview l

is now proportional to h. The decay rate of $\mathcal{J}_l$ as l increases can be seen from the following table:

l	0	1	2	3
$\mathcal{J}_l/\mathcal{J}_\infty$	4	1.2154	1.0155	1.0011

and is reminiscent of what we saw in the previous example.

26. Concluding Remarks

In this part we have addressed the L^2 optimal design of D/A converters (reconstructors) with causality constraints imposed on them. Closed-form optimal solutions have been derived in terms of state-space realizations of the given signal generators. The solutions are in form of exponential / polynomial splines, which have clear structural properties (such as continuity and consistency) and recover some known structures when preview length $l \to \infty$. State space machinery facilitates both computational and implementational efficiency of the resulted reconstructors.

Although we have discussed only noise-free measurements, discrete-time white measurement noise can be incorporated into our procedure seamlessly, see [25] (effectively, the only change is the replacement $(C_y Y C_y')^{-1} \to (\Phi_n + C_y Y C_y')^{-1}$, where Φ_n is the noise spectral density). The results can also be extended to more general sampling devices (see [56]).

Some related problems are still open. It would be interesting to have a possibility to impose FIR constraints on optimal reconstructors. This, however, might require quite different techniques to be used as the approach presented in this part cannot handle this situation. Perhaps the ideas of [32] can be exploited in this case. Another open problem is an extension of the approach to the L^∞ performance measure, which can probably be done using the method of [31]. Unlike noncausal cases, L^∞ solutions do not coincide with L^2 ones when causality constraints are imposed and even possess some qualitatively different properties, see [31].

Appendices

A. Proofs for Part II

Proof of Lemma 9.2. This is a known result, often called the Parrott lower bound, see [35, 12]. The idea is to transform the operator whose L^∞ norm we want to minimize into one of the form

$$\begin{bmatrix} \mathcal{R}_{11} - \mathcal{S} & \mathcal{R}_{12} \\ \mathcal{R}_{21} & \mathcal{R}_{22} \end{bmatrix}$$

with $\mathcal{R}_{ij}$ fixed operators and $\mathcal{S}$ our free parameter (sampler). [35] showed that then its L^∞ norm is bounded from below by

$$\max \left(\left\| \begin{bmatrix} \mathcal{R}_{12} \\ \mathcal{R}_{22} \end{bmatrix} \right\|_\infty, \left\| \begin{bmatrix} \mathcal{R}_{21} & \mathcal{R}_{22} \end{bmatrix} \right\|_\infty \right)$$

and that equality can be achieved [12]. To simplify the exposition, we assume that $\mathcal{H}^*\mathcal{H} = I$ and $\mathcal{G}_y \mathcal{G}_y^* = I$. Then $\begin{bmatrix} \mathcal{G}_y^* & I - \mathcal{G}_y^*\mathcal{G}_y \end{bmatrix}$ is co-inner, meaning that

$$\begin{bmatrix} \mathcal{G}_y^* & I - \mathcal{G}_y^*\mathcal{G}_y \end{bmatrix} \begin{bmatrix} \mathcal{G}_y^* & I - \mathcal{G}_y^*\mathcal{G}_y \end{bmatrix}^* = I.$$

Therefore $\mathcal{G}_v - \mathcal{H}\mathcal{S}\mathcal{G}_y$ and

$$(\mathcal{G}_v - \mathcal{H}\mathcal{S}\mathcal{G}_y) \begin{bmatrix} \mathcal{G}_y^* & I - \mathcal{G}_y^*\mathcal{G}_y \end{bmatrix}$$
$$= \begin{bmatrix} \mathcal{G}_v \mathcal{G}_y^* - \mathcal{H}\mathcal{S} & \mathcal{G}_v(I - \mathcal{G}_y^*\mathcal{G}_y) \end{bmatrix} \quad (140)$$

have the same L^∞ norm. Notice that the second block here does not depend on $\mathcal{S}$. Similarly $\begin{bmatrix} \mathcal{H}^* \\ I - \mathcal{H}\mathcal{H}^* \end{bmatrix}$ is inner and therefore (140) in turn has the same L^∞ norm as

$$\begin{bmatrix} \mathcal{H}^* \\ I - \mathcal{H}\mathcal{H}^* \end{bmatrix} \begin{bmatrix} \mathcal{G}_v \mathcal{G}_y^* - \mathcal{H}\mathcal{S} & \mathcal{G}_v(I - \mathcal{G}_y^*\mathcal{G}_y) \end{bmatrix}$$
$$= \begin{bmatrix} \mathcal{H}^*\mathcal{G}_v \mathcal{G}_y^* - \mathcal{S} & \mathcal{H}^*\mathcal{G}_v(I - \mathcal{G}_y^*\mathcal{G}_y) \\ (I - \mathcal{H}\mathcal{H}^*)\mathcal{G}_v \mathcal{G}_y^* & (I - \mathcal{H}\mathcal{H}^*)\mathcal{G}_v(I - \mathcal{G}_y^*\mathcal{G}_y) \end{bmatrix}$$
$$=: \begin{bmatrix} \mathcal{R}_{11} - \mathcal{S} & \mathcal{R}_{12} \\ \mathcal{R}_{21} & \mathcal{R}_{22} \end{bmatrix}.$$

Now, only the upper left block depends on $\mathcal{S}$ and it can be assigned any operator that we like and therefore Parrott's theorem applies. It is readily seen that

$$\left\| \begin{bmatrix} \mathcal{R}_{12} \\ \mathcal{R}_{22} \end{bmatrix} \right\|_\infty = \| \mathcal{G}_v(I - \mathcal{G}_y^*\mathcal{G}_y) \|_\infty$$

and

$$\left\| \begin{bmatrix} \mathcal{R}_{21} & \mathcal{R}_{22} \end{bmatrix} \right\|_\infty = \| (I - \mathcal{H}\mathcal{H}^*)\mathcal{G}_v \|_\infty.$$

The formula for the optimal $\mathcal{S}$ is very involved [12]. Yet if $\mathcal{G}_y$ is stably invertible, then (42) achieves the lower bound (44). ∎

Proof of Theorem 10.5. For $G_v(s) = 1/s^n$ the Fourier transform (50) becomes

$$\Phi_{\text{opt}}(i\omega) = \frac{1/\omega^{2n}}{\frac{1}{h} \sum_{k \in \mathbb{Z}} 1/(\omega + 2k\omega_N)^{2n}}.$$

Since $e^{i2k\omega_N h} = 1$ this Fourier transform equals

$$\Phi_{\text{opt}}(i\omega) = \frac{W(i\omega)^{2n}}{\frac{1}{h} \sum_{k \in \mathbb{Z}} (W(i(\omega + 2k\omega_N)))^{2n}} \quad (141)$$

for $W(i\omega) := (1 - e^{-i\omega h})/(i\omega)$. Now, W is the Fourier transform of the zero degree B-spline (not centered around zero) and so W^{2n} corresponds to the degree $2n - 1$ B-spline. The numerator in (141) is the result of passing W^{2n} through a stable discrete filter that makes $\phi(kh) = \bar{\delta}[k]$, see [46, §V.B]. So $\phi(t)$ is the cardinal polynomial spline of degree $2n - 1$. ∎

Proof of Equation (55). According to (7), the kernel $g(t, s)$ of the continuous-time mapping $u = \mathcal{H}\mathcal{S}y$ is $g(t, s) = \sum_{i \in \mathbb{Z}} \phi(t - ih)\psi(ih - s)$. Therefore the kernel $\breve{g}(z; \tau, \sigma)$ of the transfer function is

$$
\begin{aligned}
\breve{g}(z; \tau, \sigma) &= \sum_{k \in \mathbb{Z}} \sum_{i \in \mathbb{Z}} \phi(\tau + kh - ih)\psi(ih - \sigma)z^{-k} \\
&= \sum_{k \in \mathbb{Z}} \sum_{i \in \mathbb{Z}} \phi(\tau + (k-i)h)z^{-(k-i)}\psi(ih - \sigma)z^{-i} \\
&= \breve{\phi}(z; \tau)\breve{\psi}(z; -\sigma).
\end{aligned}
$$

This completes the proof. ∎

Proof of Theorem 11.1 (Rank Theorem). The if part is trivial. Now the only-if part. If $g \in L^2(\mathbb{R})$, then by Parseval we have that $\int_{-\pi}^{\pi} \|\breve{G}(e^{i\theta})\|_{\mathrm{HS}}^2 d\theta < \infty$. Hence $\|\breve{G}(e^{i\theta})\|_{\mathrm{HS}} < \infty$ for almost all θ (for all θ except possibly on a set of zero measure). By the definition of the Hilbert-Schmidt norm then,

$$
\int_0^h \int_0^h |\breve{g}(e^{i\theta}; \tau, \sigma)|^2 d\tau \, d\sigma < \infty \tag{142}
$$

for almost all $\theta \in [-\pi, \pi]$. For any of those θ the mapping $\int_0^h \int_0^h \breve{g}(e^{i\theta}; \tau, \sigma)\breve{u}(\sigma)d\tau \, d\sigma$ is readily seen to be a bounded mapping from $L^2[0, h]$ to $L^2[0, h]$ and therefore is a compact operator and so has an SVD with countably many singular values (at most r in fact) [9, A.3.24 and A.4.23], that is, has a representation of the form $\sum_{k=1}^r \alpha_k(\tau)\langle \breve{u}, \beta_k \rangle$ where the inner product is that of $L^2[0, h]$ (all α_ks and β_ks still depend on θ). The kernel of this mapping hence is

$$
\begin{aligned}
\breve{g}(e^{i\theta}; \tau, \sigma) &= \breve{\phi}(e^{i\theta}; \tau)\breve{\psi}(e^{i\theta}; \sigma) \\
&:= \begin{bmatrix} \alpha_1(\tau) & \cdots & \alpha_r(\tau) \end{bmatrix} \begin{bmatrix} \beta_1'(\sigma) \\ \vdots \\ \beta_r'(\sigma) \end{bmatrix}.
\end{aligned}
$$

Having finite norm (142) both parts $\breve{\psi}(e^{i\theta})$ and $\breve{\phi}(e^{i\theta})$ have finite $L^2[0, h]$ norm—which by scaling may be taken to be the same—almost everywhere and then have well defined inverse Fourier transforms in $L^2(\mathbb{R})$. The assumption of continuity on some finite partition is sufficient to guarantee that the factors are Lebesgue integrable. ∎

Proof of Lemma 14.6 (Pathological sampling). Define $G_\epsilon(i\omega)$ as the magnitude of $G(i\omega)$ upto at most $1/\epsilon$, $G_\epsilon(i\omega) = \min(1/\epsilon, |G(i\omega)|)$. This G_ϵ is stable and for every frequency $s = i\omega$ that is not a pole of $G(s)$ it converges pointwise to $G(i\omega)$ as $\epsilon \to 0$. Therefore in the case of pathological sampling two or more singular values $\sigma_k(\theta)$ of $G_\epsilon(e^{i\theta})$ converge to ∞ for some θ. So then (given the rationality of G) the error norm for the stabilized generator $\mathcal{G}_{e,\epsilon} := (I - \mathcal{F}_\epsilon)\mathcal{G}_\epsilon$ converges to ∞ as $\epsilon \to 0$. Now, since

$$
\|(I - \mathcal{F})\mathcal{G}\| \geq \|(I - \mathcal{F})\mathcal{G}_\epsilon\| \geq \|(I - \mathcal{F}_\epsilon)\mathcal{G}_\epsilon\|,
$$

we necessarily have that $\|(I - \mathcal{F})\mathcal{G}\| = \infty$ for any $\mathcal{F}$ (LCTI or LDTI), which is what we had to prove.

If we have no pathological sampling then $F_0 := \lim_{\epsilon \to 0} F_\epsilon$ is well defined (frequency-wise, and by rationality). We claim

that then $\|(I - \mathcal{F})\mathcal{G}\|_2 \geq \|(I - \mathcal{F}_0)\mathcal{G}\|_2$ so that $\mathcal{F}_0$ is optimal for G. Indeed, if $\|(I - \mathcal{F})\mathcal{G}\|_2 < \|(I - \mathcal{F}_0)\mathcal{G}\|_2$ then by continuity in ϵ also $\|(I - \mathcal{F})\mathcal{G}_\epsilon\|_2 < \|(I - \mathcal{F}_\epsilon)\mathcal{G}_\epsilon\|_2$ for some small enough ϵ. This contradicts optimality of $\mathcal{F}_\epsilon$. ∎

Mixing matrices (Eqn. (68)). We prove that (68) is the mixing matrix for the scheme of Fig. 15. The mapping from y to $\bar{u}_1$ is a sampler $\mathcal{S}_{\mathrm{Idl}}\mathcal{A}_1\mathcal{F}_{\mathrm{idl}}$ where the ideal low pass filter has cut off frequency $2\omega_\mathrm{N}$. The sampling function of this sampler is the impulse response of $\mathcal{A}_1\mathcal{F}_{\mathrm{idl}}$. Its frequency response according to the Key Lifting Formula (16b) is $\frac{1}{h}\sum_{k \in \mathbb{Z}} A_1(i\omega_k)F_{\mathrm{idl}}(i\omega_k)e^{i\omega_k\tau}$, which for $\theta \in [0, \pi)$ and by the bandlimitness of the ideal low-pass filter becomes

$$
\begin{aligned}
\frac{1}{h}&[A_1(i\omega_0)e^{i\omega_0\tau} + A_1(i\omega_{-1})e^{i\omega_{-1}\tau}] \\
&= \begin{bmatrix} A_1(i\omega_0) & A_1(i\omega_{-1}) \end{bmatrix} \begin{bmatrix} e^{i\omega_0\tau}/h \\ e^{i\omega_{-1}\tau}/h \end{bmatrix}.
\end{aligned}
$$

For the lower loop, the A_1 has to be replaced with A_2. ∎

B. Coprime Factorization over H^∞

In this appendix we review some basic facts about coprime factorization of rational transfer functions over H^∞ as needed in Part III. For an in-depth treatment a reader is referred to [52].

We say that H^∞ functions $\tilde{M}(z)$ and $\tilde{N}(z)$ are *left coprime over H^∞* it there exist compatibly dimensioned H^∞ functions $\tilde{X}(z)$ and $\tilde{Y}(z)$ such that

$$
\tilde{M}\tilde{X} + \tilde{N}\tilde{Y} = \begin{bmatrix} \tilde{M} & \tilde{N} \end{bmatrix} \begin{bmatrix} \tilde{X} \\ \tilde{Y} \end{bmatrix} = I.
$$

This equation is called the Bézout equation and corresponding $\tilde{X}$ and $\tilde{Y}$—Bézout factors of $\tilde{M}$ and $\tilde{N}$. Left coprimeness effectively says that $\tilde{M}$ and $\tilde{N}$ have no common unstable (i.e., in $\mathbb{C} \setminus \mathbb{D}$) zeros, including their multiplicity and output directions. Yet another way to say this is that $\begin{bmatrix} \tilde{M} & \tilde{N} \end{bmatrix}$ is right invertible in H^∞. Consequently, if $\tilde{M}$ and $\tilde{N}$ are left coprime, then $\tilde{T} \begin{bmatrix} \tilde{M} & \tilde{N} \end{bmatrix} \in H^\infty$ necessarily implies that $\tilde{T} \in H^\infty$ too (this fact is instrumental in proving Proposition 20.5).

Now, let $\tilde{G}(z)$ be a rational and proper (i.e., bounded in $|z| > \rho$ for a sufficiently large ρ) transfer function. In this case it can always be presented (this can be shown by construction) as

$$
\tilde{G} = \tilde{M}^{-1}\tilde{N}
$$

for some left coprime H^∞ transfer functions $\tilde{M}$ and $\tilde{N}$ such that $\tilde{M}$ is square and properly invertible. This presentation is called a *left coprime factorization* (lcf) of $\tilde{G}$ over H^∞. The factors $\tilde{M}$ and $\tilde{N}$ can then be thought of as a denominator and a numerator of $\tilde{G}$, respectively. These factors are not unique. For example, $\tilde{P}\tilde{M}$ and $\tilde{P}\tilde{N}$ are also lcf of $\tilde{G}$ for every $\tilde{P}$ such that $\tilde{P}, \tilde{P}^{-1} \in H^\infty$ (the left coprimeness of these factors follow from the fact that $\tilde{X}\tilde{P}^{-1}$ and $\tilde{Y}\tilde{P}^{-1}$ are their Bézout factors). In fact, a stronger result can be proved: if $\tilde{M}$ and $\tilde{N}$ are lcf of $\tilde{G}$, then so are $\tilde{M}_1$ and $\tilde{N}_1$ iff $\tilde{M}_1 = \tilde{P}\tilde{M}$ and $\tilde{N}_1 = \tilde{P}\tilde{N}$ for some $\tilde{P}, \tilde{P}^{-1} \in H^\infty$.

C. Technical Results

Lemma C.1. The factors $\bar{M}_y$ and $\acute{N}_y$ defined by (112) are coprime in H^∞.

Proof. Let F be any matrix such that $A_F := A + BF$ is Hutwitz (this is always possible because the pair (A, B) is controllable). Consider then the following candidates Bézout factors:

$$\bar{X}_y(z) = (I - C_y(zI - e^{A_F h})^{-1}L)\Xi^{-1},$$
$$\acute{Y}_y(z) = \acute{C}_F(zI - e^{A_F h})^{-1}L\Xi^{-1},$$

where $\acute{C}_F$ verifies $\acute{C}_F\bar{\xi} = Fe^{A_F\tau}\bar{\xi}$. Then,

$$\begin{aligned}
\bar{M}_y\bar{X}_y &= \Xi(I + C_y(zI - \bar{A}_1)^{-1}L) \\
&\quad \times (I - C_y(zI - e^{A_F h})^{-1}L)\Xi^{-1} \\
&= I + \Xi C_y(zI - \bar{A}_1)^{-1}(zI - e^{A_F h} \\
&\quad - zI + \bar{A}_1 - LC_y)(zI - e^{A_F h})^{-1}L\Xi^{-1} \\
&= I + \Xi C_y(zI - \bar{A}_1)^{-1} \\
&\quad \times (e^{Ah} - e^{A_F h})(zI - e^{A_F h})^{-1}L\Xi^{-1}.
\end{aligned}$$

Also,

$$\acute{N}_y\acute{Y}_y = \Xi C_y(zI - \bar{A}_1)^{-1}$$
$$\times \int_0^h e^{A(h-\sigma)}BFe^{A_F\sigma}\,d\sigma\,(zI - e^{A_F h})^{-1}L\Xi^{-1}.$$

The integral in the last expression can be interpreted as the response, at the time instance $t = h$, of the continuous-time system $G_1 := (sI - A)^{-1}B$ to the input $Fe^{A_F t}$, which, in turn, is the impulse response of the system $G_2 := F(sI - A_F)^{-1}$. Thus, the integral can be interpreted as the impulse response of the system $G_1 G_2$ taken at the time instance $t = h$. The cascade $G_1 G_2$ can be also represented as a parallel interconnection:

$$\begin{aligned}
G_1 G_2 &= (sI - A)^{-1}BF(sI - A_F)^{-1} \\
&= (sI - A_F)^{-1} - (sI - A)^{-1}.
\end{aligned}$$

Hence, the impulse response of $G_1 G_2$ is the difference of the impulse responses of $(sI - A_F)^{-1}$ and $(sI - A)^{-1}$:

$$\int_0^h e^{A(h-\sigma)}BFe^{A_F\sigma}\,d\sigma = e^{A_F h} - e^{Ah},$$

so that

$$\begin{aligned}
\acute{N}_y\acute{Y}_y &= \Xi C_y(zI - \bar{A}_1)^{-1}(e^{A_F h} - e^{Ah})(zI - e^{A_F h})^{-1}L\Xi^{-1} \\
&= I - \bar{M}_y\bar{X}_y.
\end{aligned}$$

Thus, $\bar{X}_y$ and $\acute{Y}_y$ are Bézout factors of $\bar{M}_y$ and $\acute{N}_y$, which proves the statement. ■

We conclude this Appendix with some technical steps required to proof our main result.

Proof of Theorem 24.1. We effectively only need to show that the optimal cost in the Theorem verifies

$$\mathcal{J}_l = \|\check{N}_v\|_2^2 - \|\dot{Q}_l\|_2^2$$

for the norms in Lemmas 23.1 and 23.3. To this end, note that a direct application of [8, Lemma 10.5.1] yields $\Gamma_v = \Delta_{21}\Sigma_{11}^{-1}$. We also know [29, Lemma 5.5] that $\mathrm{tr}(\Gamma_{vw}) = \mathrm{tr}(\Delta_{22}\Sigma_{11}')$. Finally,

$$\begin{aligned}
(Y - \Gamma_w(\tau))e^{-A'\tau} &= Y\Sigma_{22}(\tau) - \Sigma_{12}(\tau) \\
&= \begin{bmatrix} -I & Y \end{bmatrix} \exp\left(\begin{bmatrix} A & BB' \\ 0 & -A' \end{bmatrix}\tau\right)\begin{bmatrix} 0 \\ I \end{bmatrix},
\end{aligned}$$

so we can use [8, Lemma 10.5.1] again, this time applying to extended matrices, and some row / column permutations to obtain $\Gamma_V = \begin{bmatrix} -I & Y \end{bmatrix}\Delta\Sigma^{-1}\begin{bmatrix} Y \\ I \end{bmatrix}$. The rest is now a direct algebra. ■

D. References

[1] A. Aldroubi and K. Gröchenig. Nonuniform sampling and reconstruction in shift-invariant spaces. *SIAM Review*, 43(4):585–620, 2001.

[2] K. J. Åström and B. Wittenmark. *Computer-Controlled Systems: Theory and Design*. Prentice-Hall, Englewood Cliffs, NJ, 3rd edition, 1997.

[3] B. Bamieh and J. B. Pearson. A general framework for linear periodic systems with applications to H^∞ sampled-data control. *IEEE Trans. Automat. Control*, 37(4):418–435, 1992.

[4] B. Bamieh and J. B. Pearson. The $\mathcal{H}^2$ problem for sampled-data systems. *Syst. Control Lett.*, 19(1):1–12, 1992.

[5] J. Braslavsky, G. Meinsma, R. Middleton, and J. Freudenberg. On a key sampling formula relating the Laplace and $\mathcal{Z}$ transforms. *Syst. Control Lett.*, 29(4):181–190, 1997.

[6] Sheldon S. L. Chang. *Synthesis of Optimum Control Systems*. McGraw-Hill, New York, 1961.

[7] T. Chen and B. A. Francis. Design of multirate filter banks by H^∞ optimization. *IEEE Trans. Signal Processing*, 43(12):2822–2830, 1995.

[8] T. Chen and B. A. Francis. *Optimal Sampled-Data Control Systems*. Springer-Verlag, London, 1995.

[9] R. F. Curtain and H. Zwart. *An Introduction to Infinite-Dimensional Linear Systems Theory*. Springer-Verlag, New York, 1995.

[10] G. E. Dullerud. *Control of Uncertain Sampled-Data Systems*. Birkhäuser, Boston, 1996.

[11] Y. C. Eldar and M. Unser. Nonideal sampling and interpolation from noisy observations in shift-invariant spaces. *IEEE Trans. Signal Processing*, 54(7):2636–2651, 2006.

[12] K. Glover, D.J.N. Limebeer, J.C. Doyle, E.M. Kasenally, and M.G. Safonov. A characterization of all solutions to the four block general distance problem. *SIAM J. Control Optim.*, 92(2):283–324, 1991.

[13] G. H. Golub and C. F. Van Loan. *Matrix Computations*. The Johns Hopkins University Press, Baltimore, 3rd edition, 1996.

[14] B. Hassibi, A. H. Sayed, and T. Kailath. *Indefinite Quadratic Estimation and Control: A Unified Approach to H^2 and H^∞ Theories*. SIAM, Philadelphia, 1999.

[15] J. R. Higgins. *Sampling Theory in Fourier and Signal Analysis: Foundations*. Oxford University Press, Oxford, UK, 1996.

[16] J. R. Higgins and R. L. Stens, editors. *Sampling Theory in Fourier and Signal Analysis: Advanced Topics*. Oxford University Press, Oxford, UK, 1999.

[17] A. H. Jazwinski. *Stochastic Processes and Filtering Theory*. Academic Press, New York, 1970.

[18] A. J. Jerri. The Shannon sampling theorem—its various extensions and applications: A tutorial review. *Proc. IEEE*, 65(11):1565–1596, 1977.

[19] E. I. Jury. *Sampled-Data Control Systems*. John Wiley & Sons, New York, 1958.

[20] T. Kailath, A. H. Sayed, and B. Hassibi. *Linear Estimation*. Prentice-Hall, Upper Saddle River, NJ, 2000.

[21] R. E. Kalman, Y. C. Ho, and K. S. Narendra. Controllability of linear dynamical systems. *Contributions to Differential Equations*, 1(2):189–213, 1963.

[22] Y. Kannai and G. Weiss. Approximating signals by fast impulse sampling. *Math. Control, Signals and Systems*, 6:166–179, 1993.

[23] P. P. Khargonekar and Y. Yamamoto. Delayed signal reconstruction using sampled-data control. In *Proc. 35th IEEE Conf. Decision and Control*, pages 1259–1263, Kobe, Japan, 1996.

[24] P. Lancaster and L. Rodman. *Algebraic Riccati Equations*. Clarendon Press, Oxford, UK, 1995.

[25] G. Meinsma and L. Mirkin. Sampled signal reconstruction via H^2 optimization. In *Proc. 2006 IEEE Int. Conf. Acoust., Speech, Signal Processing*, volume III, pages 365–368, Toulouse, France, 2006.

[26] G. Meinsma and L. Mirkin. System theoretic perspectives of the Sampling Theorem. In *Proc. 17th MTNS Symposium*, pages 730–741, Kyoto, Japan, 2006.

[27] G. Meinsma and L. Mirkin. Noncausal sampled signal reconstruction from noisy measurements: a system-theoretic approach. In *Proc. 46th IEEE Conf. Decision and Control*, pages 444–449, New Orleans, LA, 2007.

[28] G. Meinsma and H. S. Shekhawat. Chopped norms and limitations on signal reconstruction. (paper in preparation).

[29] L. Mirkin, H. Rotstein, and Z. J. Palmor. H^2 and H^∞ design of sampled-data systems using lifting – Part I: General framework and solutions. *SIAM J. Control Optim.*, 38(1):175–196, 1999.

[30] L. Mirkin and G. Tadmor. Yet another H^∞ discretization. *IEEE Trans. Automat. Control*, 48(5):891–894, 2003.

[31] L. Mirkin and G. Tadmor. On geometric and analytic constraints in the H^∞ fixed-lag smoothing. *IEEE Trans. Automat. Control*, 52(8):1514–1519, 2007.

[32] L. Mirkin and G. Tadmor. Imposing FIR structure on H^2 preview tracking and smoothing solutions. *SIAM J. Control Optim.*, 48(4):2433–2460, 2009.

[33] A. V. Oppenheim, A. S. Willsky, and S. H. Nawab. *Signals & Systems*. Prentice-Hall, Upper Saddle River, NJ, 2nd edition, 1997.

[34] A. Papoulis. Generalized sampling expansion. *IEEE Trans. Circuits and Systems*, 24(5):652–654, 1977.

[35] S. Parrott. On a quotient norm and the sz-nagy-foias lifting theorem. *Journal of Functional Analysis*, 30:311–328, 1978.

[36] D. Petrinović. Causal cubic splines: Formulations, interpolation properties and implementations. *IEEE Trans. Signal Processing*, 56(11):5442–5453, 2008.

[37] J. G. Proakis and D. G. Manolakis. *Digital Signal Processing*. Prentice-Hall, Upper Saddle River, NJ, 4th edition, 2007.

[38] H. M. Robbins. An extension of Wiener filter theory to partly sampled systems. *IRE Trans. Circuit Theory*, CT-6:362–370, 1959.

[39] W. Rudin. *Real and Complex Analysis*. McGraw-Hill, New York, 3rd edition, 1987.

[40] A. H. Sayed and T. Kailath. A survey of spectral factorization methods. *Numer. Linear Algebra Appl.*, 8:467–496, 2001.

[41] C. Scherer. Mixed H_2/H_∞ control. In A. Isidori, editor, *Trends in Control: A European Perspective*, pages 173–216. Springer-Verlag, Berlin, 1995.

[42] J. B. Thomas. *An Introduction to Statistical Communication Theory*. John Wiley & Sons, New York, 1969.

[43] M. K. Tsatsans and G. B. Giannakis. Principal component filter banks for optimal multiresolution analysis. *IEEE Trans. Signal Processing*, 43(8):1766–1777, 1995.

[44] M. Unser. On the optimality of ideal filters for pyramid and wavelet signal approximation. *IEEE Trans. Signal Processing*, 41(12):3591–3596, 1993.

[45] M. Unser. Sampling—50 years after Shannon. *Proc. IEEE*, 88(4):569–587, 2000.

[46] M. Unser and A. Aldroubi. A general sampling theory for nonideal acquisition devices. *IEEE Trans. Signal Processing*, 42(11):2915–2925, 1994.

[47] M. Unser, A. Aldroubi, and M. Eden. B-spline signal processing: Part II—Efficiency design and applications. *IEEE Trans. Signal Processing*, 41(2):834–848, 1993.

[48] M. Unser, A. Aldroubi, and M. Eden. B-spline signal processing: Part I—Theory. *IEEE Trans. Signal Processing*, 41(2):821–833, 1993.

[49] M. Unser and T. Blu. Cardinal exponential splines: part I—theory and filtering algorithms. *IEEE Trans. Signal Processing*, 53(4):1425–1438, 2005.

[50] M. Unser and J. Zerubia. A generalized sampling theorem without band-limiting constraints. *IEEE Trans. Circuits Syst. I*, 45(8):959–969, 1998.

[51] P. P. Vaidyanathan. Generalizations of the sampling theorem: Seven decades after Nyquist. *IEEE Trans. Circuits Syst. I*, 48(9):1094–1109, 2001.

[52] M. Vidyasagar. *Control System Synthesis: A Factorization Approach*. The MIT Press, Cambridge, MA, 1985.

[53] Y. Yamamoto and P. P. Khargonekar. Frequency response of sampled-data systems. *IEEE Trans. Automat. Control*, 41(2):166–176, 1996.

[54] J. L. Yen. On nonuniform sampling of bandwidth-limited signals. *IRE Trans. Circuit Theory*, CT-3:251–257, 1956.

[55] N. Young. *An Introduction to Hilbert Space*. Cambridge University Press, Cambridge, UK, 1988.

[56] R. Zaslavsky. *Sampled-Data H^2 Estimation Problems Motivated by Tensegrity Structures*. PhD thesis, Faculty of Mechanical Eng., Technion– IIT, August 2008.